Volume 63 Issue 1

African Invertebrates 63(1): 1–18 (2022)
doi: 10.3897/AfrInvertebr.63.76934
https://africaninvertebrates.pensoft.net

RESEARCH ARTICLE

African Invertebrates
A journal of biodiversity research

A group of two: *Scrapter peringueyi* is not a synonym of *Scrapter heterodoxus* (Hymenoptera, Colletidae, Scraptrinae)

Silas Bossert[1,2], Simon van Noort[3,4]

1 *Department of Entomology, Washington State University, Pullman, WA, 99164, USA* **2** *Department of Entomology, National Museum of Natural History, Smithsonian Institution, Washington, DC, USA* **3** *Research and Exhibitions Department, South African Museum, Iziko Museums of South Africa, Cape Town, 8000, South Africa* **4** *Department of Biological Sciences, University of Cape Town, Private Bag, Rondebosch, 7701, South Africa*

Corresponding author: Silas Bossert (silas.bossert@wsu.edu)

Academic editor: D. Brothers | Received 25 October 2021 | Accepted 30 December 2021 | Published 21 January 2022

http://zoobank.org/CB17C6B2-CF80-4B11-A100-E340E5CB66A2

Citation: Bossert S, van Noort S (2022) A group of two: *Scrapter peringueyi* is not a synonym of *Scrapter heterodoxus* (Hymenoptera, Colletidae, Scraptrinae). African Invertebrates 63(1): 1–18. https://doi.org/10.3897/AfrInvertebr.63.76934

Abstract

Scrapter is a genus of colletid bees with a primary distribution centered in Southern Africa. The genus currently comprises 68 recognized species, which are divided into nine species groups, ranging from one to 29 included species. The *Scrapter heterodoxus* group is presently considered to be the only monotypic group, because of synonymization of *Scrapter heterodoxus* with *Scrapter peringueyi* in a previous revision of the genus. A comparative examination of these two species using both morphological assessment and molecular sequence data from the COI barcode region supported the recognition of *S. peringueyi* as a valid species, which we accordingly resurrect as the second species of the *Scrapter heterodoxus* species group. We provide high resolution images of the type specimens for both species and updated diagnoses to enable their separation from all other species of *Scrapter*.

Keywords

Bees, COI, DNA barcoding, Afrotropical, morphology

Introduction

Scrapter Lepeletier & Serville, 1828 is a genus of colletid bees endemic to Africa (Eardley 1996; Davies et al. 2005; Michener 2007; Eardley et al. 2010). A species-rich genus, *Scrapter* currently comprises 68 recognized species (Kuhlmann and Friehs 2020), and new species are being discovered at a remarkable pace. In the past 25 years since Eardley's (1996) revision of the genus, in which he recognized 31 valid species, more than 30 new species have been described (Davies et al. 2005; Davies and Brothers 2006; Kuhlmann 2014; Kuhlmann and Friehs 2020). As many species of *Scrapter* seem to be ephemeral in their biology, including tight hostplant associations and narrow flight periods in highly seasonal environments (Kuhlmann 2009; Kuhlmann and Eardley 2012; Kuhlmann et al. 2012; Kuhlmann and Friehs 2020), this increase of newly discovered species can be expected to continue into the upcoming decades.

In the past, the phylogenetic relationships of *Scrapter* to other colletid lineages proved difficult to establish based on morphology alone (McGinley 1981; Alexander and Michener 1995; Plant and Paulus 2016). Previously considered to be part of Paracolletini (e.g., Michener 1944), albeit without strong morphological evidence (McGinley 1981), analyses of nucleotide sequence data strongly indicated a sister group relationship of Scraptrinae and Euryglossinae, an Australian-endemic lineage of Colletidae (Almeida and Danforth 2009; Almeida et al. 2012; Kayaalp et al. 2017; Cardinal et al. 2018). Interestingly, a close relationship to Euryglossinae has been discussed as early as 1933 (Cockerell and Ireland 1933; specifically discussing *Euryglossidia* Cockerell) and a sister-group relationship is supported by certain morphological characters of the mature larvae (McGinley 1981). Fossil-based divergence-time estimates agree that the lineages forming the present-day Scraptrinae and Euryglossinae split in the early Eocene, around ~55 million years ago (Almeida et al. 2012; Kayaalp et al. 2017). *Scrapter* is the only colletid lineage endemic to Africa, and with the exception of one species reported from Kenya (Davies et al. 2005), it is geographically restricted to southern Africa. With Euryglossinae being endemic to Australia, the biogeographical puzzle leading to this exceptional distribution has been difficult to explain (Almeida et al. 2012; Kayaalp et al. 2017).

Scrapter is a morphologically heterogeneous genus (Davies and Brothers 2006) with great differences in body size (e.g., 3.5 mm, *Scrapter minutissimus* Kuhlmann, 2014 vs. 14 mm, *Scrapter heterodoxus* (Cockerell, 1921)). Eardley (1996) presented the first attempt to systematically revise the genus, including redescriptions, synonymizations, and type designations. He established eight species groups based on similar characteristics, and Kuhlmann (2014) added the 'euryglossiform' species as a ninth group. One group, the *Scrapter heterodoxus* group is currently understood as being monotypic, because Eardley (1996) synonymized *Scrapter peringueyi* (Cockerell, 1921) with *Scrapter heterodoxus*. Both these species were described by Cockerell (1921) in the same article, but based on different sexes. In the present article, we re-examine the type specimens of the two species and additional material of the *Scrapter heterodoxus* group. Studying both sexes of both species, we found strong morphological evidence that *S. peringueyi* is not a synonym of *S. heterodoxus*, but a valid species.

Nucleotide sequence data from COI barcodes of both morphotypes show a divergence of > 6%, underlining the significant discrepancy between the two lineages. Based on this combined evidence, we resurrect *S. peringueyi* as a valid species.

Materials and methods

We located and examined the type specimens of *S. heterodoxus* and *S. peringueyi* in the collections of the Iziko South African Museum, Cape Town (**SAMC**), and in the South African National Collection of Insects, Pretoria (**SANC**). Additional specimens of both species were collected during field work by Bryan Danforth in South Africa in September 2001 and were deposited in the Cornell University Insect Collection (**CUIC**). In total, we examined 133 specimens, which includes all specimens deposited in the collections of the SAMC and the CUIC. We mapped the distributions of the two recognized species using SimpleMappr (Shorthouse 2010). The terminology of surface sculpturing follows Harris (1979).

To compare the DNA sequences of *Scrapter heterodoxus* and *S. peringueyi*, we obtained sequence data for both species. One COI sequence for *S. heterodoxus* was retrieved from GenBank (identifier MH578427) and we extracted another COI barcode from a UCE assembly of the same species (from Branstetter et al. 2017). This DNA sequence data is associated with a male voucher specimen which is deposited in the CUIC. This voucher specimen was examined in the present study and is part of a series of specimens consisting of male and female *S. heterodoxus*: males and females were collected jointly at the same time and place. Since both sexes share distinct morphological features that distinguish them from what was described as *S. peringueyi*, we deemed them conspecific. For *S. peringueyi*, we generated two new barcode sequences. Two male specimens collected on 28 September 2001 and listed below under additional material were used for DNA extraction. These specimens are vouchered in the CUIC as well and are labelled with a green colored extraction code label. DNA was extracted from ground-up thorax tissue using a CTAB phenol-chloroform protocol. We used the DNA extractions to sequence ultraconserved elements (UCEs) as detailed in Bossert et al. (2021), as the *S. peringueyi* samples were processed jointly with the samples of that study. After assembling the raw read data with SPAdes (ver. 3.13.1; Bankevich et al. 2012), we extracted the COI barcode region using the script *phyluce_assembly_match_contigs_to_barcodes* of the Phyluce package (ver. 1.7.1; Faircloth 2016) and a reference COI barcode of *Apis mellifera* L., 1758. The four sequences consisting of two representative barcodes for each of *S. heterodoxus* and *S. peringueyi* were aligned with MUSCLE (ver. 3.8.425; Edgar 2004).

Examination of the sequence alignment by eye revealed that for each species the two barcode sequences differed in length but were otherwise identical across the shared positions. Since we were interested in examining the interspecific distance between *S. heterodoxus* and *S. peringueyi*, we only retained the longest DNA sequence for each species. This led to a sequence alignment of 658 nucleotides (658 present positions for *S. heterodoxus* and 657 for *S. peringueyi*). We estimated the evolutionary distance

between these two sequences by quantifying the proportion of sites at which nucleotides differed (*p*-distance). We uploaded the reference COI sequence of *S. peringueyi* to NCBI GenBank where it can be retrieved under identifier MZ682106. The sequence alignment of all four sequences can be found as Suppl. material 1.

Images were acquired at SAMC with a Leica LAS 4.9 imaging system, comprising a Leica Z16 microscope (using either a 2× or 5× objective) with a Leica DFC450 Camera and 0.63× video objective attached. The imaging process, using an automated Z-stepper, was managed using the Leica Application Suite V 4.9 software installed on a desktop computer. Diffused lighting was achieved using a Leica LED5000 HDI dome. All images presented in this paper, as well as supplementary images, are available on WaspWeb at www.waspweb.org.

Depositories

CUIC Cornell University Insect Collection, Ithaca, NY, USA.
SAMC South African Museum, Iziko Museums of South Africa, Cape Town, South Africa.
SANC National Collection of Insects, Pretoria, South Africa.

Results

Systematics

Subfamily Scraptrinae Ascher & Engel, 2005

Genus *Scrapter* Lepeletier & Serville, 1828

Scrapter Lepeletier & Serville, 1828: 403 (not *Scrapter* Lepeletier, 1841: 260). Type species: *Scrapter bicolor* Lepeletier & Serville, 1828, by subsequent designation in Vachal (1897: 63).
Polyglossa Friese, 1909: 123. Type species: *Polyglossa capensis* Friese, 1909, by subsequent designation in Cockerell (1921: 203).
Strandiella Friese, 1912: 181. Type species: *Strandiella longula* Friese, 1912 = *Scrapter niger* Lepeletier & Serville, 1828, by designation in Cockerell (1916: 430).
Polyglossa (*Parapolyglossa*) Brauns, 1929: 134. Type species: *Polyglossa heterodoxa* Cockerell, 1921, by subsequent designation in Sandhouse (1943: 584).

Comment. Michener (1997) clarified several problematic subsequent type designations.

***Scrapter heterodoxus* (Cockerell, 1921)**
Figures 1, 2, 5

Polyglossa heterodoxa Cockerell, 1921: 204.

Figure 1. Male lectotype of *Scrapter heterodoxus* (Cockerell, 1921). **A** habitus, dorsolateral view, and labels **B** habitus, lateral view **C** head, frontal view **D** propodeum **E** hind leg tibia **F** fore wing.

Material examined. ***Lectotype:*** South Africa: Cape Town, leg. F. Foly, ♂, SAMC, catalogue no. SAM-HYM-B000145. Labels associated with this specimen are shown in Fig. 1A. According to Cockerell (1921), the specimen was collected in 1914. Additional material: South Africa: Cape Province, 31 km S of Clanwilliam, 32°23.1'S, 18°56.8'E, 7 September 2001, leg. B. N. Danforth, C. D. Eardley, K. L. Walker, 6♂, 15♀, CUIC. Cape Province, Sauer, Suurfontein, –32.85, 18.5667, 25 August 1994, leg. V. B. Whitehead, 2♂, SAMC, cat. no. SAM-HYM-B007774. Cape Province, Holfontein, 20 km S. of Clanwilliam, –32.4333, 18.95, 8 August 1984, leg. V. B. Whitehead, 3♂, SAMC, cat. no. SAM-HYM-B007777. Cape Province, Piketberg, Witte-

Figure 2. Female non-type specimen of *Scrapter heterodoxus* (Cockerell, 1921), (SAM-HYM-B007786). **A** habitus, dorsal view **B** habitus, lateral view **C** head, frontal view **D** propodeum **E** labels **F** fore wing.

water, –32.9167, 18.7, 5 September 1990, leg. V. B. Whitehead, 1♀, SAMC, cat. no. SAM-HYM-B007784. Cape Province, Piketberg, farm Hartbeesrivier, Kapteinskloof, –32.875, 18.625, 23 August 1991, leg. V. B. Whitehead, 1♂, SAMC, cat. no. SAM-HYM-B007785. Cape Province, Piketberg, Banghoek, –32.75, 18.6, 20 September 1991, leg. V. B. Whitehead, 1♀, SAMC, cat. no. SAM-HYM-B007786. Cape Province, Mamre, Malmesbury Div. Cape, –33.5167, 18.4667, 25 August 1977, leg. V. B. Whitehead, 1♂, SAMC, cat. no. SAM-HYM-B007788. Cape Province, Joostenbergkloof, Stellenbosch, –33.7667, 18.7667, 14 August 1988, leg. V. B. Whitehead, 3♂,

SAMC, cat. no. SAM-HYM-B007789. Cape Province, Joostenbergkloof, Stellenbosch, –33.7667, 18.7667, 31 July 1988, leg. V. B. Whitehead, 1♂, SAMC, cat. no. SAM-HYM-B007790. Cape Province, Katberg Pass, R351, –32.4667, 26.65, 25 November 1985, 1♀, SAMC, cat. no. SAM-HYM-B007791. Cape Province, Kakamas, 16.5 km N of Orange R. bridge, Rd to Namibia, –28.6000, 20.5667, 22 July 1993, leg. V. B. Whitehead, 1♀, SAMC, cat. no. SAM-HYM-B007792. Cape Province, Leipoldtville, –32.2333, 18.4833, 14 September 1984, leg. V. B. Whitehead, 2♀, SAMC, cat. no. SAM-HYM-B007793. Cape Province, Hetkruis, Groenrivier, –32.6, 18.75, 14 August 1991, leg. V. B. Whitehead, 1♂, SAMC, cat. no. SAM-HYM-B007794. Cape Province, 7 km N. of Elandsbaai, –32.25, 18.35, 21 September 1984, leg. V. B. Whitehead, 1♂ and 1♀, SAMC, cat. no. SAM-HYM-B007795. Cape Province, Doringfontein, 33km N. of Piketberg, 30 August 1987, –32.6, 18.7667, leg. V. B. Whitehead, 1♂, SAMC, cat. no. SAM-HYM-B007796. Cape Province, Tygerberg, –33.8833, 18.6, 14 September 1990, leg. K. Steiner, 1♀, SAMC, cat. no. SAM-HYM-B009506. Cape Province, Elands Bay, –32.3, 18.35, 26 September 1985, leg. V. B. Whitehead, 1♂, SAMC, cat. no. SAM-HYM-B009507. Cape Province, Sevilla, Traveller's Rest, –32.07278, 19.08056, 25 August 2007, leg. S. van Noort, 1♀, SAMC, cat. no. SAM-HYM-B010372. Cape Province, Somerset (W.) Strand, 25 October 1925, –34.1167, 18.8333, leg. H. Brauns, 1♀, SAMC, cat. no. SAM-HYM-B007776a.

Diagnosis. ♂: the male of *S. heterodoxus* differs from all other *Scrapter* species except *S. peringueyi* in possessing the unique combination of the following characters: body size of ≥ 12 mm, hind femur greatly enlarged, hind tibia strongly broadened apically (Figs 1E, 5B), hind basitarsus unmodified (enlarged in *S. amplitarsus* Eardley, 1996) and midleg basitarsus unmodified (enlarged in *S. armatipes* (Friese, 1913)). *Scrapter heterodoxus* differs from *S. peringueyi* in the shape of the apical section of the hind tibia: the shape of the projecting apical portion is tapering in *S. heterodoxus*, resembling a triangular shape, whereas the projecting apical portion of the tibia in *S. peringueyi* is parallel-sided, resembling a rectangular shape (Figs 1E, 4E, 5A, 5B). As in the female sex, the surface sculpturing of the basal zone of the propodeum is rugulose in *S. heterodoxus*, whereas it is substrigulate in *S. peringueyi* (Figs 5C, 5D). The integument between the punctation on the mesoscutum is polished in *S. heterodoxus* and shagreened (dull) in *S. peringueyi*.

♀: The female differs from most species of *Scrapter*, except *S. caesariatus* Eardley, 1996, *S. peringueyi* and those of the *S. nitidus* and *S. basutorum* species groups, in having a medio-longitudinally depressed clypeus ("mediolongitudinal sulcus" in Eardley 1996), but the depression is shallower than in the species of the *S. nitidus* and *S. basutorum* groups. With 6.8–9.3 mm body length, *S. heterodoxus* is on average larger than *S. caesariatus* (at most 7.3 mm) and the species of the *S. nitidus* group (at most 7.7 mm long). It differs from all aforementioned *Scrapter* species except *S. peringueyi* in having a declivous propodeal surface, without a nearly horizontal basal zone. *Scrapter heterodoxus* is very similar and clearly closely related to *S. peringueyi*. It differs in having a rugulose surface sculpturing of the basal zone of the propodeum, particularly of the anterior portion, whereas the sculpturing of *S. peringueyi* is substrigulate (Figs 5E, 5F).

As in the male, the integument between the punctation on the mesoscutum is polished in *S. heterodoxus* and shagreened (dull) in *S. peringueyi*.

Comments. The females of *S. heterodoxus* and *S. peringueyi* are difficult to distinguish at times, whereas the males are easily recognized. The published sequence data of *S. heterodoxus* from previous molecular-phylogenetic treatments (Almeida and Danforth 2009; Branstetter et al. 2017; Almeida et al. 2019) is associated with a vouchered specimen deposited in the CUIC. This specimen is part of the examined series listed under additional material, which was collected in the Western Cape Province, 31 km S of Clanwilliam. The voucher corresponds to the type specimen of *S. heterodoxus*, which means that the previously published DNA data refers to the true *S. heterodoxus* and not to *S. peringueyi*.

***Scrapter peringueyi* (Cockerell, 1921), stat. rev.**
Figures 3–5

Polyglossa peringueyi Cockerell, 1921: 205.

Material examined. Holotype: South Africa: Knysna, C. C., October 1916, leg. L. Péringuey, ♀, SAMC. Additional material: South Africa: Knysna, C. C., October 1916, leg. L. Péringuey, ♀, SANC, Database No. HYMA04122. Cape Province, Hermanus, 34°24.76'S, 19°17.25'E, 28 September 2001, leg. B. N. Danforth, C. D. Eardley, K. L. Walker, 17 ♂, CUIC. Cape Province, Pearly Beach, Bredasdorp, September 1959, –34.6667, 19.51667, leg. South African Museum Expedition, 3♂ and 2♀, SAMC, cat. no. SAM-HYM-B007139. Cape Province, Pearly Beach, Bredasdorp, September 1959, –34.6667, 19.51667, leg. South African Museum Expedition, 41♂ and 5♀, SAMC, cat. no. SAM –HYM-B007773. Cape Province, Somerset (W.) Strand, 25 October 1925, –34.1167, 18.8333, leg. H. Brauns, 1♂, SAMC, cat. no. SAM-HYM-B007776b. Cape Province, Cape of Good Hope Nature Reserve, 18 September 1975, leg. V. B. Whitehead, 1♂ and 3♀, SAMC, cat. no. SAM-HYM-B007778. Cape Province, Cape of Good Hope Nature Reserve, Olifantsbos, near Skaife center, –34.2667, 18.3833, 18–19 September 1993, leg. S. van Noort, 1♀, SAMC, cat. no. SAM-HYM-B007779. Cape Province, Vermont, –34.4167, 19.1667, 10 October 1977, leg. V. B. Whitehead, 1♂, SAMC, cat. no. SAM-HYM-B007780. Cape Province, Knysna, October 1916, leg. L. Péringuey, 5♀, SAMC, cat. no. SAM-HYM-B007782. Cape Province, Hout Bay, opp. Duiker Is., –34.0333, 18.3, 11 October 1986, leg. K. Steiner, 1♀, SAMC, cat. no. SAM-HYM-B007783. Cape Province, Strandfontein, –34.0833, 18.5500, 1 November 1960, leg. F. W. Gess, 1♂, SAMC, cat. no. SAM-HYM-B007787. Cape Province, Cape of Good Hope Nature Reserve, 8 October 1986, leg. K. Steiner, 1♂, SAMC, cat. no. SAM-HYM-B009504. Cape Province, Hout Bay, Duiker Point, –34.0333, 18.3, 11 October 1986, leg. K. Steiner, 1♂, SAMC, cat. no. SAM-HYM – B009505.

Diagnosis. *Scrapter peringueyi* is morphologically very similar to *S. heterodoxus*. ♂: the male of *S. peringueyi* differs from that of *S. heterodoxus* in the shape of the projecting apical portion of the hind tibia, which is parallel-sided (tapering in *S. heterodoxus*)

Figure 3. Female holotype of *Scrapter peringueyi* (Cockerell, 1921), stat. rev. (SAM-HYM-B000144). **A** habitus, dorsolateral view **B** habitus, lateral view **C** head, frontal view **D** propodeum **E** labels **F** fore wing.

(Figs 1E, 4E, 5A, 5B). It further differs from *S. heterodoxus* in the surface sculpturing of the basal zone of the propodeum, which is substrigulate in *S. peringueyi* and rugulose in *S. heterodoxus* (Figs 1D, 3D, 5C, 5D). The integument on the mesoscutum is shagreened between the punctation, whereas it is polished in *S. heterodoxus.*

♀: the female of *S. peringueyi* differs from *S. heterodoxus* in the same characters as the male, except for the shape of the hind tibia. The surface sculpturing of the basal zone of the propodeum is substrigulate, whereas it is rugulose in *S. heterodoxus* (Figs 2D, 3D, 5E, 5F). The integument between the punctation on the mesoscutum is shagreened in *S. peringueyi* and it is polished in *S. heterodoxus*.

Figure 4. Non-type male specimen of *Scrapter peringueyi* (Cockerell, 1921), stat. rev. **A** habitus, dorsal view **B** habitus, lateral view **C** head, frontal view **D** propodeum **E** hind leg tibia **F** fore wing.

Discussion

Scrapter heterodoxus and *S. peringueyi* were described as species by Cockerell in the same publication (Cockerell 1921). Subsequently, in his major revisionary work on *Scrapter*, Eardley (1996) synonymized the two species and regarded only *Scrapter heterodoxus* as valid. Thus, the *Scrapter heterodoxus* species 'group' was regarded as monotypic over the past decades. In the present study, we reassess the status of both species using morphological and molecular methods, and find strong support for the re-recognition of *S. peringueyi*

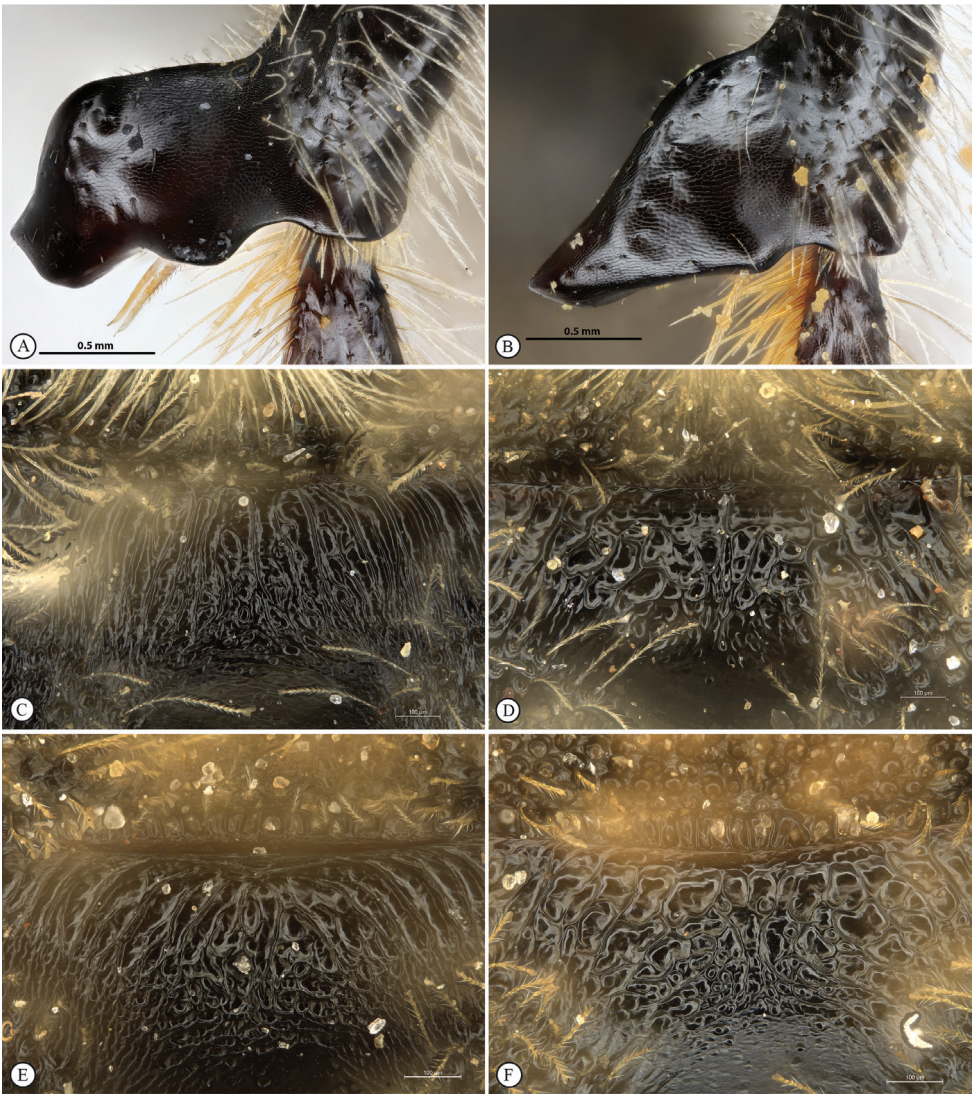

Figure 5. Comparison of the shape of the male hind leg tibia and propodeal sculpture. **A** *Scrapter peringueyi* (Cockerell, 1921), stat. rev. hind leg tibial apex, non-type male specimen (deposited in CUIC) **B** *Scrapter heterodoxus* (Cockerell, 1921) hind leg tibial apex, non-type male specimen (deposited in CUIC) **C** *Scrapter peringueyi* (Cockerell, 1921), stat. rev. propodeal sculpture, non-type male specimen (SAM-HYM-B007139) **D** *Scrapter heterodoxus* (Cockerell, 1921) propodeal sculpture, lectotype male (SAM-HYM-B000145) **E** *Scrapter peringueyi* (Cockerell, 1921), stat. rev. propodeal sculpture, holotype female (SAM-HYM-B000144) **F** *Scrapter heterodoxus* (Cockerell, 1921) propodeal sculpture, non-type female (SAM-HYM-B007786).

as a valid second species in the *Scrapter heterodoxus* group. While both species are morphologically very similar, clearly closely related, and not particularly like any other species of *Scrapter*, they can be readily separated using morphological characters and molecular

data. Differentiation of the species is particularly clear in the male sex based on the species-specific shape of the hind tibia (Fig. 5), which shows no intraspecific variation among the examined specimens or in illustrations in the literature (Brauns 1929; Eardley 1996). Other structures that are often diagnostic for species-recognition of *Scrapter*, such as the genital capsule and terminal sterna, seem identical between the two species and cannot be used to separate *S. heterodoxus* and *S. peringueyi*. However, both sexes can also be separated by the different surface sculpturing of the basal zone of the propodeum and the polished or shagreened interspaces on the mesoscutum. These morphological differences that distinguish both males and females of *S. heterodoxus* from *S. peringueyi* allowed us to associate the female sex for both species, since we only generated COI sequence data from male individuals. In line with these morphological differences is the significant genetic distance between the examined specimens, which is 6.1% for the 657 base-pair long COI barcode region. Species delimitation based on pairwise genetic distances of this partial gene region is common practice in modern insect systematics and has been routinely applied for many insect groups such as Lepidoptera (e.g., Hausmann et al. 2011; Nneji et al. 2020), Coleoptera (e.g., Oba et al. 2015; Huang et al. 2020), Hymenoptera (e.g., Sheffield et al. 2009; Stahlhut et al. 2013), and specifically for certain African bees (Bossert et al. 2020). While the threshold for delimiting species boundaries is not universal, varies among studies, and is not ultimate proof, a distance of 2–3% is common practice to recognize a barcoding gap (Ratnasingham and Hebert 2013; Hebert et al. 2003; and references above). The calculated distance between *S. heterodoxus* and *S. peringueyi* exceeds such thresholds considerably, underlining the need to recognize them as distinct species.

Prior and subsequent to Eardley's (1996) revision of *Scrapter* and the synonymization of *S. peringueyi* with *S. heterodoxus*, samples of '*Scrapter heterodoxus*' have been included in a number of morphological-phylogenetic studies (Alexander and Michener 1995; Davies and Brothers 2006; Packer 2008; Mthethwa 2016; Plant and Paulus 2016; Porto and Almeida 2019), or assessments of pollinator communities (Tribe 2007; Goldblatt et al. 2009). As the distinguishing characters between *S. heterodoxus* and *S. peringueyi* are not specifically mentioned in these works, it is not immediately clear which of the two species were actually included in the respective studies. It is therefore possible that some of the examined specimens may in fact have corresponded to *S. peringueyi*. For example, the material examined in Mthethwa (2016) almost certainly consists of a mixed sample of both *S. heterodoxus* and *S. peringueyi*, since the specimens for morphological study were collected in Citrusdal and Hermanus. According to the distributional patterns discussed below, these collection localities make it very likely that both species were included. However, given the overall very similar, or seemingly identical shape of most examined morphological structures and the close evolutionary relationship of the two species, we do not expect that this combined interpretation could significantly impact results and conclusions of any of these phylogenetic studies. More care would need to be taken in assessing pollination networks, given that there may be disparity in host plant fidelity between the two species. Interestingly, the two species were confused early on: in one of the very first treatments of *S. heterodoxus* after Cockerell's description (Cockerell 1921), Brauns (1929) redescribed the species and illustrated the hindleg tibia based on a male specimen. The shape of the tibia, however, clearly corresponds to that of *S. peringueyi* (cf., Fig. 5A) and not of *S. heterodoxus*.

Figure 6. Distribution map of *Scrapter peringueyi* (Cockerell, 1921) and *Scrapter heterodoxus* (Cockerell, 1921) based on 133 examined specimens. If several specimens were collected at the same site, they are shown as a single occurrence.

Mapping the distributions of *S. peringueyi* and *S. heterodoxus* based on the 133 examined specimens reveals slightly different distribution patterns for the two species (Fig. 6). *Scrapter peringueyi* is a southern Cape coastal species, without any records north of the Cape Town area. All localities are in close proximity to the shoreline, without any records from inland regions. *Scrapter heterodoxus* in turn extends from Cape Town northwards up the south-western coast of South Africa, with most occurrences recorded from inland of the western coastline. The two species are sympatric in the Cape Town vicinity. Additionally, we recovered two isolated records for *S. heterodoxus*, one from the interior of the Eastern Cape (Katberg), and another one from Kakamas in the interior Northern Cape region. These records are particularly interesting as they significantly expand the distributional range of *S. heterodoxus*, but they also warrant further study: the surface sculpturing of these two specimens is slightly less rugulose than in the females from the Cape Town region, which is where the type locality is located. Additional study of specimens from the interior Northern and Eastern Cape regions is required to determine the degree of variation of this propodeal character and could possibly reveal additional, yet to be described species of the *S. heterodoxus* species group.

Acknowledgements

We thank Bryan N. Danforth (Cornell University) for providing us access to the specimens deposited in the Cornell University Insect Collection and Werner Strumpher (South African National Collection of Insects) for help in locating the type specimens. We thank the reviewers and the editorial team of African Invertebrates for their constructive feedback on the manuscript. This work was supported by U.S. National Science Foundation grants DEB-2127744 and DEB-0814544.

References

Alexander BA, Michener CD (1995) Phylogenetic studies of the families of short-tongued bees (Hymenoptera: Apoidea). The University of Kansas Science Bulletin 55: 377–424.

Almeida EAB, Danforth BN (2009) Phylogeny of colletid bees (Hymenoptera: Colletidae) inferred from four nuclear genes. Molecular Phylogenetics and Evolution 50(2): 290–309. https://doi.org/10.1016/j.ympev.2008.09.028

Almeida EAB, Pie MR, Brady SG, Danforth BN (2012) Biogeography and diversification of colletid bees (Hymenoptera: Colletidae): emerging patterns from the southern end of the world. Journal of Biogeography 39(3): 526–544. https://doi.org/10.1111/j.1365-2699.2011.02624.x

Almeida EAB, Packer L, Melo GAR, Danforth BN, Cardinal SC, Quinteiro FB, Pie MR (2019) The diversification of neopasiphaeine bees during the Cenozoic (Hymenoptera: Colletidae). Zoologica Scripta 48(2): 226–242. https://doi.org/10.1111/zsc.12333

Bankevich A, Nurk S, Antipov D, Gurevich AA, Dvorkin M, Kulikov AS, Lesin VM, Nikolenko SI, Pham S, Prjibelski AD, Pyshkin AV, Sirotkin AV, Vyahhi N, Tesler G, Alekseyev MA, Pevzner PA (2012) SPAdes: A new genome assembly algorithm and its applications to single-cell sequencing. Journal of Computational Biology 19(5): 455–477. https://doi.org/10.1089/cmb.2012.0021

Bossert S, Copeland RS, Sless TJL, Branstetter MG, Gillung JP, Brady SG, Danforth BN, Policarová J, Straka J (2020) Phylogenomic and morphological reevaluation of the bee tribes Biastini, Neolarrini, and Townsendiellini (Hymenoptera: Apidae) with description of three new species of *Schwarzia.* Insect Systematics and Diversity 4(6): 1–29. https://doi.org/10.1093/isd/ixaa013

Bossert S, Wood TJ, Patiny S, Michez D, Almeida EAB, Minckley RL, Packer L, Neff JL, Copeland RS, Straka J, Pauly A, Griswold T, Brady SG, Danforth BN, Murray EA (2021) Phylogeny, biogeography and diversification of the mining bee family Andrenidae. Systematic Entomology, 1–20. https://doi.org/10.1111/syen.12530

Branstetter MG, Danforth BN, Pitts JP, Faircloth BC, Ward PS, Buffington ML, Gates MW, Kula RR, Brady SG (2017) Phylogenomic insights into the evolution of stinging wasps and the origins of ants and bees. Current Biology 27(7): 1019–1025. https://doi.org/10.1016/j.cub.2017.03.027

Brauns H (1929) Neue und auffallende Apiden aus Süd-Afrika. Zeitschrift für wissenschaftliche Insektenbiologie 24: 130–143.

Cardinal S, Buchmann SL, Russell AL (2018) The evolution of floral sonication, a pollen foraging behavior used by bees (Anthophila). Evolution 72(3): 590–600. https://doi.org/10.1111/evo.13446

Cockerell TDA (1915) XXX.–Descriptions and records of bees.–LXVI. Annals and Magazine of Natural History (Ser 8) 15: 341–350. https://doi.org/10.1080/00222931508693649

Cockerell TDA (1916) LI.–Descriptions and records of bees.–LXXII. Annals and Magazine of Natural History (Ser 8) 17: 428–435. https://doi.org/10.1080/00222931608693809

Cockerell TDA (1921) XXV.–Descriptions and Records of Bees.–XC. Annals and Magazine of Natural History (Ser 9) 7: 201–212. https://doi.org/10.1080/00222932108632512

Cockerell TDA, Ireland LM (1933) The relationships of *Scrapter*, a genus of African bees. Proceedings of the National Academy of Sciences of the United States of America 19(11): 972–978. https://doi.org/10.1073/pnas.19.11.972

Davies GBP, Brothers DJ (2006) Morphology of *Scrapter* (Hymenoptera: Anthophila: Colletidae), with description of three new species and taxonomic status of five Cockerell taxa. African Invertebrates 47: 135–183.

Davies GBP, Eardley C, Brothers DJ (2005) Eight new species of *Scrapter* (Hymenoptera: Apoidea: Colletidae), with descriptions of *S. albifumus* and *S. amplispinatus* females and a major range extension of the genus. African Invertebrates 46: 141–179.

Eardley CD (1996) The genus *Scrapter* Lepeletier & Serville (Hymenoptera: Colletidae). African Entomology 4: 37–92.

Eardley CD, Kuhlmann M, Pauly A (2010) The bee genera and subgenera of sub-Saharan Africa. Abc Taxa 7: 1–139.

Edgar RC (2004) MUSCLE: Multiple sequence alignment with high accuracy and high throughput. Nucleic Acids Research 32(5): 1792–1797. https://doi.org/10.1093/nar/gkh340

Faircloth BC (2016) PHYLUCE is a software package for the analysis of conserved genomic loci. Bioinformatics 32(5): 786–788. https://doi.org/10.1093/bioinformatics/btv646

Friese H (1909) Die Bienen Afrikas nach dem Stande unserer heutigen Kenntnisse. In: Schultze, L (Ed.) Zoologische und Anthropologische Ergebnisse einer Forschungsreise im Westlichen und Zentralen Südafrika ausgeführt in den Jahren 1903–1905, Band 2. Denkschriften der Medizinisch-Naturwissenschaftlichen Gesellschaft zu Jena 14: 83–476. https://doi.org/10.5962/bhl.title.10343

Friese H (1912) Neue und wenig bekannte Bienen Süd-Afrikas. (Hym.). Archiv für Naturgeschichte 78A: 181–189.

Friese H (1913) II. Nachtrag zu 'Bienen Afrika'. Zoologische Jahrbücher 35: 581–598. https://doi.org/10.5962/bhl.part.16721

Goldblatt P, Manning JC, Nänni I (2009) New species of *Geissorhiza* (Iridaceae: Crocoideae) from the southern African winter rainfall zone, range extensions, taxonomic changes, and notes on pollen morphology and floral ecology. Bothalia 39(2): 123–152. https://doi.org/10.4102/abc.v39i2.240

Harris RA (1979) A glossary of surface sculpturing. Occasional Papers in Entomology, State of California Department of Food and Agriculture 28: 1–31.

Hausmann A, Haszprunar G, Hebert PD (2011) DNA barcoding the geometrid fauna of Bavaria (Lepidoptera): Successes, surprises, and questions. PLoS One 6(2): e17134. https://doi.org/10.1371/journal.pone.0017134

Hebert PDN, Ratnasingham S, de Waard JR (2003) Barcoding animal life: Cytochrome c oxidase subunit 1 divergences among closely related species. Proceedings of the Royal Society of London. Series B, Biological Sciences 270(Supplement): S96–S99. https://doi.org/10.1098/rsbl.2003.0025

Huang W, Xie X, Huo L, Liang X, Wang X, Chen X (2020) An integrative DNA barcoding framework of ladybird beetles (Coleoptera: Coccinellidae). Scientific Reports 10(1): 10063. https://doi.org/10.1038/s41598-020-66874-1

Kayaalp P, Stevens MI, Schwarz MP (2017) 'Back to Africa': Increased taxon sampling confirms a problematic Australia-to-Africa bee dispersal event in the Eocene. Systematic Entomology 42(4): 724–733. https://doi.org/10.1111/syen.12241

Kuhlmann M (2009) Patterns of diversity, endemism and distribution of bees (Insecta: Hymenoptera: Anthophila) in southern Africa. South African Journal of Botany 75(4): 726–738. https://doi.org/10.1016/j.sajb.2009.06.016

Kuhlmann M (2014) Revision of the "euryglossiform" species of the Afrotropical bee genus *Scrapter* Lepeletier & Serville, 1828 (Hymenoptera: Apoidea: Colletidae). European Journal of Taxonomy 95(95): 1–69. https://doi.org/10.5852/ejt.2014.95

Kuhlmann M, Eardley CD (2012) Pollen resources of non-*Apis* bees in southern Africa. In: Patiny S (Ed.) Evolution of Plant-Pollinator Relationships. Cambridge University Press, Cambridge, United Kingdom, 439–457. https://doi.org/10.1017/CBO9781139014113.017

Kuhlmann M, Friehs T (2020) Nine new species and new records of euryglossiform *Scrapter* Lepeletier & Serville (Hymenoptera: Colletidae) from South Africa. European Journal of Taxonomy 647(647): 1–33. https://doi.org/10.5852/ejt.2020.647

Kuhlmann M, Guo D, Veldtman R, Donaldson J (2012) Consequences of warming up a hotspot: Species range shifts within a centre of bee diversity. Diversity & Distributions 18(9): 885–897. https://doi.org/10.1111/j.1472-4642.2011.00877.x

Lepeletier de Saint Fargeau ALM, Audinet-Serville JG (1828) In: Diderot et al. (Eds) Encyclopedie Méthodique, Histoire Naturelle. Insectes, Vol. 10. Agasse, Paris, 345–832.

McGinley RJ (1981) Systematics of the Colletidae based on mature larvae with phenetic analysis of apoid larvae. University of California Publications in Entomology 91: 1–307.

Michener CD (1944) Comparative external morphology, phylogeny, and a classification of the bees (Hymenoptera). Bulletin of the American Museum of Natural History 82: 151–326.

Michener CD (1997) Genus-group names of bees and supplemental family-group names. Scientific Papers, Natural History Museum. The University of Kansas 1: 1–81. https://doi.org/10.5962/bhl.title.4052

Michener CD (2007) The Bees of the World. Second Edition. The Johns Hopkins University Press, Baltimore, Maryland, 953 pp.

Mthethwa QM (2016) The taxonomy and systematics of the bee genus *Scrapter* (Colletidae: Colletinae: Scraptrini). MSc dissertation: University of KwaZulu-Natal, 69 pp. https://researchspace.ukzn.ac.za/handle/10413/15817 [Accessed July 30, 2021]

Nneji LM, Adeola AC, Ayoola AO, Oladipo SO, Wang YY, Malann YD, Anyaele O, Nneji IC, Rahman MM, Olory CS (2020) DNA barcoding and species delimitation of butterflies (Lepidoptera) from Nigeria. Molecular Biology Reports 47(12): 9441–9457. https://doi.org/10.1007/s11033-020-05984-5

Oba Y, Ôhira H, Murase Y, Moriyama A, Kumazawa Y (2015) DNA Barcoding of Japanese Click Beetles (Coleoptera, Elateridae). PLoS One 10(1): e0116612. https://doi.org/10.1371/journal.pone.0116612

Packer L (2008) Phylogeny and classification of the Xeromelissinae (Hymenoptera: Apoidea, Colletidae) with special emphasis on the genus *Chilicola.* Systematic Entomology 33(1): 72–96. https://doi.org/10.1111/j.1365-3113.2007.00398.x

Plant JD, Paulus HF (2016) Evolution and phylogeny of bees – a review and a cladistic analysis in light of morphological evidence (Hymenoptera, Apoidea). Zoologica 161: 1–364.

Porto DS, Almeida EAB (2019) A comparative study of the pharyngeal plate of Apoidea (Hymenoptera: Aculeata), with implications for the understanding of phylogenetic relationships of bees. Arthropod Structure & Development 50: 64–77. https://doi.org/10.1016/j.asd.2019.04.002

Ratnasingham S, Hebert PDN (2013) A DNA-based registry for all animal species: the Barcode Index Number (BIN) system. PloS One 8(8): e66213. https://doi.org/10.1371/journal.pone.0066213

Sandhouse GA (1943) The type species of the genera and subgenera of bees. Proceedings of the United States National Museum 92(3156): 519–619. https://doi.org/10.5479/si.00963801.3156.519

Sheffield CS, Hebert PDN, Kevan PG, Packer L (2009) DNA barcoding a regional bee (Hymenoptera: Apoidea) fauna and its potential for ecological studies. Molecular Ecology Resources 9: 196–207. https://doi.org/10.1111/j.1755-0998.2009.02645.x

Shorthouse DP (2010) SimpleMappr, an online tool to produce publication-quality point maps. http://www.simplemappr.net [Accessed October 20, 2021]

Stahlhut JK, Fernández-Triana J, Adamowicz SJ, Buck M, Goulet H, Hebert PDN, Huber JT, Merilo MT, Sheffield CS, Woodcock T, Smith MA (2013) DNA barcoding reveals diversity of Hymenoptera and the dominance of parasitoids in a sub-arctic environment. BMC Ecology 13(1): 1–13. https://doi.org/10.1186/1472-6785-13-2

Tribe G (2007) Fruit crops: deciduous fruit in South Africa. African Pollinators Initiative (Producers) Crops, Browse and Pollinators in Africa: an Initial Stock-taking. Food and Agricultural Organization of the United Nations, Rome, Italy, 14–19.

Vachal J (1897) Éclaircissements sur de genre *Scrapter* et description d'une espèce nouvelle de *Dufourea*. Bulletin de la Société Entomologique de France 1897: 61–64. http://dx.doi.org/10.3406/bsef.1897.21997

Supplementary material 1

Multiple sequence alignment of the examined species of *Scrapter*

Authors: Silas Bossert

Data type: multiple sequence alignment

Explanation note: Multiple sequence alignment of the *Scrapter heterodoxus* and *Scrapter peringueyi* sequences analyzed in the present study. The alignment file is in Fasta format.

Link: https://doi.org/10.3897/AfrInvertebr.63.76934.suppl1

Supplementary material 2

Specimen metadata

Authors: Simon van Noort, Silas Bossert

Data type: occurences

Explanation note: Specimen metadata for the 133 examined specimens in Darwin Core format.

Link: https://doi.org/10.3897/AfrInvertebr.63.76934.suppl2

African Invertebrates 63(1): 19–75 (2022)
doi: 10.3897/AfrInvertebr.63.76309
https://africaninvertebrates.pensoft.net

RESEARCH ARTICLE

African Invertebrates
A journal of biodiversity research

Taxonomic revision of the mydas-fly genera *Eremohaplomydas* Bequaert, 1959, *Haplomydas* Bezzi, 1924, and *Lachnocorynus* Hesse, 1969 (Insecta, Diptera, Mydidae)

Claire Boschert[1], Torsten Dikow[2]

1 *Rice University, Houston, TX, USA* **2** *Department of Entomology, National Museum of Natural History, Smithsonian Institution, 10th Street and Constitution Avenue NW, Washington, DC 20560, USA*

Corresponding author: Torsten Dikow (DikowT@si.edu)

Academic editor: John Midgley | Received 8 October 2021 | Accepted 1 March 2022 | Published 25 March 2022

http://zoobank.org/F849C700-225A-4923-AE19-62882F933E83

Citation: Boschert C, Dikow T (2022) Taxonomic revision of the mydas-fly genera *Eremohaplomydas* Bequaert, 1959, *Haplomydas* Bezzi, 1924, and *Lachnocorynus* Hesse, 1969 (Insecta, Diptera, Mydidae). African Invertebrates 63(1): 19–75. https://doi.org/10.3897/AfrInvertebr.63.76309

Abstract

The genera *Eremohaplomydas* Bequaert, 1959, *Haplomydas* Bezzi, 1924, and *Lachnocorynus* Hesse, 1969 (Diptera: Mydidae: Syllegomydinae) are revised. Currently, four species are known from southern Africa, *i.e.*, *Eremohaplomydas desertorum* Bequaert, 1959 from north-western Namibia, *Haplomydas crassipes* Bezzi, 1924 widespread in southern Africa, *Lachnocorynus chobeensis* Hesse, 1969 from northern Botswana, and *Lachnocorynus kochi* Hesse, 1969 from northern Namibia. Four new species, *Eremohaplomydas gobabebensis* **sp. nov.** and *Eremohaplomydas whartoni* **sp. nov.** from the central Namib desert of Namibia, *Eremohaplomydas stomachoris* **sp. nov.** from the northern Namib desert in Namibia, and *Lachnocorynus stenocephalus* **sp. nov.** from north-eastern Zimbabwe are described. *Lachnocorynus kochi* is synonymized with *Lachnocorynus chobeensis*. Distribution, biology, occurrence in biodiversity hotspots *sensu* Conservation International and seasonal imago flight activity are discussed. Descriptions/redescriptions, photographs, specimen occurrence data, and identification keys (both dichotomous and matrix-based) to species are provided and made openly accessible in data repositories to support and accelerate future studies of the included taxa. An updated identification key to the Mydidae genera of the Afrotropical Region is provided. The placement of the three genera in the subfamily taxon Syllegomydinae is discussed and several morphological features, such as an extremely reduced proboscis in some species, a unique wing venation in *Eremohaplomydas gobabebensis* **sp. nov.**, and the unique metathoracic coxa, are discussed.

Keywords

Afrotropical, cybertaxonomy, Karoo, Mydas flies, Namib Desert, open-access

Introduction

The Mydidae fauna of southern Africa is the most diverse and richest in the world with 179 (37%) of 480 species world-wide occurring in this region south of the Kunene and Zambesi rivers (Botswana, Mozambique, Namibia, South Africa, and Zimbabwe; no records exist for Eswatini (Swaziland) and Lesotho) alone (Hesse 1969; Dikow 2017). At the generic level, this diversity is similarly striking as 20 of the 38 genera in the Afrotropics, of the 66 genera in the world, are endemic to southern Africa. This revision aims to review the three small and rarely collected southern African endemic genera *Eremohaplomydas* Bequaert, 1959, *Haplomydas* Bezzi, 1924, and *Lachnocorynus* Hesse, 1969 and describe four new species.

This study was instigated by the discovery of yet undescribed species of *Eremohaplomydas* from Namibia, including the discovery of a species by Wharton (1982), and *Lachnocorynus* from Zimbabwe in several natural history collections and by the collection of an undescribed species of *Eremohaplomydas* in Namibia in 2018 (Figs 1–3).

The three genera *Eremohaplomydas*, *Haplomydas*, and *Lachnocorynus* are here revised together as they share a number of morphological features that could provide evidence for a close phylogenetic relationship. Most strikingly, all three genera exhibit a distinctly clubbed metathoracic femur (Figs 20, 36, 42), the metathoracic tibia is arched medially and a distinct ventral keel is developed (Fig. 20), the metathoracic coxa and the metakatepisternum are developed in a unique fashion that allows the metathoracic leg to be moved laterally (Figs 53–55), and wing cell r_5 is open (Fig. 40).

The taxonomic history of the three genera can be summarized as follows:

Bezzi (1924) described the genus *Haplomydas* with its type species *Haplomydas crassipes* Bezzi, 1924 from Bulawayo in south-western Zimbabwe.

Brunetti (1929) described *Rhopalia flavomarginata* Brunetti, 1929 from Matopos south of Bulawayo in Zimbabwe.

Séguy (1929) described the genus *Heleomydas* with its type species *Heleomydas lesnei* Séguy, 1929 from Nova Chupanga on the banks of the Zambesi River in central Mozambique.

Bequaert (1959) described the genus *Eremohaplomydas* with its type species *Eremohaplomydas desertorum* Bequaert, 1959 from the Namib Desert in north-western Namibia.

Bequaert (1963) synonymized *Rhopalia flavomarginata* with *Haplomydas crassipes* as well as *Heleomydas* with *Haplomydas* resulting in the synonymy of *Heleomydas lesnei* with *Haplomydas crassipes*.

Hesse (1969) described the genus *Lachnocorynus* with its type species *Lachnocorynus chobeensis* Hesse, 1969 from the Chobe River at Kabulabula in northern-most Botswana and *Lachnocorynus kochi* Hesse, 1969 from Oshikango in northern-most Namibia. He furthermore provided a key to all southern African Mydidae genera.

Bowden (1980) catalogued the following species: *Haplomydas crassipes* with both *Rhopalia flavomarginata* and *Heleomydas lesnei* as junior synonyms, *Eremohaplomydas desertorum*, *Lachnocorynus chobeensis*, and *Lachnocorynus kochi*.

Wharton (1982) reviewed the Mydidae species of the central Namib Desert, Namibia and recorded an undescribed species of *Eremohaplomydas* active on the gravel plains in May and provided some biological information on this species.

Dikow (2017) provided a review of the Afrotropical Mydidae with an updated key to the genera including *Eremohaplomydas*, *Haplomydas*, and *Lachnocorynus*.

At the commencement of this study the three genera included here were, therefore, known from four species: *E. desertorum*, *H. crassipes*, *L. chobeensis*, and *L. kochi*.

Materials and methods

Morphological features were examined using an Olympus SZ60 and a Zeiss SteREO Discovery.V12 stereo microscopes. Wing length is measured from the tegula to the distal tip of the wing. The female and male terminalia were first excised and macerated in 10% potassium hydroxide (KOH) at 55 °C followed by neutralization in acetic acid (glacial, CH_3COOH) and rinsing in distilled water (H_2O). They were temporarily stored in 75% ethanol (C_2H_5OH) for examination and photography and eventually sealed in polyethylene vials containing 100% glycerine (C_3H_8O) and attached to the specimen's pin.

Terminology

Terminology follows Dikow (2009), Cumming and Wood (2017), and Dikow (2017, general morphology and abbreviations for setae), Stuckenberg (1999, antennae), and Wootton and Ennos (1989, wing venation). Setae are abbreviated as follows: **dc** = discal setae, **acr** = acrostichal setae, **npl** = notopleural setae, **spal** = supra-alar setae, **pal** = post-alar setae. Abdominal tergites are abbreviated in the descriptions with 'T', and sternites

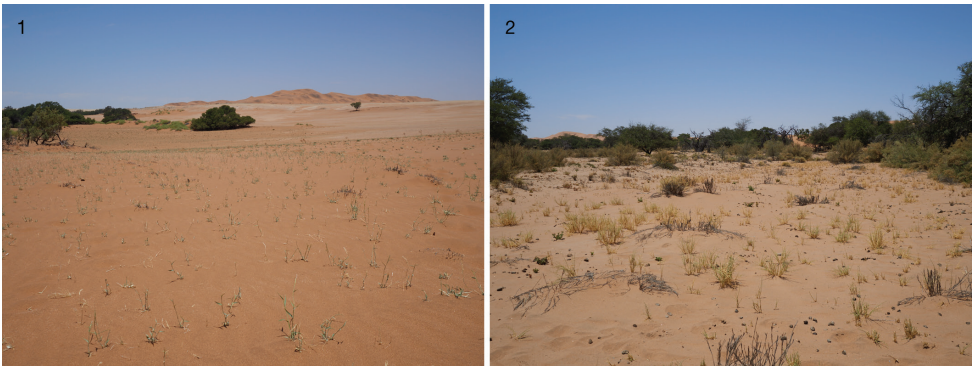

Figures 1–2. Habitat photographs where *Eremohaplomydas gobabebensis* sp. nov. was observed and collected: **1** sparsely vegetated small sand dune West of Kuiseb riverbed at Gobabeb, Namibia (23°33'50"S, 015°01'59"E, note grass *Centropodia glauca* in foreground), taken on 23 Nov 2018 (Zenodo https://doi.org/10.5281/zenodo.6263467) **2** margin of dry Kuiseb riverbed, 20 km NW on D1983 of Gobabeb, Namibia (23°24'56"S, 014°54'43"E, note grass *Cladoraphis spinosa* in foreground), taken on 24 Nov 2018 (https://doi.org/10.5281/zenodo.6263266). Photographs by T. Dikow.

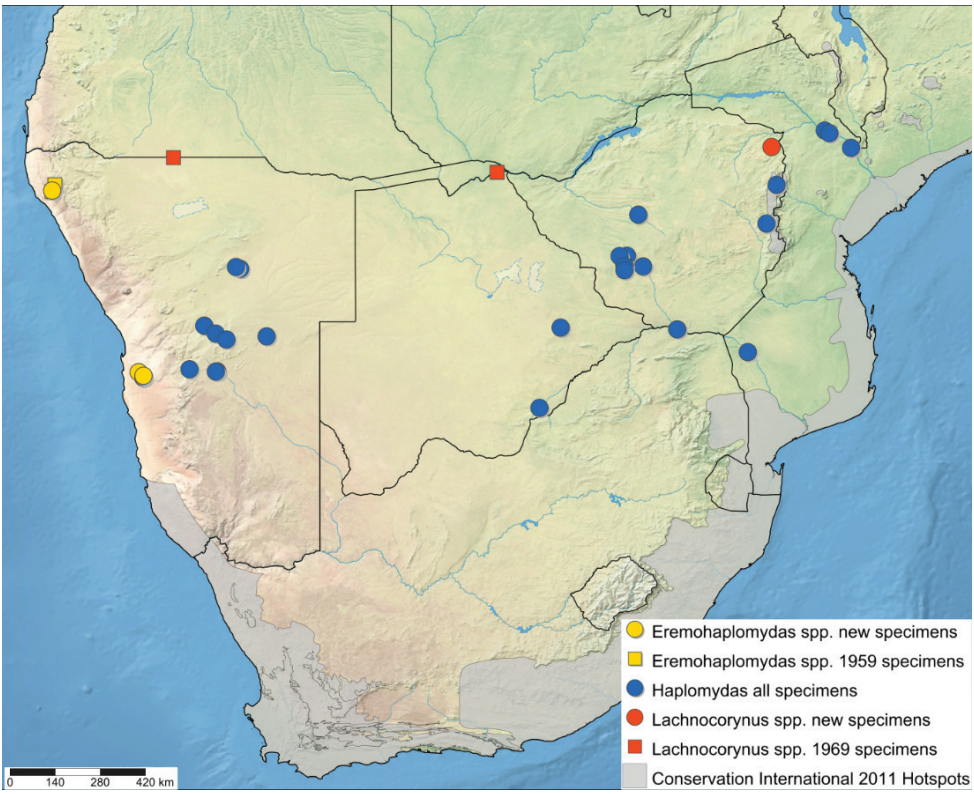

Figure 3. Map of southern Africa with elevational relief and biodiversity hotspots (*sensu* Conservation International in grey) and distribution of *Eremohaplomydas*, *Haplomydas*, and *Lachnocorynus* specimens studied in respective most recent review and now (SimpleMappr https://www.simplemappr.net/map/14084). Distribution and occurrence data available in Google Earth KML file https://www.simplemappr.net/map/14084.kml and also through GBIF (data-set https://www.gbif.org/dataset/993875DD-5915-4107-8707-835D5A8D1022, DOI https://doi.org/10.15468/awpjz9).

are abbreviated with 'S'. The terms prothoracic, mesothoracic, and metathoracic are abbreviated 'pro', 'mes', and 'met', respectively. The term pubescence (adjective pubescent) refers to the short, fine microtrichia densely covering certain body parts. Other generalized terms follow the Torre-Bueno Glossary of Entomology (Nichols 1989).

Species descriptions and re-descriptions

Species descriptions are based on composites of all specimens and not exclusively on the holotype and are compiled from a character matrix of 196 features and 496 character states assembled with Lucid Builder (version 4.0.10) and eventually exported as natural-language descriptions. These species descriptions have been deposited in the Zenodo data depository and can be accessed in XML-format following the SDD (Structure of Descriptive Data) standard. All taxon names have been registered in ZooBank (Pyle and Michel 2008). If available, permanent URLs or Digital Object Identifiers (**DOIs**) to the original species

descriptions on the Biodiversity Heritage Library (**BHL**, www.biodiversitylibrary.org) or other online sources are provided. The species record for each species at the Global Biodiversity Information Facility (**GBIF**, www.gbif.org) provides a summary of occurrence data, images, or taxonomic treatments from natural history collections. Some previous taxon descriptions have been marked-up in TaxonX XML language (Catapano 2010) and uploaded to the Plazi TreatmentBank (http://plazi.org/treatmentbank/) from where they are accessible in human- and machine-readable formats and a permanent URL provided.

Specimen occurrence data

The following data on species occurrences are given (where available): country, state/province, county, locality, geographic co-ordinates (formatted in both degrees minutes seconds and decimal latitude/longitude for type localities), elevation (in meters), date of collection (format: yyyy-mm-dd), time of day at collection, habitat information, sampling protocol (if other than hand netting), collector, catalog number (a unique specimen identifier and any other identifying number), depository (institution code), number of specimens, sex, life stage, name of person who identified the specimen, and any other previous identifications. Each specimen is listed with a unique specimen identifier (either an institutional catalog number or an AAM-XXXXXX number used by the junior author) that will allow the re-investigation as well as provide a unique Life Science Identifier (**LSID**). The occurrence of all species is illustrated in distribution maps plotted with SimpleMappr (http://www.simplemappr.net; Shorthouse 2010) with all of those localities for which co-ordinates are available or could be gathered from online gazetteers or Google Earth. Type localities are plotted with a square symbol while all other specimens are plotted with a circular symbol. The distribution maps include Biodiversity Hotspots *sensu* Conservation International (Mittermeier et al. 1998; Myers et al. 2000; Mittermeier et al. 2005). The specimen occurrence data are deposited as a Darwin Core Archive (**DwC-A**) at GBIF using the Integrated Publishing Toolkit (**IPT**) at the NMNH. Annual rainfall and temperature averages for geographically restricted species were obtained from either World Weather Information Service (https://worldweather.wmo.int) or World Weather Online (www.worldweatheronline.com).

Photographs and illustrations

Whole habitus photographs of pinned specimens were taken with a GIGAmacro Magnify^2 system, a Canon EOS D5 Mark IV full-frame DSLR, a Canon MP-E 65 mm f2.8 macro-lens, and illuminated by a twin-flash. Some whole habitus photographs were taken using a Visionary Digital Passport II system (base and StackShot only), an Olympus OM-D E-M5 Micro 4/3 camera, a 60 mm f2.8 macro lens (equivalent to 120 mm focal length in 35 mm photography), and illuminated with a Falcon FLDM-i200 LED dome-light for even and soft light. Photographs of the female and male terminalia were taken on a Zeiss SteREO Discovery.V12 stereo microscope with a PlanApo S 1.0× lens at 50–75× magnification and an attached Olympus OM-D E-M1 MicroFourThirds digital camera. The dissected terminalia were placed in 75%

ethanol in a glass dish and illuminated by a Schott VisiLED light source utilizing mixed bright-field (dorsal), dark-field (lateral), and transillumination (ventral). The MicroFourThirds camera was tethered to a laptop and controlled by Olympus Capture software (version 2.2.1) and the vertical movement for obtaining photographs for later image stacking was done manually using the fine drive. Individual RAW-format images were stacked using HeliconFocus Pro (version 7.+) and exported in Adobe DNG-format. All photographs have been deposited in full-resolution in both tif-format and RAW dng-format at Zenodo in the Biodiversity Literature Repository (BLR, http://zenodo.org/communities/biosyslit) community and the individual photo and specimen DOIs are included in the figure captions for access and downloading.

Keys

The online, interactive dichotomous key and the multi-access, matrix-based key have been built with Lucid Builder (version 4.0.10) and both can be accessed on Lucidcentral and the junior author's research web-site.

Institutions providing specimens

Institutions providing specimens are listed below, together with the abbreviations used in the text when citing depositories (institutionCode), a link to the record in the Global Registry of Scientific Collections (**GRSciColl**, https://www.gbif.org/grscicoll), and the people who kindly assisted (some no longer working at these institutions):

AMGS Albany Museum, Grahamstown, Eastern Cape, South Africa (S. Gess, F. Gess) https://www.gbif.org/grscicoll/institution/8F04EE40-D146-4B05-82B2-E31D08381EB4;

AMNH American Museum of Natural History, New York City, New York, USA (D. Grimaldi) https://www.gbif.org/grscicoll/institution/DC02E848-9E1F-4DD0-8078-2EB60620D39B;

BMSA National Museum, Bloemfontein, Free State, South Africa (A. Kirk-Spriggs, B. Muller) https://www.gbif.org/grscicoll/institution/55BD4595-00F6-448A-BD54-34B16A40412B;

CAS California Academy of Sciences, San Francisco, California, USA (N. Penny, M. Trautwein) http://biocol.org/urn:lsid:biocol.org:col:15690;

CSCA California State Collection of Arthropods, Sacramento, California, USA (M. Hauser) https://www.gbif.org/grscicoll/institution/E4829E9C-D657-4AC0-B26E-D659AD09D4CB;

MNHN Museum national d'Histoire naturelle, Paris, France (C. Daugeron, E. Delfosse) https://www.gbif.org/grscicoll/institution/CC3E1F45-E430-4835-951E-4DD33C4B7201;

MZLU Museum of Zoology, Lund University, Lund, Sweden (R. Danielsson) https://www.gbif.org/grscicoll/institution/13EDC77B-7023-4DDD-89C7-D883A480B294;

NHMUK The Natural History Museum, London, UK (E. McAlister) https://www.gbif.org/grscicoll/institution/1D808A7C-1F9E-4379-9616-EDB749ECF10E;

NHMW Naturhistorisches Museum, Wien, Austria (P. Sehnal) https://www.gbif.org/grscicoll/institution/08EA694E-0C7F-446F-B1C2-BB7B1ED6FBAC;

NMBZ Natural History Museum of Zimbabwe, Bulawayo, Bulawayo, Zimbabwe (D. Madamba) https://www.gbif.org/grscicoll/institution/EC9F47D3-BCB0-4262-96DB-6F2AC529872B;

NMNW National Museum of Namibia, Windhoek, Khomas, Namibia (F. Becker) https://www.gbif.org/grscicoll/institution/827515F9-6AB3-4ED9-B825-7AFD7181BEA7;

NMSA KwaZulu-Natal Museum, Pietermaritzburg, KwaZulu-Natal, South Africa (B. Muller, T. Pillay, K. Williams) https://www.gbif.org/grscicoll/institution/F7612BDF-65B0-4B26-A734-7494A5E6CE85;

RBINS Royal Belgian Institute of Natural Sciences, Brussels, Belgium (P. Grootaert) https://www.gbif.org/grscicoll/institution/C2BFDEEF-9C03-435E-8465-C483DADD6995;

SAMC Iziko South African Museum, Cape Town, Western Cape, South Africa (M. Cochrane) https://www.gbif.org/grscicoll/institution/ACE2B65E-D36F-4727-84D5-6FFE047C4BF2;

SANC South African National Collection of Insects, Pretoria, Gauteng, South Africa (R. Urban) https://www.gbif.org/grscicoll/institution/C1681A5E-61EA-491A-9340-910F76546022;

SDEI Senckenberg Deutsches Entomologisches Institut, Müncheberg, Brandenburg, Germany (F. Menzel) https://www.gbif.org/grscicoll/institution/2796E2F5-C160-4E3C-942F-D6D64AB8465F;

SNSB-ZSM Zoologische Staatssammlung, München, Bayern, Germany (M. Kotrba) http://grscicoll.org/institution/zoologische-staatssammlung;

USNM United States National Museum, Smithsonian Institution, Washington, DC, USA https://www.gbif.org/grscicoll/institution/586ee56e-b0fe-4dff-b7f9-aeb104f3308a.

Data resources

GBIF: specimen occurrence data-set – http://www.gbif.org/dataset/993875DD-5915-4107-8707-835D5A8D1022 – DOI https://doi.org/10.15468/awpjz9.

Lucid Builder: illustrated, multi-entry, matrix-based identification key – http://keys.lucidcentral.org/keys/v4/eremohaplomydas-matrix (archived in SDD format at Zenodo – DOI https://doi.org/10.5281/zenodo.6320960).

Lucid Builder: illustrated, dichotomous, pathway identification key – https://keys.lucidcentral.org/keys/v4/eremohaplomydas-dichotomous (archived in SDD format at Zenodo – DOI https://doi.org/10.5281/zenodo.6320934).

Lucid Builder: illustrated, dichotomous, pathway identification key to Afrotropical Mydidae genera v2 – https://keys.lucidcentral.org/keys/v4/Afrotropical-Mydidae-genera-dichotomous (archived in SDD format at Zenodo – DOI https://doi.org/10.5281/zenodo.5295621).
Plazi TreatmentBank taxon treatments:
Bequaert 1959 – http://tb.plazi.org/GgServer/summary/FFEFFFD55963FFF0FFE3FFE9FFBEFFB3

SimpleMappr: distribution maps – https://www.simplemappr.net/map/14084?width=1000&height=750&legend=true (as in Fig. 3; Google Earth KML file http://www.simplemappr.net/map/14084.kml); https://www.simplemappr.net/map/14089?width=1000&height=750&legend=true (as in Fig. 56; Google Earth KML file http://www.simplemappr.net/map/14089.kml); https://www.simplemappr.net/map/14090?width=1000&height=750&legend=true (as in Fig. 57; Google Earth KML file http://www.simplemappr.net/map/14090.kml).

Zenodo: natural-language species descriptions from Lucid Builder 4.0 in SDD format – DOI https://doi.org/10.5281/zenodo.5139987.

Zenodo BLR: full-resolution specimen photographs – DOI https://doi.org/10.5281/zenodo.6115471.

ZooBank new nomenclatorial acts: http://zoobank.org/F849C700-225A-4923-AE19-62882F933E83.

Taxonomy

***Eremohaplomydas* Bequaert, 1959**
http://zoobank.org/F170BC4E-DC90-4903-8836-53E3B693CB13
GBIF https://www.gbif.org/species/1591415
Plazi TreatmentBank http://treatment.plazi.org/id/03D687AD-5962-FFF1-FDA9-FB4AF93AF63F

Eremohaplomydas Bequaert, 1959: 357. Type-species: *Eremohaplomydas desertorum* Bequaert, 1959, by monotypy.

Diagnosis. The genus can be delineated by the very small to minute proboscis, the costal vein terminating at the point where R_1 joins the wing margin, the small body size of the majority of species, and the restricted distribution in the Namib Desert.

Distribution, biodiversity hotspots, phenology, and biology. Known only from five disjunct localities in the northern and central Namib Desert in Namibia (Figs 56–57) to which the genus is endemic. A rarely collected genus known only from 18 specimens in museum collections from nine collecting events between 1951–2018 (Table 1). The genus is not known to occur in any currently recognized biodiversity hotspot. Adult flies are either active in early summer or mid-autumn to early winter (Table 2). Nothing is known of the biology.

Table 1. Collecting event summary for *Eremohaplomydas*, *Haplomydas*, and *Lachnocorynus* species.

Species	# specimens	#♀/#♂	# collecting events	earliest collection	most recent collection	iNaturalist observation
E. desertorum	3	1/2	2	1951	1951	–
E. gobabebensis sp. nov.	7	0/7	3	2018	2018	–
E. stomachoris sp. nov.	1	1/0	1	1970	1970	–
E. whartoni sp. nov.	7	2/5	4	1979	1979	–
summary	18	4/14	9	1951	2018	
L. chobeensis	4	1/3	3	1930	1948	2019
L. stenocephalus sp. nov.	1	0/1	1	1986	1986	–
summary	4	1/3	3	1930	1986	2019
H. crassipes	67	22/44	25	1917	1999	–
summary total	89	27/60	37	1917	2018	2019

Table 2. Seasonal imago flight activity of *Eremohaplomydas*, *Haplomydas*, and *Lachnocorynus* species through number of specimens collected and unique collecting events in each month (data given as # specimens/# collecting events). Months abbreviated starting with July. * = iNaturalist observation.

species	Jul	Aug	Sep	Oct	Nov	Dec	Jan	Feb	Mar	Apr	May	Jun
E. desertorum	-	-	-	-	-	-	-	-	-	-	-	3/2
E. gobabebensis sp. nov.	-	-	-	-	7/3	-	-	-	-	-	-	-
E. whartoni sp. nov.	-	-	-	-	-	-	-	-	-	-	7/4	-
E. stomachoris sp. nov.	-	-	-	-	-	-	-	-	-	-	1/1	-
L. chobeensis	3/2	-	-	-	-	-	-	-	-	-	-	1/1*
L. stenocephalus sp. nov.	-	1/1	-	-	-	-	-	-	-	-	-	-
H. crassipes	-	-	-	-	-	-	-	3/1	19/9	35/9	7/7	-
total	3/2	1/1	-	-	7/3	-	-	3/1	19/9	35/9	15/10	4/3

Eremohaplomydas desertorum Bequaert, 1959

http://zoobank.org/DD434890-73C0-429E-AE09-670889346232
GBIF https://www.gbif.org/species/1591416
Plazi TreatmentBank http://treatment.plazi.org/id/03D687AD-5962-FFF7-FFD5-F63AFEF3F788
Figs 4–9, 56

Diagnosis. The species is distinguished from congeners by the overall brown colouration, the greatly expanded metathoracic femora, the apubescent abdominal tergites 3–8 in females, and the restricted distribution in the northern Namib Desert.

Description. Female. ***Head*****:** black, facial gibbosity brown, in general grey to light brown pubescent, white setose, regular, cylindrical setae; width distinctly greater than thorax (at postpronotal lobe), interocular distance on vertex same as at ventral eye margin; vertex between compound eyes ± horizontally straight, medially only slightly below dorsal eye margin, vertex light brown pubescent, white setose; ocellar triangle apubescent; facial gibbosity distinct, well-developed and discernible in lateral view, mystax covering entire facial gibbosity, white; parafacial area approximately as wide as ¾ width of central gibbosity (at same level); frons not elevated, light brown pubescent, white setose; occiput grey pubescent, yellowish to light brown setose, median

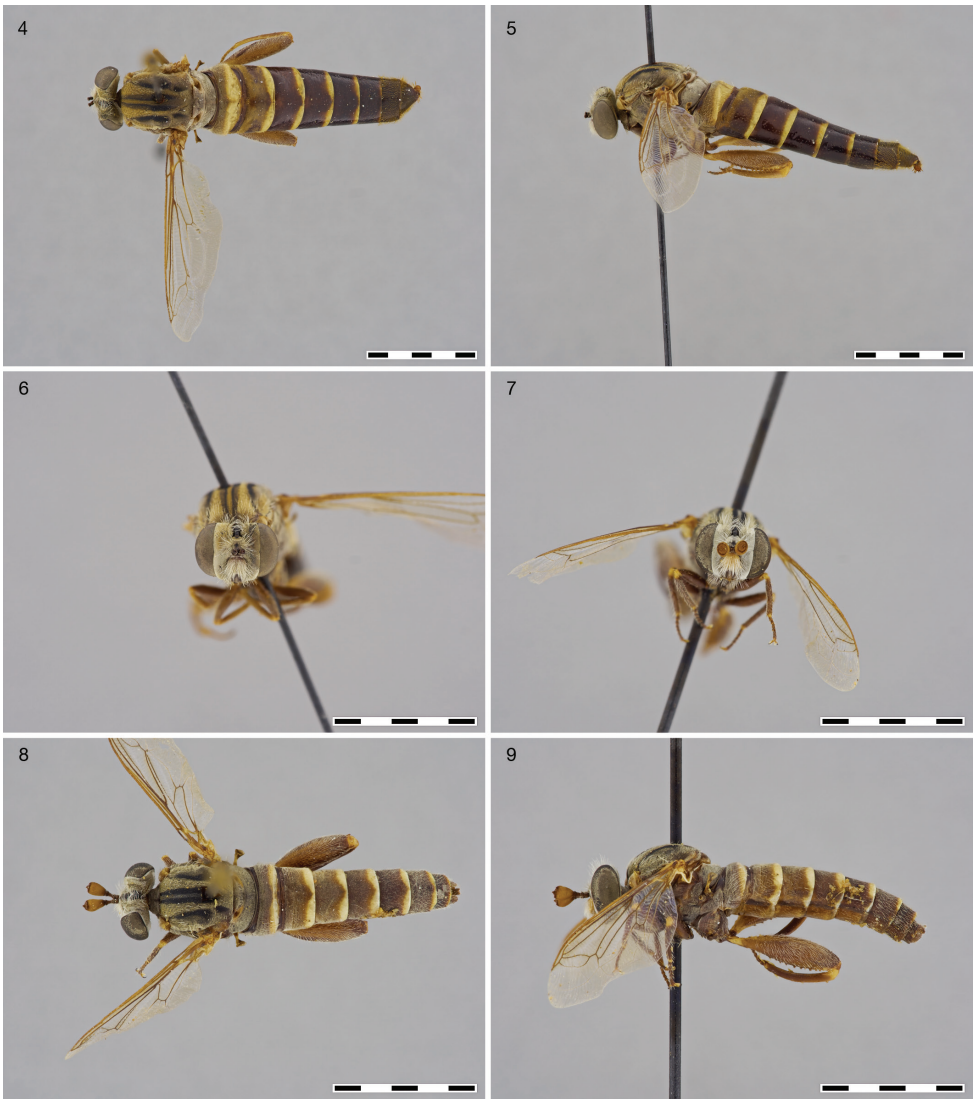

Figures 4–9. *Eremohaplomydas desertorum*: **4** ♀ holotype (MZLU-2143:1, Zenodo https://doi.org/10.5281/zenodo.6083924), dorsal (https://doi.org/10.5281/zenodo.6083955) **5** same, lateral (https://doi.org/10.5281/zenodo.6083957) **6** same, head anterior (https://doi.org/10.5281/zenodo.6083959) **7** ♂ paratype (MZLU-2143:2, https://doi.org/10.5281/zenodo.6083926), head anterior (https://doi.org/10.5281/zenodo.6083965) **8** same, dorsal (https://doi.org/10.5281/zenodo.6083961) **9** same, lateral (https://doi.org/10.5281/zenodo.6083963). Scale bars: 5 mm.

occipital sclerite yellowish macrosetose; pocl macrosetae absent; postgena sparsely grey pubescent, long, sparsely white setose; clypeus comprised of single sclerite, entirely sclerotized medially, flat to protruding (convex) ventrally, ventrally expanded, anterior to proboscis (almost covering it), laterally connected to face by sclerotized cuticle; proboscis very short, vestigial, knob-like, brown; labellum indiscernible,

length indiscernible, sclerotization indiscernible; maxillary palpus cylindrical, brown, longer than proboscis.

***Antenna*:** brown; scape white setose dorsally, asetose ventrally; pedicel white setose dorsally and ventrally; postpedicel indiscernible (broken).

***Thorax*:** dark brown, predominantly light brown pubescent; scutum uniformly black, surface microrugose (slightly rugose 'imitating' pubescence), predominantly light brown pubescent, broad sublateral stripes (interrupted by transverse suture) and narrow paramedian stripes merging postsuturally and not reaching posterior margin apubescent, scutal setation comprised of long white to yellow setae in pubescent areas; dc setae presuturally white, postsuturally absent, acr setae absent, lateral scutal setae white, npl setae 0, spal setae 0, pal setae 0; proepisternum apubescent medially, grey pubescent laterally, long yellowish macrosetose; proepimeron grey pubescent, asetose, antepronotum antero-medially smooth (without any indentation); lateral postpronotum short yellowish setose; postpronotal lobe yellow, white pubescent, short yellowish setose; scutellum light brown pubescent, discal scutellar setae absent, apical scutellar setae absent; mesopostnotum light brown pubescent, asetose; anatergite light brown pubescent, asetose; katatergite light brown pubescent, long white setose, elevated and smoothly convex; anepisternum light brown pubescent, anteriorly asetose, posteriorly asetose, otherwise asetose; katepisternum light brown pubescent, asetose; anepimeron light brown pubescent, single long yellowish seta dorso-medially; katepimeron light brown pubescent, asetose; meron light brown pubescent, asetose; metakatepisternum large; metanepisternum light brown pubescent, asetose; metepimeron brown (same color as T1), light brown pubescent, short white setose, ± flat, infra-halter sclerite absent.

***Legs*:** light brown to brown, setation comprised of white setae, yellow macrosetae; pro coxa sparsely grey pubescent, long yellowish macrosetose; mes coxa sparsely grey pubescent, long yellowish macrosetose; met coxa laterally unsclerotized (membrane between coxa and metakatepisternum clearly visible), sparsely grey pubescent, long yellowish macrosetose; met trochanter sparsely setose medially; pro + mes femur brown, met femur brown, distinctly clubbed for nearly entire length, macrosetose with thickened spine-like macrosetae on protuberances in 1 antero-ventral and 1 postero-ventral rows, 2–3 macrosetae distally in anterior row, postero-ventrally long white, appressed setose; pro tibia straight; mes tibia straight; met tibia laterally arched, met tibia cylindrical with distinct ventral keel terminating into distinct spur, macroseta at tip of spur, almost reaching tip of 1st tarsomere, postero-laterally short white, appressed setose; pro + mes tarsomere 1 approximately as long as individual tarsomeres 2, 3, or 4, met tarsomere 1 as long as individual tarsomeres 2, 3, or 4; pulvillus reduced, ½ length of well-developed claw; setiform empodium absent.

***Wing*:** length = 9.9 mm; slightly brown stained throughout, veins brown, microtrichia absent; cells r_1, r_4, m_3, + cua closed, r_5 open; C terminating at junction with R_1; Sc long, terminating in C proximal to r-m; R_4 terminates in R_1; R_5 terminates in R_1; auxiliary vein (R_3) at base of R_4 absent; R_4 and R_5 widest apart medially; r-m distinct, R_{4+5} and M_1 apart, connected by crossvein; M_1 straight at r-m (not curving anteriorly), M_1 (or M_1+M_2) terminates in C; base of M_3+M_4 present, M_3+M_4 not terminating together in C (not reaching wing margin), M_4 and CuA split proximally to m-cu (cell m_3

narrow proximally); CuP straight, cell cup wide, CuP and wing margin further apart proximally than distally; alula entirely reduced (nearly straight wing margin); halter light brown, pubescent, dorsally asetose, ventrally yellow setose.

***Abdomen*:** brown, setation comprised of scattered short white setae, T2–4 parallel-sided and not constricted waist-like, T surface entirely smooth; T1–6 dark brown with light yellow posterior margin narrowest medially, T7 dark brown; T1–2 sparsely grey pubescent, T3–7 apubescent; T1–7 short white setose; S1–7 brown; S apubescent; S1–7 sparsely short white setose; bullae on T2 oval, small, yellow, surface entirely smooth, T2 surface anterior to bullae smooth.

♀ abdomen and genitalia: densely arranged anteriorly directed setae present on T7–8 and S7–8; T8 anterior apodeme indiscernible (not dissected), auxiliary spiracle indiscernible (not dissected); T9 formed by wide, rectangular sclerite with median protuberance; T9+10 entirely fused (sclerites indistinguishable), T10 divided into 2 heavily sclerotized acanthophorite plates; 6 acanthophorite spines per plate.

Male. *Head*: black, facial gibbosity yellow, in general densely grey pubescent, white setose, regular, cylindrical setae; width distinctly greater than thorax (at postpronotal lobe), interocular distance on vertex same as at ventral eye margin; vertex between compound eyes ± horizontally straight, medially only slightly below dorsal eye margin, vertex grey pubescent, white setose; ocellar triangle apubescent; facial gibbosity distinct, well-developed and discernible in lateral view, mystax covering entire facial gibbosity, white; parafacial area approximately as wide as ¾ width of central gibbosity (at same level); frons not elevated, grey pubescent, white setose; occiput grey pubescent, white setose, median occipital sclerite yellowish macrosetose; pocl macrosetae absent; postgena sparsely grey pubescent, long, sparsely white setose; clypeus comprised of single sclerite, entirely sclerotized medially, flat to protruding (convex) ventrally, ventrally expanded, anterior to proboscis (almost covering it), laterally connected to face by sclerotized cuticle; proboscis very short, vestigial, knob-like, brown; labellum indiscernible, length indiscernible, sclerotization indiscernible; maxillary palpus cylindrical, brown, longer than proboscis.

***Antenna*:** brown; scape white setose dorsally, asetose ventrally; pedicel white setose dorsally and ventrally; postpedicel cylindrical in proximal ⅓, symmetrically bulbous in distal 2/3, ≥ 3.0 times as long as combined length of scape and pedicel, asetose; apical seta-like sensory element situated apically in cavity on postpedicel.

***Thorax*:** dark brown, predominantly grey pubescent; scutum uniformly black, surface microrugose (slightly rugose 'imitating' pubescence), predominantly grey pubescent, broad sublateral stripes (interrupted by transverse suture) and narrow paramedian stripes merging postsuturally and not reaching posterior margin apubescent, scutal setation comprised of long white to yellow setae in pubescent areas; dc setae presuturally white, postsuturally absent, acr setae absent, lateral scutal setae white, npl setae 0, spal setae 0, pal setae 0; proepisternum apubescent medially, grey pubescent laterally, long yellowish macrosetose; proepimeron grey pubescent, asetose, antepronotum antero-medially smooth (without any indentation); lateral postpronotum short yellowish setose; postpronotal lobe yellow, white pubescent, short yellowish setose; scutellum sparsely grey pubescent, discal scutellar setae absent, apical scutellar setae absent; mesopostnotum grey pubescent, asetose; anatergite grey pubescent, asetose;

katatergite grey pubescent, long white setose, elevated and smoothly convex; anepisternum sparsely grey pubescent, anteriorly asetose, posteriorly asetose, otherwise asetose; katepisternum sparsely grey pubescent, few white setae posteriorly; anepimeron sparsely grey pubescent, single long yellowish seta dorso-medially; katepimeron sparsely grey pubescent, white setose; meron sparsely grey pubescent, asetose; metakatepisternum large; metanepisternum grey pubescent, asetose; metepimeron brown (same color as T1), grey pubescent, short white setose, ± flat, infra-halter sclerite absent.

***Legs*:** light brown to brown, setation comprised of white setae, yellow macrosetae; pro coxa sparsely grey pubescent, long white macrosetose; mes coxa sparsely grey pubescent, short white setose; met coxa laterally unsclerotized (membrane between coxa and metakatepisternum clearly visible), sparsely grey pubescent, short white setose; met trochanter sparsely setose medially; pro + mes femur brown, met femur brown, distinctly clubbed for nearly entire length, macrosetose with thickened spine-like macrosetae on protuberances in 1 antero-ventral and 1 postero-ventral rows, 2–3 macrosetae distally in anterior row, postero-ventrally long white, appressed setose; pro tibia straight; mes tibia straight; met tibia laterally arched, met tibia cylindrical with distinct ventral keel terminating into distinct spur, spur almost reaching tip of 1st tarsomere, postero-laterally short white, appressed setose; pro + mes tarsomere 1 approximately as long as individual tarsomeres 2, 3, or 4, met tarsomere 1 as long as individual tarsomeres 2, 3, or 4; pulvillus well-developed, as long as well-developed claw, and as wide as base of claw; setiform empodium absent.

***Wing*:** length = 5.6–7.6 mm; slightly brown stained throughout, veins brown, microtrichia absent; cells r_1, r_4, m_3, + cua closed, r_5 open; C terminating at junction with R_1; Sc long, terminating in C proximal to r-m; R_4 terminates in R_1; R_5 terminates in R_1; auxiliary vein (R_3) at base of R_4 absent; R_4 and R_5 widest apart medially; r-m distinct, R_{4+5} and M_1 apart, connected by crossvein; M_1 straight at r-m (not curving anteriorly), M_1 (or M_1+M_2) terminates in C; base of M_3+M_4 present, M_3+M_4 not terminating together in C (not reaching wing margin), M_4 and CuA split proximally to m-cu (cell m_3 narrow proximally); CuP straight, cell cup wide, CuP and wing margin further apart proximally than distally; alula entirely reduced (nearly straight wing margin); halter light brown, pubescent, dorsally asetose, ventrally yellow setose.

***Abdomen*:** brown, setation comprised of scattered short white setae, T2–4 parallel-sided and not constricted waist-like, T surface entirely smooth; T1–7 brown with narrow yellow posterior margin; T sparsely grey pubescent; T1–7 short white setose; S1–7 light brown; S apubescent; S1–7 sparsely short white setose; bullae on T2 oval, small, yellow, surface entirely smooth, T2 surface anterior to bullae smooth.

♂ ***abdomen and terminalia*:** T1–7 well-developed, entirely sclerotized, T8 postero-medially weakly sclerotized, with anterior transverse sclerotized bridge connecting lateral sclerites; T7–8 anteriorly with 2 lateral apodemes; T8 auxiliary spiracle present; S6 regular, without any special setation postero-medially; S8 simple plate, entire (undivided) ventro-medially, not fused to T8 dorso-laterally; epandrium formed by 2 sclerites, separated medially and fused anteriorly, distally in dorsal view blunt, evenly rounded; subepandrial sclerite without lateral or median protuberances; hypandrium concave, cup-shaped, entirely sclerotized ventrally, entirely fused with gonocoxite, forming a gonocoxite-

hypandrial complex, supra-hypandrial sclerite absent; gonocoxite simple, short, hook-like, without median or lateral protuberance, gonocoxal apodeme absent; 2 functional phallic prongs, short and wide, medio-distally connected, parallel or diverging laterally, distally straight or only diverging slightly laterally; phallic epimere absent; lateral ejaculatory process absent; ejaculatory apodeme formed by single dorso-ventrally oriented plate; ventro-median margin of parameral sheath heavily sclerotized (appearing entirely closed); parameral sheath long, sperm sac entirely covered; sperm sac appearing weakly sclerotized.

Type locality. Namibia: Kunene: Orupembe (= Anabib), 24 km S (18°23'00"S, 012°13'00"E, -18.38333, 12.21667).

Material examined. Namibia: Kunene: 1♀ Kaokoveld, Orupembe, 24 km S, 18°21'21"S, 012°28'35"E, 1951-06-09, Swedish South Africa Expedition (MZLU-2143:1, Holotype, MZLU); 2♂ Kaokoveld, Orupembe, 18°09'37"S, 012°33'44"E, 1951-06-07–1951-06-09, Swedish South Africa Expedition (MZLU-2143:2, MZLU-2143:3, Paratypes, MZLU).

Distribution, biodiversity hotspots, phenology, and biology. Known only from two localities in the northern Namib Desert in Namibia (Fig. 56). A rarely collected species known only from three specimens from two collecting events in 1951 (Table 1). The species is not known to occur in any currently recognized biodiversity hotspot. Adult flies are active in June in early winter (Table 2), which is a time following a moister period and lower temperatures in this part of the Namib Desert (data for Anabib, Namibia, see https://www.worldweatheronline.com/anabib-weather/kunene/na.aspx). Nothing is known of the biology.

Remarks. The size difference among the three known specimens is quite significant. The ♀ holotype (wing length 9.9 mm) is much larger than the two ♂ paratypes (wing length 5.6–7.7 mm) and represents the largest fly in the genus *Eremohaplomydas*.

***Eremohaplomydas gobabebensis* sp. nov.**

http://zoobank.org/745D49C1-62B8-4884-9F7F-2B82523373D3
GBIF https://www.gbif.org/species/1591415 (genus record)
Figs 10–15, 32, 53, 56

Diagnosis. The species is distinguished from congeners by the densely arranged dorso-ventrally flattened setae on legs, the absence of the base of vein M_3+M_4, the overall golden pubescence, and the restricted distribution in the central Namib Desert.

Etymology. This species is named after the Gobabeb Namib Research Institute (www.gobabeb.org) where it was collected for the first time in November 2018. The specific epithet is to be treated as a noun in apposition.

Description. Female. unknown.

Male. *Head*: black, facial gibbosity brown, in general golden pubescent, ventrally and posteriorly white pubescent, white setose, laterally compressed setae; width distinctly greater than thorax (at postpronotal lobe), interocular distance on vertex larger than at ventral eye margin; vertex between compound eyes ± horizontally straight, medially only slightly below dorsal eye margin, vertex golden pubescent, white setose;

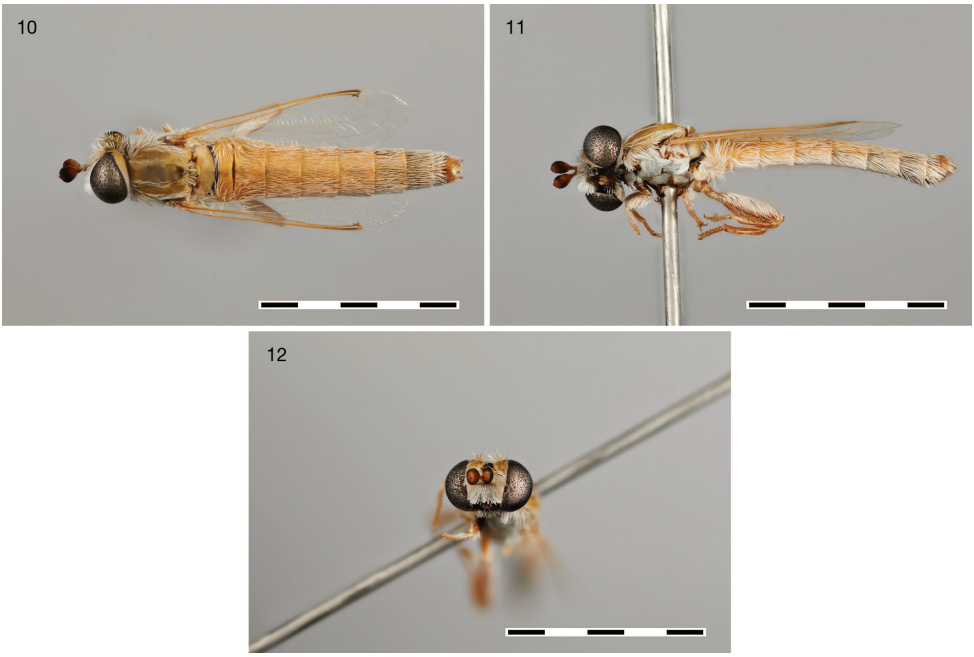

Figures 10–12. *Eremohaplomydas gobabebensis* sp. nov. (♂ paratype, USNMENT01518012, Zenodo https://doi.org/10.5281/zenodo.6083928): **10** dorsal (Zenodo https://doi.org/10.5281/zenodo.6083969) **11** lateral (https://doi.org/10.5281/zenodo.6083971) **12** head anterior (https://doi.org/10.5281/zenodo.6083979). Scale bars: 5 mm.

ocellar triangle apubescent; facial gibbosity distinct, well-developed and discernible in lateral view, mystax covering entire facial gibbosity, white; parafacial area approximately as wide as ½ width of central facial gibbosity (at same level); frons not elevated, golden pubescent, white setose; occiput predominantly white pubescent, dorsally golden pubescent, white setose, median occipital sclerite white setose, laterally compressed setae; pocl macrosetae absent; postgena apubescent, long, sparsely white setose; clypeus comprised of inverted U-shaped sclerite, dorsal ½ sclerotized medially to form plate, recessed (concave), ventrally simple, posterior to proboscis, laterally connected to face by sclerotized cuticle; proboscis very short, vestigial, knob-like, yellow; labellum small, as wide as prementum, length indiscernible, sclerotization indiscernible; maxillary palpus laterally compressed (triangular), light brown, slightly longer than proboscis.

***Antenna*:** light brown to brown; scape white setose dorsally, asetose ventrally; pedicel white setose dorsally and ventrally; postpedicel cylindrical in proximal 1/5, symmetrically bulbous in distal 4/5, ≥ 5.0 times as long as combined length of scape and pedicel, asetose; apical seta-like sensory element situated apically in cavity on postpedicel.

***Thorax*:** brown, scutum golden pubescent, pleura white pubescent; scutum uniformly black, surface entirely smooth, golden pubescent, scutal setation comprised of long white setae with distinct rows of long dorsocentral setae and dense lateral scutal setae; dc setae pre- and postsuturally white, acr setae absent, lateral scutal setae white, npl setae 0, spal setae 0, pal setae 0; proepisternum apubescent, long white setose; proepimeron grey pubescent,

asetose; antepronotum antero-medially smooth (without any indentation); lateral postpronotum long white setose; postpronotal lobe light brown, golden to light brown pubescent, long white setose; scutellum golden pubescent, discal scutellar setae absent, apical scutellar setae absent; mesopostnotum golden pubescent, asetose; anatergite golden pubescent, asetose; katatergite white pubescent, long white setose, slightly elevated, smoothly convex; anepisternum white pubescent, anteriorly white setose, posteriorly densely long white setose, scattered long white setose centrally; katepisternum dorsally white pubescent, ventrally apubescent, asetose; anepimeron white pubescent, long white setose; katepimeron white pubescent, asetose; meron white pubescent dorsally, sparsely white pubescent ventrally, asetose; metakatepisternum large; metanepisternum white pubescent, asetose; metepimeron yellow (same color as T1), white pubescent, long white setose, ± flat, infra-halter sclerite absent.

***Legs*:** light brown to brown, setation comprised of white laterally compressed setae predominantly covering surface; pro coxa apubescent, sparse white laterally compressed setae; mes coxa apubescent, asetose anteriorly, short white laterally compressed setae posteriorly; met coxa laterally unsclerotized (membrane between coxa and metakatepisternum clearly visible), apubescent, asetose anteriorly, short white laterally compressed setae posteriorly; met trochanter setose medially; pro + mes femur light brown to brown, met femur light brown to brown, distinctly clubbed for nearly entire length, macrosetose, 1 antero-ventral and 1 postero-ventral row of macrosetae, postero-ventrally long white, appressed setose; pro tibia laterally arched; mes tibia laterally arched; met tibia laterally arched, met tibia cylindrical with ventral keel terminating into distinct spur, spur not projecting beyond tip of tibia, postero-laterally long white, appressed setose; pro + mes tarsomere 1 approximately as long as individual tarsomeres 2, 3, or 4, met tarsomere 1 as long as individual tarsomeres 2, 3, or 4; pulvillus well-developed, as long as well-developed claw, and as wide as base of claw; setiform empodium absent.

***Wing*:** length = 4.2–5.7 mm; hyaline throughout, veins light yellow, microtrichia absent; cells r_1, r_4, m_3, + cua closed, r_5 open; C terminating at junction with R_1; Sc long, terminating in C proximal to r-m; R_4 terminates in R_1; R_5 terminates in R_1 and R_4 simultaneously; auxiliary vein (R_3) at base of R_4 absent; R_4 and R_5 widest apart medially; r-m distinct, R_{4+5} and M_1 apart, connected by crossvein; M_1 curves slightly anteriorly at r-m, M_1 (or M_1+M_2) terminates in C (not reaching wing margin); base of M_3+M_4 absent, M_3+M_4 not terminating together in C (not reaching wing margin), M_4 and CuA split proximally to m-cu (cell m_3 narrow proximally); CuP straight, cell cup wide, CuP and wing margin further apart proximally than distally; alula well-developed; halter light yellow, apubescent, asetose.

***Abdomen*:** light brown to brown, setation comprised of dense long white setae, T2–4 parallel-sided and not constricted waist-like, T surface entirely smooth; T1–4 light brown, T5–7 brown; T entirely golden pubescent; T1–7 long white setose; S1–5 brown with white posterior margin, S6–7 dark brown; S apubescent; S1 asetose, S2–7 long white setose; bullae on T2 oval, brown, surface entirely smooth, T2 surface anterior to bullae smooth.

♂ ***abdomen and terminalia*:** T1–8 well-developed; T7–8 anteriorly with 2 lateral apodemes; S6 regular, without any special setation postero-medially; S8 simple plate, entire (undivided) ventro-medially, not fused to T8 dorso-laterally; epandrium formed by single sclerite (fused medially ± entirely), distally in dorsal view pointed postero-

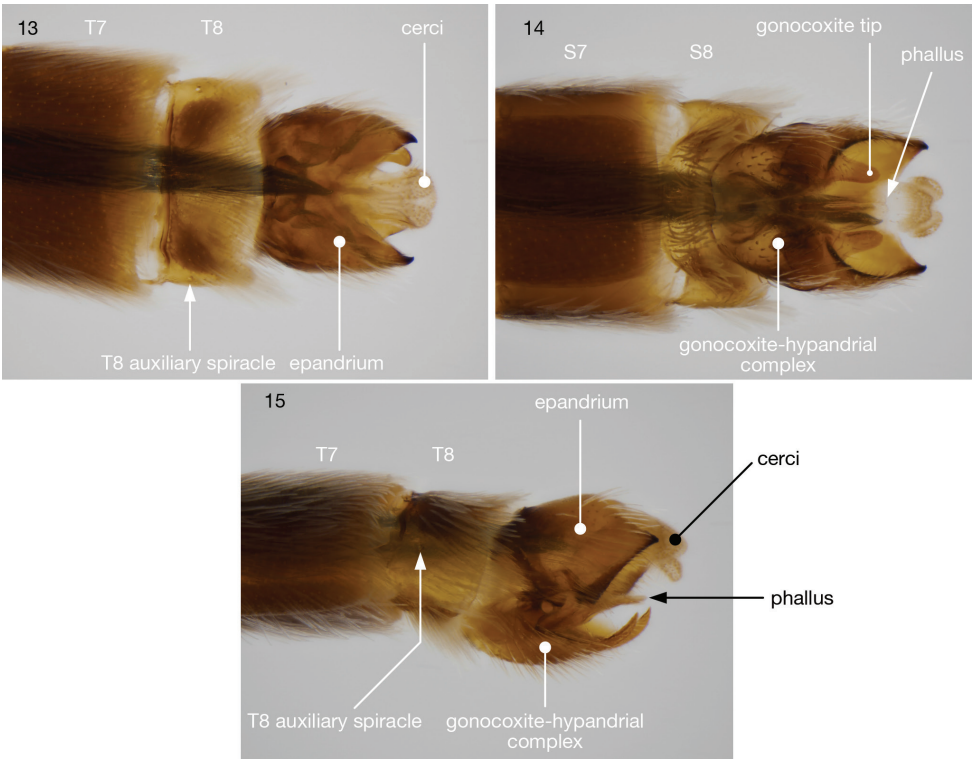

Figures 13–15. *Eremohaplomydas gobabebensis* sp. nov. ♂ terminalia (paratype, USNMENT01518012): **13** dorsal (Zenodo https://doi.org/10.5281/zenodo.6083973) **14** ventral (https://doi.org/10.5281/zenodo.6083977) **15** lateral (https://doi.org/10.5281/zenodo.6083975). Magnification = 75×.

laterally; subepandrial sclerite without lateral or median protuberances; hypandrium ± flat, divided ventro-medially by unsclerotized area into 2 sclerotized halves, entirely fused with gonocoxite, forming a gonocoxite-hypandrial complex, supra-hypandrial sclerite absent; gonocoxite simple, short, hook-like, without median or lateral protuberance, gonocoxal apodeme absent; 2 functional phallic prongs, short with broad lateral flange, medio-distally connected, parallel or diverging laterally, distally straight or only diverging slightly laterally; phallic epimere absent; lateral ejaculatory process absent; ejaculatory apodeme formed by single dorso-ventrally oriented plate; ventro-median margin of parameral sheath heavily sclerotized (appearing entirely closed); parameral sheath long, sperm sac entirely covered; sperm sac appearing ± heavily sclerotized.

Type locality. Namibia: Erongo: Namib-Naukluft National Park, Gobabeb 20 km NW on D1983, Kuiseb riverbed (23°24'56"S, 014°54'43"E, -23.41556, 14.91194).

Material examined. Namibia: Erongo: 1♂ Namib-Naukluft National Park, Gobabeb 20 km NW on D1983, Kuiseb riverbed, 23°24'56"S, 014°54'43"E, 317 m, 2018-11-24 collected a.m. (9:00–noon), dry, sandy, partly wooded riverbed, resting on sand, Dikow, T. (USNMENT01518262, Holotype, NMNW); 1♂ Namib-Naukluft National Park, Gobabeb 20 km NW on D1983, Kuiseb riverbed, 23°24'56"S, 014°54'43"E, 317 m, 2018-11-24 collected a.m. (9:00–noon), dry, sandy, partly wooded riverbed,

resting on sand, Dikow, T. (USNMENT01518263, Paratype, NMNW); 1♂ Namib-Naukluft National Park, Gobabeb 20 km NW on D1983, Kuiseb riverbed, 23°24'56"S, 014°54'43"E, 317 m, 2018-11-24 collected a.m. (9:00–noon), dry, sandy, partly wooded riverbed, resting on sand, Dikow, T. (USNMENT01518261, Paratype, USNM); 1♂ Namib-Naukluft National Park, Gobabeb 20 km NW on D1983, Kuiseb riverbed, 23°24'56"S, 014°54'43"E, 317 m, 2018-11-24 collected a.m. (9:00–noon), dry, sandy, partly wooded riverbed, resting on sand, Dikow, T. (USNMENT01518260, Paratype, USNM); 1♂ Namib-Naukluft National Park, Gobabeb, dunes W of Kuiseb riverbed, 23°33'48"S, 015°01'58"E, 401 m, 2018-11-21 collected a.m. (9:00–noon), small vegetated dunes, resting on sand, Dikow, T. (USNMENT01518012, Paratype, USNM); 1♂ Namib-Naukluft National Park, Gobabeb, small dunes W of Kuiseb River, 23°33'50"S, 015°01'59"E, 398 m, 2018-11-23 collected p.m. (noon–15:00), partly vegetated dune, resting on sand, Dikow, T. (USNMENT01518339, Paratype, USNM).

Distribution, biodiversity hotspots, phenology, and biology. Known only from two localities in the central Namib Desert in Namibia (Fig. 56). A rarely collected species known only from seven specimens from three collecting events in 2018 (Table 1). The species is not known to occur in any currently recognized biodiversity hotspot. Adult flies are active in November in late spring (Table 2), which is a time at the beginning of a moister period and rising temperatures in this part of the Namib Desert (data for Gobabeb, Namibia, see https://www.worldweatheronline.com/gobabeb-weather/erongo/na.aspx). So far, only males have been collected and they were observed to fly very low above the ground and appeared to inspect the base of single grass plants and dart at high speed across the sand to the next plant. At the Gobabeb locality, the flies were collected flying among *Centropodia glauca* (Poaceae, Gha Grass, https://www.gbif.org/species/5680035) and at the 20 km N Gobabeb locality the flies darted among *Cladoraphis spinosa* (Poaceae, Spiny Love Grass, https://www.gbif.org/species/4152290, see habitat photographs with the grasses in the foreground in Figs 1, 2). Both grass species are native and widely distributed in the western parts of southern Africa including the Namib Desert (van Oudtshoorn 2012). The male flies possibly inspected the grasses in search for females resting in the shade although the junior author was not able to observe or collect any females. In general, the flies were very difficult to observe and collect due to their high flight speed, light colouration, and small size.

Remarks. Wharton (1982) did not collect this species in his seminal year-long study of Mydidae at Gobabeb.

Eremohaplomydas stomachoris sp. nov.

http://zoobank.org/47E76F26-91AF-4DFD-80ED-6CDCC4DBF994
GBIF https://www.gbif.org/species/1591415 (genus record)
Figs 16–18, 33, 57

Diagnosis. The species is distinguished from congeners by the macrosetose dorso-median occipital setae, the small and slender size (wing length 6.3 mm), and the restricted distribution in the northern Namib Desert.

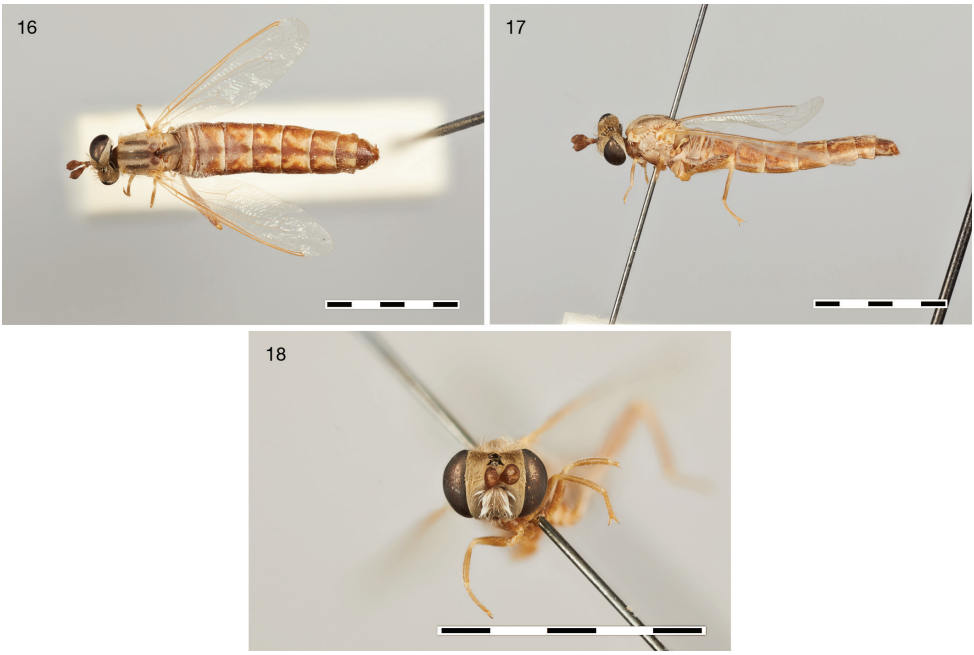

Figures 16–18. *Eremohaplomydas stomachoris* sp. nov. (♀ holotype, AAM-003035, Zenodo https://doi.org/10.5281/zenodo.6083930): **16** dorsal (https://doi.org/10.5281/zenodo.6083983) **17** lateral (https://doi.org/10.5281/zenodo.6083985) **18** head anterior (https://doi.org/10.5281/zenodo.6083987). Scale bars: 5 mm.

Etymology. Greek *stoma* = mouth, *choris* = without. The specific epithet refers to the extremely short and minute proboscis in this species.

Description. Female. ***Head*****:** black, facial gibbosity brown, in general golden pubescent, ventrally and posteriorly white pubescent, white setose, regular, cylindrical setae; width distinctly greater than thorax (at postpronotal lobe), interocular distance on vertex larger than at ventral eye margin; vertex between compound eyes ± horizontally straight, medially only slightly below dorsal eye margin, vertex golden pubescent, light brown; ocellar triangle apubescent; facial gibbosity distinct, well-developed and discernible in lateral view, mystax covering entire facial gibbosity, sparse, white; parafacial area approximately as wide as ½ width of central facial gibbosity (at same level); frons not elevated, golden pubescent, yellow; occiput predominantly grey pubescent, dorsally golden pubescent, yellowish to light brown setose, median occipital sclerite yellowish macrosetose; pocl macrosetae absent; postgena sparsely white pubescent, long, sparsely white setose; clypeus comprised of single sclerite, entirely sclerotized medially, flat to protruding (convex) ventrally, ventrally simple, posterior to proboscis, laterally connected to face by sclerotized cuticle; proboscis very short, vestigial, knob-like, light brown; labellum small, as wide as prementum, length indiscernible, sclerotization indiscernible; maxillary palpus laterally compressed (triangular), light brown, slightly longer than proboscis.

Antenna**:** brown; scape brown setose dorsally, asetose ventrally; pedicel light brown setose dorsally and ventrally; postpedicel cylindrical in proximal ¼, symmetrically

bulbous in distal ¾, ≥ 4.0 times as long as combined length of scape and pedicel, asetose; apical seta-like sensory element situated apically in cavity on postpedicel.

***Thorax*:** light brown, predominantly grey pubescent; scutum black, brown posteriorly, surface entirely smooth, predominantly grey pubescent, broad median and sublateral stripes reaching transverse suture brown pubescent, postsuturally with 2 large sublateral sparsely grey pubescent spots, scutal setation comprised of distinct rows of long dorsocentral setae and lateral scutal setae; dc setae pre- and postsuturally white or yellow, acr setae absent, lateral scutal setae yellow, npl setae 0, spal setae 0, pal setae 0; proepisternum apubescent, long white setose; proepimeron grey pubescent, asetose; antepronotum antero-medially smooth (without any indentation); lateral postpronotum long white setose; postpronotal lobe yellow, white pubescent, long white setose; scutellum grey pubescent, discal scutellar setae absent, apical scutellar setae absent; mesopostnotum grey pubescent, asetose; anatergite grey pubescent, asetose; katatergite grey pubescent, long white setose, slightly elevated, smoothly convex; anepisternum grey pubescent, anteriorly white setose, posteriorly long white setose, scattered white setose antero-ventrally; katepisternum dorsally grey pubescent, ventrally apubescent, single white seta posteriorly; anepimeron grey pubescent, long white setose; katepimeron grey pubescent, asetose; meron grey pubescent dorsally, apubescent ventrally, asetose; metakatepisternum large; metanepisternum grey pubescent, asetose; metepimeron yellow (contrasting color of T1), grey pubescent, long white setose, ± flat, infra-halter sclerite absent.

***Legs*:** light brown to brown, setation comprised of white to yellowish setae, femur with laterally compressed setae; pro coxa sparsely white pubescent, short white macrosetose; mes coxa sparsely white pubescent, short white macrosetose anteriorly, long white laterally compressed setae posteriorly; met coxa laterally unsclerotized (membrane between coxa and metakatepisternum clearly visible), sparsely white pubescent, short white macrosetose anteriorly, long white laterally compressed setae posteriorly; met trochanter sparsely setose medially; pro + mes femur light brown to brown, met femur light brown to brown, evenly clubbed in distal ¾, macrosetose, 1 antero-ventral and 1 postero-ventral row of macrosetae, postero-ventrally long white, appressed setose; pro tibia laterally arched; mes tibia laterally arched; met tibia straight, met tibia cylindrical with distinct ventral keel without terminal spur, 2 long macrosetae originating near tip of keel, postero-laterally regular setose only; pro + mes tarsomere 1 approximately as long as individual tarsomeres 2, 3, or 4, met tarsomere 1 as long as individual tarsomeres 2, 3, or 4; pulvillus well-developed, as long as well-developed claw, and as wide as base of claw; setiform empodium absent.

***Wing*:** length = 6.3 mm; hyaline throughout, veins light brown, microtrichia absent; cells r_1, r_4, m_3, + cua closed, r_5 open; C terminating at junction with R_1; Sc long, terminating in C proximal to r-m; R_4 terminates in R_1; R_5 terminates in R_1 and R_4 simultaneously; auxiliary vein (R_3) at base of R_4 absent; R_4 and R_5 widest apart medially; r-m distinct, R_{4+5} and M_1 apart, connected by crossvein; M_1 straight at r-m (not curving anteriorly), M_1 (or M_1+M_2) terminates in C (not reaching wing margin); base of M_3+M_4 present, M_3+M_4 not terminating together in C (not reaching wing margin), M_4 and CuA split proximally to m-cu (cell m_3 narrow proximally); CuP straight, cell

cup wide, CuP and wing margin further apart proximally than distally; alula well-developed; halter light yellow, apubescent, asetose.

***Abdomen*:** light brown to brown, setation comprised of scattered white setae, T2–4 parallel-sided and not constricted waist-like, T surface entirely smooth; T1 brown with yellowish posterior margin, T2–7 brown medially and laterally with yellowish posterior margins, sub-laterally yellowish, slightly angled longitudinal striping; T1 grey pubescent, T2–3 sparsely grey pubescent narrowly anteriorly and medially, T4–7 apubescent; T1–7 short white setose; S1–7 light brown; S apubescent; S1–7 sparsely short white setose; bullae on T2 oval, small, yellow, surface entirely smooth, T2 surface anterior to bullae smooth.

♀ ***abdomen and genitalia*:** densely arranged anteriorly directed setae present on T7–8 and S7–8; T8 anterior apodeme indiscernible (not dissected), auxiliary spiracle indiscernible (not dissected); T9 formed by wide, rectangular sclerite with median protuberance; T9+10 entirely fused (sclerites indistinguishable), T10 divided into 2 heavily sclerotized acanthophorite plates; 5–7 acanthophorite spines per plate.

Male. unknown.

Type locality. Namibia: Kunene: Kaokoveld, Orupembe, 21 km S (18°19'24"S, 012°29'12"E, -18.32333, 12.48667).

Material examined. Namibia: Kunene: 1♀ Kaokoveld, Orupembe, 21 km S, 18°19'24"S, 012°29'12"E, 1970-05-01, Brown, H. (AAM-003035, Holotype, SANC).

Distribution, biodiversity hotspots, phenology, and biology. Known only from a single locality in the Namib Desert in northern Namibia (Fig. 57). A rarely collected species known only from a single female specimen collected in 1970 (Table 1). The species is not known to occur in any currently recognized biodiversity hotspot. Adult flies are active in May in mid-autumn (Table 2), which is a time at the end of a moister period and decreasing temperatures in this part of the Namib Desert (data for Anabib, Namibia, see https://www.worldweatheronline.com/anabib-weather/kunene/na.aspx). Nothing is known of the biology.

Remarks. The type locality of *Eremohaplomydas stomachoris* sp. nov. lies geographically very close to that of *Eremohaplomydas desertorum*. However, the single female specimen of *E. stomachoris* sp. nov. is morphologically more similar to *Eremohaplomydas gobabebensis* sp. nov. from the central Namib Desert (more than 600 km further south) than it is to *E. desertorum* (see also Discussion). Furthermore, *E. stomachoris* sp. nov. has been collected in early May, at least a month earlier in autumn than *E. desertorum* (Table 2).

Eremohaplomydas whartoni sp. nov.

http://zoobank.org/6F6B399B-4FB1-4C20-835F-FF5728D529F4
GBIF https://www.gbif.org/species/1591415 (genus record)
Figs 19–30, 34, 57

Diagnosis. The species is distinguished from congeners by the overall light brown colouration, the reduced alula on the wing, the apubescent abdominal tergites 5–8 in females, and the restricted distribution in the central Namib Desert.

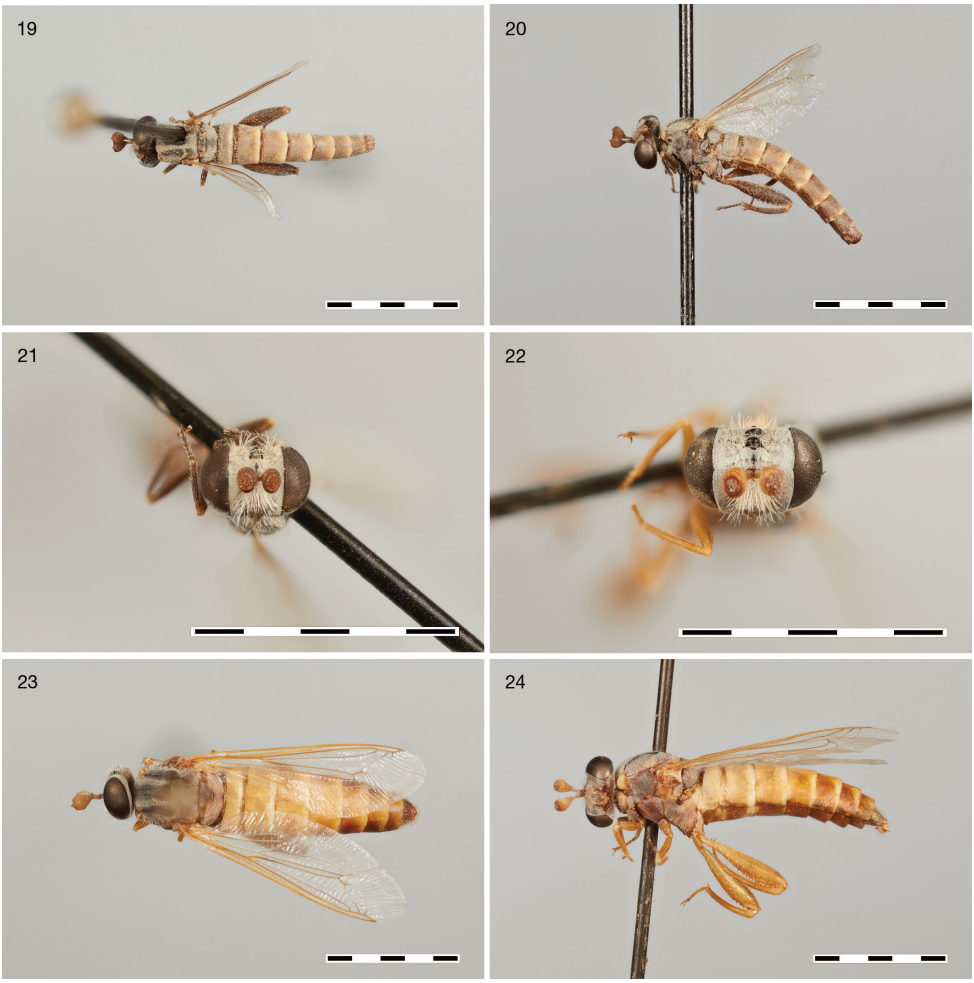

Figures 19–24. *Eremohaplomydas whartoni* sp. nov.: **19** ♂ holotype (NMSA-DIP-92011, Zenodo https://doi.org/10.5281/zenodo.6083939), dorsal (https://doi.org/10.5281/zenodo.6084009) **20** same, lateral (https://doi.org/10.5281/zenodo.6084011) **21** same, head anterior (https://doi.org/10.5281/zenodo.6084013) **22** ♀ paratype (NMSA-DIP-92012, https://doi.org/10.5281/zenodo.6083936), head anterior (https://doi.org/10.5281/zenodo.6084007) **23** same, dorsal (https://doi.org/10.5281/zenodo.6084003) **24** same, lateral (https://doi.org/10.5281/zenodo.6084005). Scale bars: 5 mm.

Etymology. This species is named after Dr Robert Wharton, the only collector of this species, in recognition of his year-long seminal study of the Mydidae (and other taxa) of the central Namib Desert at the Gobabeb Namib Research Institute in 1978–1979 (Wharton 1982). The specific name is to be treated as a noun in apposition.

Description. Female. ***Head*****:** black, facial gibbosity light brown, in general grey pubescent, white setose, regular, cylindrical setae; width distinctly greater than thorax (at postpronotal lobe), interocular distance on vertex same as at ventral eye margin; vertex between compound eyes ± horizontally straight, medially only slightly below dorsal eye

margin, vertex grey pubescent, white setose; ocellar triangle apubescent; facial gibbosity distinct, well-developed and discernible in lateral view, mystax covering entire facial gibbosity, white; parafacial area more than ½ width of central facial gibbosity (at same level); frons not elevated, grey pubescent, white setose; occiput grey pubescent, white setose, median occipital sclerite light brown macrosetose; pocl macrosetae absent; postgena sparsely grey pubescent, long, sparsely white setose; clypeus comprised of single sclerite, entirely sclerotized medially, flat to protruding (convex) ventrally, ventrally expanded, anterior to proboscis (almost covering it), laterally connected to face by sclerotized cuticle; proboscis very short, vestigial, knob-like, brown; labellum indiscernible, length indiscernible, sclerotization indiscernible; maxillary palpus cylindrical, light brown, minute.

***Antenna*:** light brown to brown; scape asetose; pedicel white setose dorsally and ventrally; postpedicel cylindrical in proximal ¼, symmetrically bulbous in distal ¾, ≥ 5.0 times as long as combined length of scape and pedicel, asetose; apical seta-like sensory element situated apically in cavity on postpedicel.

***Thorax*:** dark brown, predominantly grey pubescent; scutum uniformly black, surface microrugose (slightly rugose 'imitating' pubescence), predominantly grey pubescent, broad sublateral stripes (interrupted by transverse suture) sparsely grey pubescent, narrow paramedian stripes merging postsuturally and not reaching posterior margin sparsely grey pubescent, scutal setation comprised of long white setae in pubescent areas; dc setae pre- and postsuturally white, acr setae absent, lateral scutal setae white, npl setae 0, spal setae 0, pal setae 0; proepisternum apubescent medially, grey pubescent laterally, long yellowish macrosetose; proepimeron grey pubescent, asetose; anteprono-tum antero-medially smooth (without any indentation); lateral postpronotum long white setose; postpronotal lobe yellow, grey pubescent, short yellowish setose; scutellum grey pubescent, discal scutellar setae absent, apical scutellar setae absent; mesopostnotum grey pubescent, asetose; anatergite grey pubescent, asetose; katatergite grey pubescent, long white setose, elevated and smoothly convex; anepisternum grey pubescent, anteriorly asetose, posteriorly asetose, otherwise asetose; katepisternum sparsely grey pubescent, asetose; anepimeron sparsely grey pubescent, asetose; katepimeron sparsely grey pubescent, asetose; meron sparsely grey pubescent, asetose; metakatepisternum large; metanepisternum grey pubescent, asetose; metepimeron light brown (same color as T1), grey pubescent, long yellowish setose, ± flat, infra-halter sclerite absent.

***Legs*:** yellow to brown, setation comprised of white setae, yellow macrosetae; pro coxa sparsely grey pubescent, short white macrosetose; mes coxa sparsely grey pubescent, short white setose and macrosetose; met coxa laterally unsclerotized (membrane between coxa and metakatepisternum clearly visible), sparsely grey pubescent, short white setose and macrosetose; met trochanter setose medially; pro + mes femur yellow to light brown, met femur light brown to brown, distinctly clubbed for nearly entire length, macrosetose with thickened spine-like macrosetae on protuberances in 1 antero-ventral and 1 postero-ventral rows, 2–3 macrosetae distally in anterior row, postero-ventrally sparse, short white setose; pro tibia laterally arched; mes tibia laterally arched; met tibia laterally arched, met tibia cylindrical with distinct ventral keel terminating into distinct spur, macroseta at tip of spur, almost reaching tip of 1st tarsomere, postero-

laterally sparse long white, erect setose with setae arranged in distinct row; pro + mes tarsomere 1 as long as tarsomere 2, met tarsomere 1 as long as individual tarsomeres 2, 3, or 4; pulvillus reduced, ½ length of well-developed claw; setiform empodium absent.

***Wing*:** length = 7.0–7.9 mm; hyaline throughout, veins light brown, microtrichia absent; cells r_1, r_4, m_3, + cua closed, r_5 open; C terminating at junction with R_1; Sc long, terminating in C proximal to r-m; R_4 terminates in R_1; R_5 terminates in R_1; auxiliary vein (R_3) at base of R_4 absent; R_4 and R_5 widest apart medially; r-m distinct, R_{4+5} and M_1 apart, connected by crossvein; M_1 straight at r-m (not curving anteriorly), M_1 (or M_1+M_2) terminates in C (not reaching wing margin), rarely C; base of M_3+M_4 present, M_3+M_4 not terminating together in C (not reaching wing margin), M_4 and CuA split proximally to m-cu (cell m_3 narrow proximally); CuP straight, cell cup wide, CuP and wing margin further apart proximally than distally; alula entirely reduced (nearly straight wing margin); halter light brown, apubescent, dorsally asetose, ventrally yellow setose.

***Abdomen*:** light brown to brown, setation comprised of scattered short white setae, T2–4 parallel-sided and not constricted waist-like, T surface entirely smooth; T1–4 light brown with narrow yellowish posterior margins, T5–7 brown with narrow yellowish posterior margins; T1–4 grey pubescent, T5 sparsely grey pubescent medially, T6–7 apubescent; T1 short white setose, T2–6 sparsely very short white setose, T7 short erect white setose; S1 light brown, S2–3 brown with yellowish posterior margins, S4–7 brown; S apubescent; S1–7 sparsely short white setose; bullae on T2 transversely elongate, yellow, surface entirely smooth, T2 surface anterior to bullae smooth.

♀ ***abdomen and genitalia*:** densely arranged anteriorly directed setae present on T7–8 and S7–8; T8 anterior apodeme present, broad and rectangular, auxiliary spiracle present; T9 formed by wide, rectangular sclerite with median protuberance; T9+10 entirely fused (sclerites indistinguishable), T10 divided into 2 heavily sclerotized acanthophorite plates; 6 acanthophorite spines per plate; 2 spermathecae, all equally large, not differentiated from spermathecal ducts, weakly sclerotized; individual spermathecal duct short; S9 (furca) formed by 1 sclerite, inverted U-shaped (joined anteriorly, separated posteriorly), anterior furcal apodeme present, 2 lateral projections forming divided apodeme, lateral furcal apodeme absent, median furcal bridge absent.

Male. ***Head*:** black, facial gibbosity brown, in general grey pubescent, white setose, regular, cylindrical setae; width distinctly greater than thorax (at postpronotal lobe), interocular distance on vertex same as at ventral eye margin; vertex between compound eyes ± horizontally straight, medially only slightly below dorsal eye margin, vertex grey pubescent, white setose; ocellar triangle apubescent; facial gibbosity distinct, well-developed and discernible in lateral view, mystax covering entire facial gibbosity, white; parafacial area approximately as wide as ½ width of central facial gibbosity (at same level); frons not elevated, grey pubescent, white setose; occiput grey pubescent, white setose, median occipital sclerite light brown macrosetose; pocl macrosetae absent; postgena sparsely grey pubescent, long, sparsely white setose; clypeus comprised of single sclerite, entirely sclerotized medially, flat to protruding (convex) ventrally, ventrally expanded, anterior to proboscis (almost covering it), laterally connected to face by sclerotized cuticle; proboscis very short, vestigial, knob-like, brown; labellum indiscernible, length indiscernible, sclerotization indiscernible; maxillary palpus cylindrical, light brown, minute.

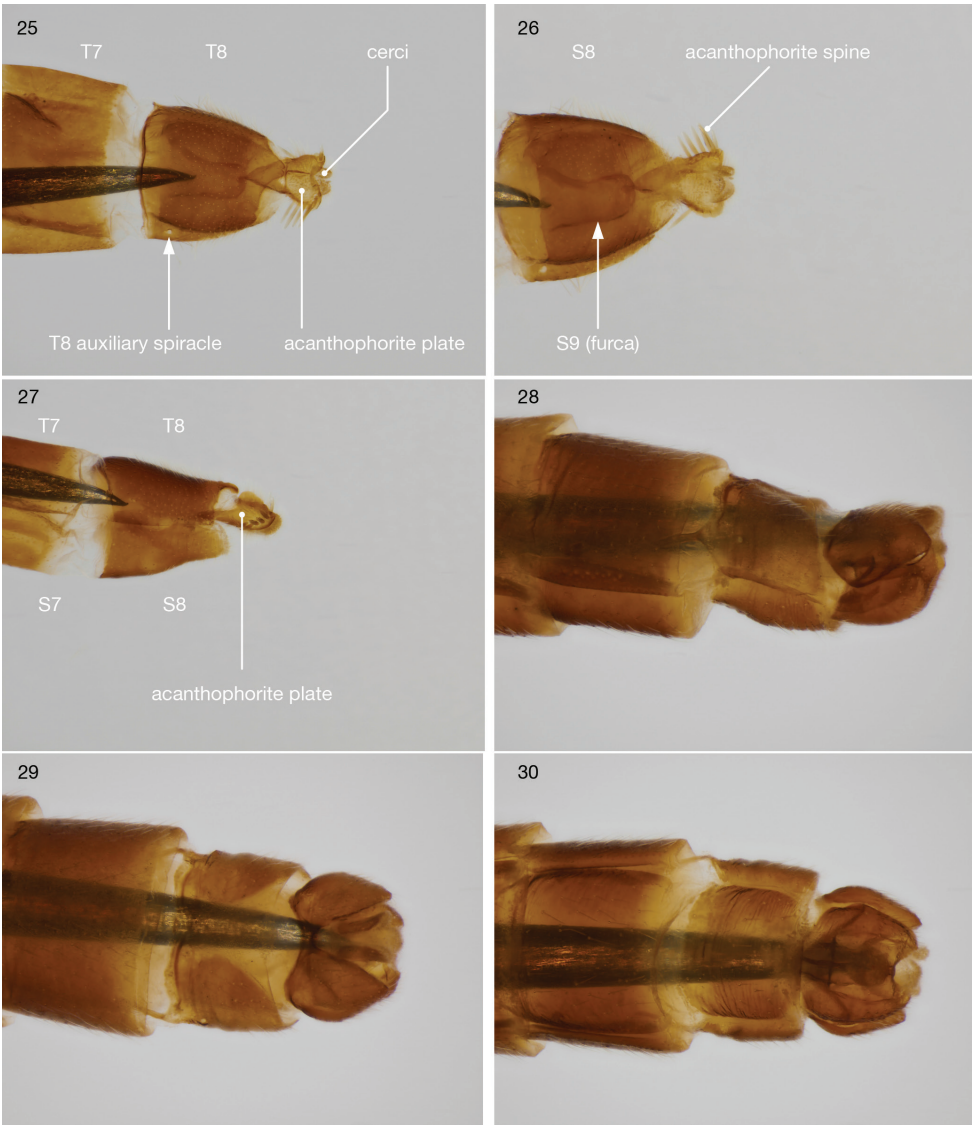

Figures 25–30. *Eremohaplomydas whartoni* sp. nov. ♀ and ♂ terminalia: **25** ♀ paratype (NMSA-DIP-52578, Zenodo https://doi.org/10.5281/zenodo.6083932), dorsal (https://doi.org/10.5281/zenodo.6083991) **26** same, ventral (https://doi.org/10.5281/zenodo.6083995) **27** same, lateral (https://doi.org/10.5281/zenodo.6083993) **28** ♂ paratype (NMSA-DIP-52577, https://doi.org/10.5281/zenodo.6083934), lateral (https://doi.org/10.5281/zenodo.6083999) **29** same, dorsal (https://doi.org/10.5281/zenodo.6083997) **30** same, ventral (https://doi.org/10.5281/zenodo.6084001). Magnification 25–27 = 50×, 28–30 = 75×.

***Antenna*:** light brown to brown; scape white setose dorsally, asetose ventrally; pedicel white setose dorsally and ventrally; postpedicel cylindrical in proximal ⅓, symmetrically bulbous in distal 2/3, ≥ 3.0 times as long as combined length of scape and pedicel, asetose; apical seta-like sensory element situated apically in cavity on postpedicel.

***Thorax*:** black, predominantly grey pubescent; scutum uniformly black, surface microrugose (slightly rugose 'imitating' pubescence), predominantly grey pubescent, broad sublateral stripes (interrupted by transverse suture) and narrow paramedian stripes merging postsuturally and not reaching posterior margin apubescent, scutal setation comprised of long white setae in pubescent areas; dc setae pre- and postsuturally white, acr setae absent, lateral scutal setae white, npl setae 0, spal setae 0, pal setae 0; proepisternum apubescent medially, grey pubescent laterally, long yellowish macrosetose; proepimeron grey pubescent, asetose; antepronotum antero-medially smooth (without any indentation); lateral postpronotum long white setose; postpronotal lobe light brown, grey pubescent, short yellowish setose; scutellum grey pubescent, discal scutellar setae absent, apical scutellar setae absent; mesopostnotum grey pubescent, asetose; anatergite grey pubescent, asetose; katatergite grey pubescent, long white setose, elevated and smoothly convex; anepisternum grey pubescent, anteriorly asetose, posteriorly asetose, otherwise asetose; katepisternum grey pubescent, asetose; anepimeron grey pubescent, single long yellowish seta dorso-medially; katepimeron grey pubescent, asetose; meron grey pubescent, asetose; metakatepisternum large; metanepisternum grey pubescent, asetose; metepimeron brown (same color as T1), grey pubescent, long white setose, ± flat, infra-halter sclerite absent.

***Legs*:** brown, setation comprised of white setae, yellow macrosetae; pro coxa sparsely grey pubescent, short white macrosetose; mes coxa sparsely grey pubescent, short white setose; met coxa laterally unsclerotized (membrane between coxa and metakatepisternum clearly visible), sparsely grey pubescent, short white setose; met trochanter setose medially; pro + mes femur brown, met femur brown, distinctly clubbed for nearly entire length, macrosetose with thickened spine-like macrosetae on protuberances in 1 antero-ventral and 1 postero-ventral rows, 2–3 macrosetae distally in anterior row, postero-ventrally sparse, long white erect setose; pro tibia laterally arched; mes tibia laterally arched; met tibia laterally arched, met tibia cylindrical with distinct ventral keel terminating into distinct spur, macroseta at tip of spur, almost reaching tip of 1st tarsomere, postero-laterally sparse long white, erect setose with setae arranged in distinct row; pro + mes tarsomere 1 as long as tarsomere 2, met tarsomere 1 as long as individual tarsomeres 2, 3, or 4; pulvillus well-developed, as long as well-developed claw, and as wide as base of claw; setiform empodium absent.

***Wing*:** length = 5.0–7.0 mm; hyaline throughout, veins light brown, microtrichia absent; cells r_1, r_4, m_3, + cua closed, r_5 open; C terminating at junction with R_1; Sc long, terminating in C proximal to r-m; R_4 terminates in R_1; R_5 terminates in R_1; auxiliary vein (R_3) at base of R_4 absent; R_4 and R_5 widest apart medially; r-m distinct, R_{4+5} and M_1 apart, connected by crossvein; M_1 straight at r-m (not curving anteriorly), M_1 (or M_1+M_2) terminates in C (not reaching wing margin), rarely C; base of M_3+M_4 present, M_3+M_4 not terminating together in C (not reaching wing margin), M_4 and CuA split proximally to m-cu (cell m_3 narrow proximally); CuP straight, cell cup wide, CuP and wing margin further apart proximally than distally; alula entirely reduced (nearly straight wing margin); halter light brown, apubescent, dorsally asetose, ventrally yellow setose.

***Abdomen*:** brown, setation comprised of scattered short white setae, T2–4 parallel-sided and not constricted waist-like, T surface entirely smooth; T1–7 brown with yellow posterior margins, dark brown lateral margins; T entirely grey pubescent; T1–7 short white setose; S1 brown, S2–6 brown with yellow posterior margins, S7 brown; S apubescent; S1–7 short white setose; bullae on T2 oval, small, yellow, surface entirely smooth, T2 surface anterior to bullae smooth.

♂ ***abdomen and terminalia*:** T1–7 well-developed, entirely sclerotized, T8 postero-medially weakly sclerotized, with anterior transverse sclerotized bridge connecting lateral sclerites; T7–8 anteriorly with 2 lateral apodemes; T8 auxiliary spiracle present; S6 regular, without any special setation postero-medially; S8 simple plate, entire (undivided) ventro-medially, not fused to T8 dorso-laterally; epandrium formed by 2 sclerites, separated medially and fused anteriorly, distally in dorsal view blunt, evenly rounded; subepandrial sclerite without lateral or median protuberances; hypandrium concave, cup-shaped, entirely sclerotized ventrally, entirely fused with gonocoxite, forming a gonocoxite-hypandrial complex, supra-hypandrial sclerite absent; gonocoxite simple, long, slightly curved dorsally, without median or lateral protuberance, gonocoxal apodeme absent; 2 functional phallic prongs, short and wide, medio-distally connected, parallel or diverging laterally, distally straight or only diverging slightly laterally; phallic epimere absent; lateral ejaculatory process absent; ejaculatory apodeme formed by single dorso-ventrally oriented plate; ventro-median margin of parameral sheath heavily sclerotized (appearing entirely closed); parameral sheath long, sperm sac entirely covered; sperm sac appearing ± heavily sclerotized.

Type locality. Namibia: Erongo: Gobabeb, 5 km N (23°30'54"S, 015°02'35"E, -23.515, 15.04306).

Material examined. Namibia: Erongo: 1♂ Gobabeb, 5 km N, 23°30'54"S, 015°02'35"E, 1979-05-08, Wharton, R. (NMSA-DIP-92011, Holotype, NMSA); 1♂ Gobabeb, 5 km N, 23°30'54"S, 015°02'35"E, 1979-05-08, Wharton, R. (NMSA-DIP-52603, Paratype, NMSA); 1♂ Gobabeb, plains, 23°33'20"S, 015°02'40"E, 1979-05-12, Wharton, R. (AAM-007357, Paratype, NMNW); 1♂ Gobabeb, plains, 23°33'20"S, 015°02'40"E, 1979-05-12, Wharton, R. (NMSA-DIP-52577, Paratype, NMSA); 1♀ Gobabeb, plains, 23°33'20"S, 015°02'40"E, 1979-05-12, Wharton, R. (NMSA-DIP-92012, Paratype, NMSA); 1♀ Gobabeb, plains, 23°33'20"S, 015°02'40"E, 1979-05-14, Wharton, R. (NMSA-DIP-52578, Paratype, NMSA); 1♂ Gobabeb, plains, 23°33'20"S, 015°02'40"E, 1979-05-11, Wharton, R. (NMSA-DIP-52599, Paratype, NMSA).

Distribution, biodiversity hotspots, phenology, and biology. Known only from two nearby localities in the central Namib Desert in Namibia (Fig. 57). A rarely collected species known only from seven specimens from three collecting events in 1979 (Table 1). The species is not known to occur in any currently recognized biodiversity hotspot. Adult flies are active in May in mid-autumn (Table 2), which is after a usually moister period and high temperatures in this part of the Namib Desert (data for Gobabeb, Namibia, see www.worldweatheronline.com/gobabeb-weather-averages/erongo/na.aspx). Wharton (1982, p. 149) stated that he observed an attempted mating by two males with the same female at

13 h 00 on 1979-05-12, which was unsuccessful due to interference (female specimen NMSA-DIP-92012 and male specimens AAM-007357 and NMSA-DIP-52577 (Wharton number 332)). Wharton (1982) furthermore highlighted the fact that *E. whartoni* sp. nov. might only emerge as an imago following the onset of strong autumn winds.

Remarks. Wharton (1982) in his seminal year-long study of Mydidae at Gobabeb discovered this species for the first time (identified as *Eremohaplomydas* sp.) and remains the only collector.

Haplomydas Bezzi, 1924

http://zoobank.org/AA86F72F-7319-43C5-9104-A618FA521E5E
Original description online https://www.biodiversitylibrary.org/page/40677714
GBIF https://www.gbif.org/species/1591511

Haplomydas Bezzi, 1924: 199. Type-species: *Haplomydas crassipes* Bezzi, 1924, by original designation.
Heleomydas Séguy, 1929 - junior synonym; ZooBank http://zoobank.org/48330D1D-A176-4042-9F3C-97EC14FCD173

Diagnosis. The genus can be delineated by the greatly expanded metathoracic femora, the distinct ventral keel terminating into a spur on the metathoracic tibiae, the presence of setae on the posterior anepisternum, the yellow to light brown colouration, and the absence of M_3+M_4 terminating into the costa.

Distribution, biodiversity hotspots, phenology, and biology. Known from diverse localities in Botswana, Mozambique, Namibia, and Zimbabwe (Fig. 57). A relatively commonly collected genus with collecting events between 1917 and 1999 (Table 1). The genus occurs in the Eastern Afromontane biodiversity hotspot in eastern-most Zimbabwe (Fig. 57). Adult flies are active in late summer to autumn (Table 2). Nothing is known of the biology.

Haplomydas crassipes Bezzi, 1924

http://zoobank.org/0D555493-5F42-4B0B-8F43-058DCA9CF4EA
Original description online https://www.biodiversitylibrary.org/page/40677715
GBIF https://www.gbif.org/species/1591512
Figs 35–40, 54, 57

Rhopalia flavomarginata Brunetti, 1929 - junior synonym; ZooBank http://zoobank.org/NomenclaturalActs/82C1F003-57A2-4559-9BB6-0AABDAC5285E
Heleomydas lesnei Séguy, 1929 - junior synonym; ZooBank http://zoobank.org/NomenclaturalActs/3566EA36-0139-4B9C-80CA-3BD2A3BE2250

Diagnosis. See above for genus.

Figures 31–34. Heads of *Eremohaplomydas* species in ventro-lateral view: **31** *E. desertorum* ♂ paratype (MZLU-2143:2, 60× magnification, Zenodo https://doi.org/10.5281/zenodo.6083967) **32** *E. gobabebensis* sp. nov. ♂ holotype (USNMENT01518012, 75×, https://doi.org/10.5281/zenodo.6083981) **33** *E. stomachoris* sp. nov. ♀ holotype (AAM-003035, 75×, https://doi.org/10.5281/zenodo.6083989) **34** *E. whartoni* sp. nov. ♂ holotype (NMSA-DIP-92011, 75×, https://doi.org/10.5281/zenodo.6084015).

Redescription. Female. ***Head*****:** brown, facial gibbosity yellow, in general densely white pubescent, white setose, regular, cylindrical setae; width distinctly greater than thorax (at postpronotal lobe), interocular distance on vertex larger than at ventral eye margin; vertex between compound eyes ± horizontally straight, medially only slightly below dorsal eye margin, vertex medially apubescent, laterally white pubescent, white setose; ocellar triangle apubescent; facial gibbosity distinct, well-developed and discernible in lateral view, mystax covering entire facial gibbosity, white; parafacial area approximately as wide as ½ width of central facial gibbosity (at same level); frons not elevated, medially apubescent, laterally white pubescent, medially asetose, latero-ventrally white; occiput grey pubescent, white setose, median occipital sclerite brown macrosetose; pocl macrosetae absent; postgena sparsely grey pubescent, long, sparsely white setose; clypeus comprised of single sclerite, entirely sclerotized medially, recessed (concave), ventrally simple, posterior to proboscis, laterally connected to face by membranous cuticle; proboscis long, reaching fronto–clypeal suture, brown; labellum large, much wider than prementum, as long as prementum, unsclerotized laterally; maxillary palpus laterally compressed, bilobed apically, light brown, approximately ⅓ length of proboscis.

***Antenna*:** brown; scape white setose dorsally, asetose ventrally; pedicel white setose dorsally and ventrally; postpedicel cylindrical in proximal ⅓, symmetrically bulbous in distal 2/3, ≥ 4.0 times as long as combined length of scape and pedicel, asetose; apical seta-like sensory element situated apically in cavity on postpedicel.

***Thorax*:** brown, predominantly grey pubescent; scutum predominantly black, surface microrugose (slightly rugose 'imitating' pubescence), grey pubescent except for brown pubescent broad median stripe (not reaching posterior margin) and sublateral stripes (interrupted by transverse suture), scutal setation comprised of short white setae in primarily grey pubescent areas; dc setae presuturally white, postsuturally absent, acr setae absent, lateral scutal setae white, npl setae 0, spal setae 0, pal setae 0; proepisternum apubescent medially, grey pubescent laterally, long white setose; proepimeron grey pubescent, asetose; antepronotum antero-medially smooth (without any indentation); lateral postpronotum long white setose; postpronotal lobe yellow, grey pubescent, long white setose; scutellum grey pubescent, discal scutellar setae absent, apical scutellar setae absent; mesopostnotum grey pubescent, asetose; anatergite grey pubescent, asetose; katatergite apubescent, long white setose, elevated and smoothly convex; anepisternum grey pubescent dorsally, apubescent ventrally, anteriorly asetose, posteriorly short white setose, otherwise asetose; katepisternum apubescent, asetose; anepimeron apubescent, asetose; katepimeron apubescent, asetose; meron grey pubescent dorsally, apubescent ventrally, asetose; metakatepisternum large; metanepisternum grey pubescent, asetose; metepimeron yellow (same color as T1), white pubescent, long white setose, ± flat, infra-halter sclerite absent.

***Legs*:** yellow to brown, setation comprised of white setae and brown macrosetae; pro coxa apubescent, short white setose; mes coxa apubescent, long white setose; met coxa laterally unsclerotized (membrane between coxa and metakatepisternum clearly visible), apubescent, long white setose; met trochanter sparsely setose medially; pro + mes femur yellow anteriorly, posteriorly brown, met femur yellow anteriorly, posteriorly brown, distinctly clubbed for nearly entire length, macrosetose with thickened spine-like macrosetae on protuberance in 2 antero-ventral and 2 postero-ventral rows, postero-ventrally sparse, short white setose; pro tibia straight; mes tibia straight; met tibia laterally arched, met tibia cylindrical with distinct ventral keel terminating into distinct spur, spur almost reaching tip of 1st tarsomere, postero-laterally short white, appressed setose; pro + mes tarsomere 1 approximately as long as individual tarsomeres 2, 3, or 4, met tarsomere 1 as long as individual tarsomeres 2, 3, or 4; pulvillus well-developed, as long as well-developed claw, and as wide as base of claw; setiform empodium absent.

***Wing*:** length = 7.8–10.4 mm; hyaline throughout, slightly brown stained along veins, veins light brown, microtrichia absent; cells r_1, r_4, m_3, + cua closed, r_5 open; C terminating at junction with M_1 (or M_1+M_2); Sc long, terminating in C proximal to r-m; R_4 terminates in R_1; R_5 terminates in R_1; auxiliary vein (R_3) at base of R_4 absent; R_4 and R_5 widest apart medially; r-m indistinct, R_{4+5} and M_1 fused, forming an X; M_1 curves slightly anteriorly at r-m, M_1 (or M_1+M_2) terminates in C; base of M_3+M_4 present, M_3+M_4 not terminating together in C (not reaching wing margin), M_4 and CuA split proximally to m-cu (cell m_3 narrow proximally); CuP straight, cell cup wide, CuP

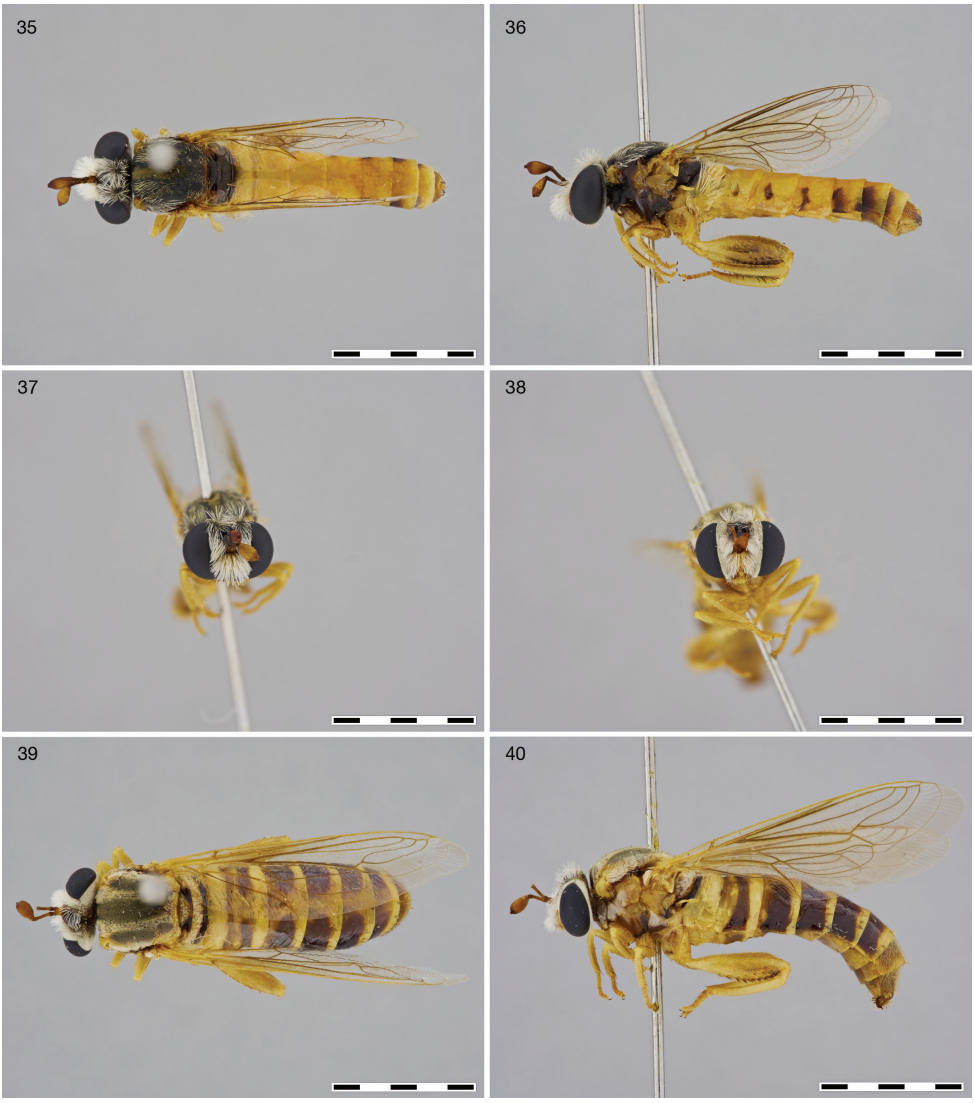

Figures 35–40. *Haplomydas crassipes*: **35** ♂ (NMSA-DIP-77049, Zenodo https://doi.org/10.5281/zenodo.6083941), dorsal (https://doi.org/10.5281/zenodo.6084017) **36** same, lateral (https://doi.org/10.5281/zenodo.6084019) **37** same, head anterior (https://doi.org/10.5281/zenodo.6084021) **38** ♀ (NMSA-DIP-77048, https://doi.org/10.5281/zenodo.6083943), head anterior (https://doi.org/10.5281/zenodo.6084027) **39** same, dorsal (https://doi.org/10.5281/zenodo.6084023) **40** same, lateral (https://doi.org/10.5281/zenodo.6084025). Scale bars: 5 mm.

and wing margin further apart proximally than distally; alula well-developed; halter light yellow, pubescent, dorsally asetose, ventrally yellow setose.

***Abdomen*:** light brown to brown, setation comprised of scattered short white setae, T2–4 parallel-sided and not constricted waist-like, T surface entirely smooth; T1

yellow, T2–7 brown (sometimes medially light brown) with yellow posterior margins; T apubescent; T1 long white setose, T2–7 sparsely short white setose; S1 yellow, S2–7 light brown to brown with yellow posterior margins; S apubescent; S1 and S7 short white setose, S2–6 asetose; bullae on T2 absent.

♀ ***abdomen and genitalia*:** densely arranged anteriorly directed setae present on T7–8 and S8, only few on S7; T8 anterior apodeme present, broad and rectangular, auxiliary spiracle present; T9 formed by wide, rectangular sclerite with median protuberance; T9+10 entirely fused (sclerites indistinguishable), T10 divided into 2 heavily sclerotized acanthophorite plates; 6–8 acanthophorite spines per plate; 2 spermathecae, all equally large, not differentiated from spermathecal ducts, unsclerotized; individual spermathecal duct long; S9 (furca) formed by 1 sclerite, ring-like (joined anteriorly and posteriorly), anterior furcal apodeme present, 2 lateral projections forming divided apodeme, lateral furcal apodeme absent, median furcal bridge absent.

Male. ***Head*:** black, facial gibbosity yellow to light brown, in general densely white pubescent, white setose, regular, cylindrical setae; width distinctly greater than thorax (at postpronotal lobe), interocular distance on vertex larger than at ventral eye margin; vertex between compound eyes ± horizontally straight, medially only slightly below dorsal eye margin, vertex medially apubescent, laterally white pubescent, white setose; ocellar triangle apubescent; facial gibbosity distinct, well-developed and discernible in lateral view, mystax covering entire facial gibbosity, white; parafacial area less than ½ width of central facial gibbosity (at same level); frons not elevated, medially apubescent, laterally white pubescent, medially asetose, latero-ventrally white; occiput grey pubescent, white setose, median occipital sclerite brown macrosetose; pocl macrosetae absent; postgena sparsely grey pubescent, long, sparsely white setose; clypeus comprised of single sclerite, entirely sclerotized medially, recessed (concave), ventrally simple, posterior to proboscis, laterally connected to face by membranous cuticle; proboscis long, reaching fronto–clypeal suture, brown; labellum large, much wider than prementum, as long as prementum, unsclerotized laterally; maxillary palpus laterally compressed, bilobed apically, light brown, approximately ⅓ length of proboscis.

***Antenna*:** brown; scape white setose dorsally, asetose ventrally; pedicel white setose dorsally and ventrally; postpedicel cylindrical in proximal ½, symmetrically bulbous in distal ½, ≥ 4.0 times as long as combined length of scape and pedicel, asetose; apical seta-like sensory element situated apically in cavity on postpedicel.

***Thorax*:** dark brown, predominantly grey pubescent; scutum uniformly black, surface microrugose (slightly rugose 'imitating' pubescence), grey pubescent except for brown pubescent broad median stripe (not reaching posterior margin) and sublateral stripes (interrupted by transverse suture), scutal setation comprised of short white setae in primarily grey pubescent areas; dc setae presuturally white, postsuturally absent, acr setae absent, lateral scutal setae white, npl setae 0, spal setae 0, pal setae 0; proepisternum apubescent medially, grey pubescent laterally, long white setose; proepimeron grey pubescent, asetose; antepronotum antero-medially smooth (without any indentation); lateral postpronotum long white setose; postpronotal lobe yellow, grey pubescent, long white setose; scutellum grey pubescent, discal scutellar setae absent,

apical scutellar setae absent; mesopostnotum grey pubescent, asetose; anatergite grey pubescent, asetose; katatergite apubescent, long white setose, elevated and smoothly convex; anepisternum grey pubescent dorsally, apubescent ventrally, anteriorly asetose, posteriorly short white setose, otherwise asetose; katepisternum apubescent, asetose; anepimeron apubescent, long white setose ventrally; katepimeron apubescent, asetose; meron grey pubescent, median stripe apubescent, asetose; metakatepisternum large; metanepisternum grey pubescent, asetose; metepimeron yellow (same color as T1), white pubescent, long white setose, ± flat, infra-halter sclerite absent.

***Legs*:** yellow to brown, setation comprised of white setae and black macrosetae; pro coxa apubescent, short white setose; mes coxa apubescent, long white setose; met coxa laterally unsclerotized (membrane between coxa and metakatepisternum clearly visible), apubescent, long white setose; met trochanter sparsely setose medially; pro + mes femur yellow anteriorly, posteriorly brown, met femur yellow anteriorly, posteriorly brown, distinctly clubbed for nearly entire length, macrosetose with thickened spine-like macrosetae on protuberance in 2 antero-ventral and 2 postero-ventral rows, postero-ventrally sparse, long white erect setose; pro tibia straight; mes tibia straight; met tibia laterally arched, met tibia cylindrical with distinct ventral keel terminating into distinct spur, spur almost reaching tip of 1st tarsomere, postero-laterally short white, appressed setose; pro + mes tarsomere 1 approximately as long as individual tarsomeres 2, 3, or 4, met tarsomere 1 as long as individual tarsomeres 2, 3, or 4; pulvillus well-developed, as long as well-developed claw, and as wide as the base of the claw; setiform empodium absent.

***Wing*:** length = 7.1–7.6 mm; hyaline throughout, slightly brown stained along veins, veins brown, microtrichia absent; cells r_1, r_4, m_3, + cua closed, r_5 open; C terminating at junction with M_1 (or M_1+M_2); Sc long, terminating in C proximal to r-m; R_4 terminates in R_1; R_5 terminates in R_1; auxiliary vein (R_3) at base of R_4 absent; R_4 and R_5 widest apart medially; r-m indistinct, R_{4+5} and M_1 fused, forming an X, rarely distinct, R_{4+5} and M_1 apart, connected by crossvein; M_1 curves slightly anteriorly at r-m, M_1 (or M_1+M_2) terminates in C; base of M_3+M_4 present, M_3+M_4 not terminating together in C (not reaching wing margin), M_4 and CuA split proximally to m-cu (cell m_3 narrow proximally); CuP straight, cell cup wide, CuP and wing margin further apart proximally than distally; alula well-developed; halter light yellow, pubescent, dorsally asetose, ventrally yellow setose.

***Abdomen*:** yellow to brown, setation comprised of scattered short white setae, T2–4 parallel-sided and not constricted waist-like, T surface entirely smooth; T1–7 yellow to orange, T2–7 antero-laterally brown; T apubescent; T1 and anterior ¼ of T2 long white setose, remaining T2 and T3–T7 sparsely white setose laterally; S1–7 yellow, brown medially; S predominantly apubescent; S1–7 sparsely short white setose; bullae on T2 transversely elongate, long (almost occupying entire lateral aspect of tergite), light brown, surface entirely smooth, T2 surface anterior to bullae smooth.

♂ ***abdomen and terminalia*:** T1–7 well-developed, entirely sclerotized, T8 postero-medially weakly sclerotized, with anterior transverse sclerotized bridge connecting lateral sclerites; T7–8 anteriorly with 2 lateral apodemes; T8 auxiliary spiracle present;

S6 regular, without any special setation postero-medially; S8 simple plate, entire (undivided) ventro-medially, not fused to T8 dorso-laterally; epandrium formed by 2 sclerites, separated disto-medially and fused antero-medially, distally in dorsal view blunt with short, strong macrosetae at tip; subepandrial sclerite without lateral or median protuberances; hypandrium concave, cup-shaped, entirely sclerotized ventrally, entirely fused with gonocoxite, forming a gonocoxite-hypandrial complex, supra-hypandrial sclerite absent; gonocoxite simple, long, slightly curved dorsally, with median protuberance, gonocoxal apodeme absent; 2 functional phallic prongs, short and wide, medio-distally connected, parallel or diverging laterally, distally straight or only diverging slightly laterally; phallic epimere absent; lateral ejaculatory process absent; ejaculatory apodeme formed by single dorso-ventrally oriented plate; ventro-median margin of parameral sheath heavily sclerotized (appearing entirely closed); parameral sheath long, sperm sac entirely covered; sperm sac appearing ± heavily sclerotized.

Type locality. Zimbabwe: Bulawayo: Bulawayo (20°09'00"S, 028°35'00"E, -20.15, 28.58333).

Material examined. Botswana: Central: 1♂ Serowe, Farmers Brigade, 22°09'58"S, 026°43'31"E, 1990-04-00, Malaise trap, Forchhammer, P. (AAM-000809, NMSA); 4♂ Serowe, Farmers Brigade, 22°09'58"S, 026°43'31"E, 1987-04-00, Malaise trap, Forchhammer, P. (USNMENT00832025, USNMENT00832027, USNMENT00832028, USNMENT00891896, USNM); 1♀ Serowe, Farmers Brigade, 22°09'58"S, 026°43'31"E, 1987-04-00, Malaise trap, Forchhammer, P. (USNMENT00832026, USNM); Kgatleng: 2♀ Mochudi, 24°25'00"S, 026°08'00"E, 1982-04-19–1982-04-21, Louw, S. (BMSA(D)00087, BMSA(D)00091, BMSA); 4♂ Mochudi, 24°25'00"S, 026°08'00"E, 1982-04-19–1982-04-21, Louw, S. (BMSA(D)00088, BMSA(D)00089, BMSA(D)00090, BMSA(D)00092, BMSA); Mozambique: Gaza: 1♀ Mapai, 22°51'08"S, 031°58'02"E, 1951-05-00, Zumpt, F. (NMSA-DIP-044922, NMSA); Manica: 2♂ Zambéze amont de Tambara (= Nhacolo) Njanassé, Lac Msica, 16°38'21"S, 034°07'28"E, 1929-00-00, Lesne, P. (AAM-001199, AAM-001200, MNHN); 1♂ Inhacoro (= Nhacolo), 16°42'57"S, 034°15'10"E, 1928-05-00, Lesne, P. (Paratype *Heleomydas lesnei*, MNHN); Sofala: 1♂ Nova Chupanga, 17°07'32"S, 034°51'34"E, 0000-05-00, Lesne, P. (Holotype *Heleomydas lesnei*, MNHN); Namibia: Hardap: 2♂ Rehoboth, 9 km S, 23°23'28"S, 017°06'23"E, 1990-03-16, Pulawski, W. (CASENT8380010, CASENT8380011, CAS); 1♂ Rehoboth, 9 km S, 23°23'59"S, 017°04'12"E, 1990-03-16, Schwarz, M. (AAM-000872, Coll. Hauser); Khomas: 2♂ Seeis, 9 km ESE, 20°28'00"S, 017°38'00"E, 1976-03-12, Rozen, J. (AAM-000097, AAM-000098, AMNH); 1♂ Seeis, 22 km ESE, 20°31'00"S, 017°45'00"E, 1976-03-14, Rozen, J. (AAM-000099, AMNH); 1♀ Seeis, 22 km ESE, 20°31'00"S, 017°45'00"E, 1976-03-14, Rozen, J. (AAM-000100, AMNH); 2♀ Windhoek, 26 km N Road 1/6, 22°20'00"S, 017°04'00"E, 1984-03-29, dry stream bed *Acacia* riparian woodland, Londt, J., Stuckenberg, B. (NMSA-DIP-77046, NMSA-DIP-77050, NMSA); 1♂ Windhoek, 26 km N Road 1/6, 22°20'00"S, 017°04'00"E, 1984-03-29, dry stream bed *Acacia*

riparian woodland, Londt, J., Stuckenberg, B. (NMSA-DIP-77047, NMSA); 1♀ Windhoek, 36 km E Road 6/1, 22°30'00"S, 017°22'00"E, 1984-03-17, dry river bed *Acacia* savanna / grassland, Londt, J., Stuckenberg, B. (NMSA-DIP-77048, NMSA); 1♂ Windhoek, 36 km E Road 6/1, 22°30'00"S, 017°22'00"E, 1984-03-17, dry river bed *Acacia* savanna / grassland, Londt, J., Stuckenberg, B. (NMSA-DIP-77049, NMSA); 1♂ Gamsberg, E of pass, 23°20'00"S, 016°20'00"E, 1999-03-12, Gess, F., Gess, S. (AAM-000203, AMGS); Omaheke: 2♀ Witvlei, 22°24'35"S, 018°29'30"E, 1970-03-01, Ross, E. (CASENT8380006, CASENT8380007, CAS); 1♂ Witvlei, 22°24'35"S, 018°29'30"E, 1970-03-01, Ross, E. (CASENT8380008, CASENT8380009, CAS); Otjozondjupa: 1♂ Gross Barmen Resort, 22°06'42"S, 016°44'48"E, 1992-03-19, at night, O'Brian, C., O'Brian, L., Marshall, G. (AAM-009904, CSCA); Zimbabwe: Bulawayo: 1♀ Bulawayo, 20°09'00"S, 028°35'00"E, 1917-05-00, Tucker, R. (SAM-DIP-A007141, Holotype, SAMC); Zimbabwe: 1♂ Worlds View, 18°09'49"S, 032°46'29"E, 1925-04-24, Stevenson, R. (NMSA-DIP-044922, NMSA); 1♂ Bazely Bridge, 19°15'01"S, 032°29'23"E, 1965-04-20, Cookson, D. (NMSA-DIP-031720, NMSA); Matabeleland North: 1♀ Khami Ruins, 20°09'30"S, 028°22'36"E, 1924-04-19, Rhodesia Museum (AAM-000647, NHMUK); 1♂ Khami Ruins, 20°09'30"S, 028°22'36"E, 1924-04-19, Rhodesia Museum (AAM-000648, NHMUK); 1♂ Khami, 20°09'30"S, 028°22'36"E, 1927-04-17, Rhodesia Museum (AAM-009508, NHMW); 1♀ Khami Ruins, 20°09'30"S, 028°22'36"E, 1924-04-19, Rhodesia Museum (NMZ1701, NMBZ); 1♂ Khami, 20°09'30"S, 028°22'36"E, 1927-04-17, Rhodesia Museum (NMZ1707, NMBZ); Matabeleland South: 1♀ Matopos, 20°23'02"S, 028°30'28"E, 1920-05-02, Rhodesia Museum (Holotype *Rhopalia flavomarginata*, BMNH(E)241675, NHMUK); 1♂ Matopos, 20°23'02"S, 028°30'28"E, 1925-04-22, Stevenson, R. (NMSA-DIP-044921, NMSA); 3♀ 6♂ Matopos Hills, 20°26'39"S, 028°30'58"E, 1932-04-00, Ogilvie, L. (AAM-000652–AAM-000660, NHMUK); 1♂ Matopos Hills, 20°26'39"S, 028°30'58"E, 1932-04-00, Ogilvie, L. (AAM-003022, RBINS); 1?* Balla-Balla (= Mbalabala), 20°26'60"S, 029°02'09"E, no date, along sandy path in Mopane forest (AAM-000072, RBINS); 1♀ Balla-Balla (= Mbalabala), 20°26'60"S, 029°02'09"E, 1933-03-00, Cuthbertson, A. (AAM-001357, RBINS); 1♀ 2♂ Balla-Balla (= Mbalabala), 20°26'60"S, 029°02'09"E, 1933-02-00, Cuthbertson, A. (AAM-000095–AAM-000096, AMNH); 1♀ Ori River, Matopos, 20°33'26"S, 028°30'49"E, 1930-05-01, Stevenson, R. (NMZ1709, NMBZ); 3♂ Beit Bridge, 22°12'51"S, 029°59'29"E, 1932-04-00, Ogilvie, L. (AAM-000071, AAM-000649, AAM-000650, NHMUK); 1♀ Beit Bridge, 22°12'51"S, 029°59'29"E, 1932-04-00, Ogilvie, L. (AAM-008033, NHMUK); 1♀ Beit Bridge, 22°12'51"S, 029°59'29"E, 1932-04-00, Ogilvie, J. (SDEI); Midlands: 1♂ Shangani, De Beer's Ranch, 19°00'00"S, 028°54'00"E, 1932-05-00, Ogilvie, L. (AAM-000651, NHMUK).

Distribution, biodiversity hotspots, phenology, and biology. See above for genus.

Remarks. Dikow (2017) reported that the females of *H. crassipes* appear to lack bullae on the postero-lateral surface of abdominal tergite 2.

***Lachnocorynus* Hesse, 1969**
http://zoobank.org/16632F70-15EE-4FF7-8DA7-D2B97BEF5505
Original description online https://www.biodiversitylibrary.org/page/40724405
GBIF https://www.gbif.org/species/1591101

Lachnocorynus Hesse, 1969: 46. Type-species: *Lachnocorynus chobeensis* Hesse, 1969, by original designation.

Diagnosis. The genus can be delineated by the densely setose head, the distinctly and deeply rugose scutum, and the costal vein terminating where M_1 joins the wing margin.

Distribution, biodiversity hotspots, phenology, and biology. Known only from three disjunct localities in northern Namibia, north-eastern Botswana, and north-eastern Zimbabwe (Fig. 56). A rarely collected genus known only from four specimens in museum collections, three collecting events between 1930–1986 (Table 1), and one observation on iNaturalist in 2019 (https://www.inaturalist.org/observations/26760859). The genus is not known to occur in any biodiversity hotspot. Adult flies are active in mid to late winter (Table 2), which corresponds to the dry season and lower temperatures. Nothing is known of the biology.

***Lachnocorynus chobeensis* Hesse, 1969**
http://zoobank.org/2AFB5F72-F10D-4836-A113-EC20704E6EB5
Original description online https://www.biodiversitylibrary.org/page/40724407
GBIF https://www.gbif.org/species/1591103
Figs 41–49, 55, 56

Lachnocorynus kochi Hesse, 1969, syn. nov. ZooBank http://zoobank.org/F341EDA4-F1C6-4B14-8015-F95D23C30BF9. Original description online https://www.biodiversitylibrary.org/page/40724409

Diagnosis. The species is distinguished from congeners by the wide face and vertex (similar width), the entirely apubescent anepimeron, and the sparsely grey pubescent abdominal tergites.

Redescription. Female. *Head*: brown, facial gibbosity yellow, in general white pubescent, white setose, regular, cylindrical setae; width distinctly greater than thorax (at postpronotal lobe), interocular distance on vertex larger than at ventral eye margin; vertex between compound eyes ± horizontally straight, medially only slightly below dorsal eye margin, vertex white pubescent, white setose; ocellar triangle apubescent; facial gibbosity distinct, well-developed and discernible in lateral view, mystax covering entire facial gibbosity, white; parafacial area approximately as wide as ¾ width of central gibbosity (at same level); frons not elevated, medially apubescent, laterally white pubescent, white setose; occiput grey pubescent, white setose, median occipital sclerite brown macrosetose; pocl macrosetae absent; postgena sparsely grey pubescent, long, sparsely white setose; clypeus comprised of single sclerite, entirely sclerotized medially,

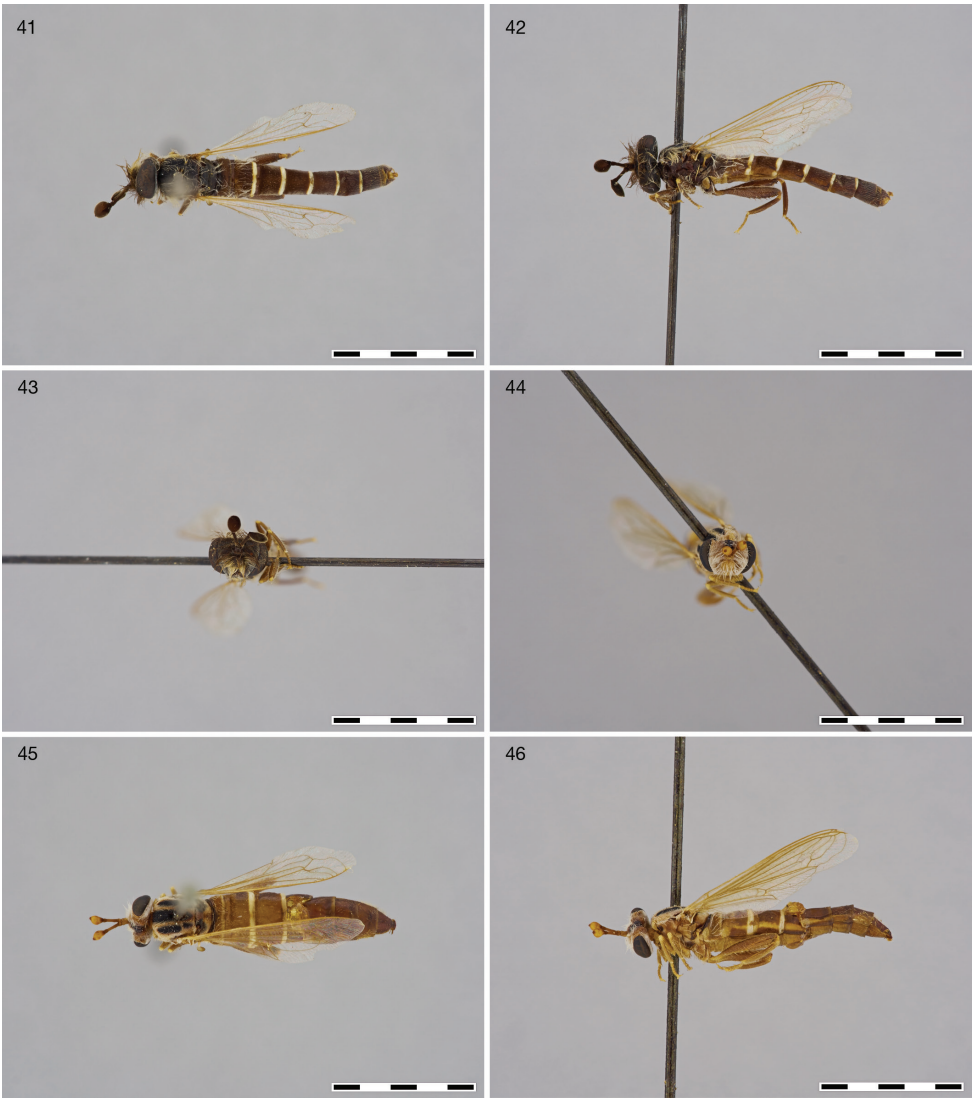

Figures 41–46. *Lachnocorynus chobeensis*: **41** ♂ holotype (NMSA-Dip-43314, Zenodo https://doi.org/10.5281/zenodo.6083945), dorsal (https://doi.org/10.5281/zenodo.6084029) **42** same, lateral (https://doi.org/10.5281/zenodo.6084031) **43** same, head anterior (https://doi.org/10.5281/zenodo.6084033) **44** ♀ paratype (NMSA-Dip-57787, https://doi.org/10.5281/zenodo.6083949), head anterior (https://doi.org/10.5281/zenodo.6084045) **45** same, dorsal (https://doi.org/10.5281/zenodo.6084041) **46** same, lateral (https://doi.org/10.5281/zenodo.6084043). Scale bars: 5 mm.

recessed (concave), ventrally simple, posterior to proboscis, laterally connected to face by membranous cuticle; proboscis short, nob-like, occupying approximately ⅓ length of oral cavity, light brown; labellum small, as wide as prementum, as long as prementum, unsclerotized laterally; maxillary palpus laterally compressed (triangular), light brown, approximately ½ length of proboscis.

***Antenna*:** brown; scape white setose dorsally, asetose ventrally; pedicel light brown setose dorsally and ventrally; postpedicel cylindrical in proximal ½, symmetrically bulbous in distal ½, ≥ 2.0 times as long as combined length of scape and pedicel, asetose; apical seta-like sensory element situated apically in cavity on postpedicel.

***Thorax*:** black or light brown to black, predominantly white pubescent; scutum black, light brown stripes medially and laterally, surface macrorugose (distinctly and deeply rugose), predominantly apubescent, paramedian stripes (merging on posterior margin) and lateral margins grey pubescent, scutal setation comprised of long white setae in pubescent areas; dc setae pre- and postsuturally white, acr setae absent, lateral scutal setae white, npl setae 0, spal setae 0, pal setae 0; proepisternum apubescent medially, grey pubescent laterally, long white setose; proepimeron grey pubescent, asetose; antepronotum antero-medially smooth (without any indentation); lateral postpronotum long white setose; postpronotal lobe yellow, white pubescent, long white setose; scutellum grey pubescent, discal scutellar setae absent, apical scutellar setae absent; mesopostnotum grey pubescent, asetose; anatergite grey pubescent, asetose; katatergite apubescent, long white setose, elevated and smoothly convex; anepisternum white pubescent, anteriorly asetose, posteriorly 1–2 white setae postero-ventrally, otherwise asetose; katepisternum white pubescent dorsally, apubescent ventrally, asetose; anepimeron white pubescent, posterior ½ apubescent, asetose; katepimeron white pubescent, asetose; meron white pubescent, median stripe apubescent, asetose; metakatepisternum large; metanepisternum white pubescent, asetose; metepimeron yellow (same color as T1), white pubescent, long white setose, ± flat, infra-halter sclerite absent.

***Legs*:** light brown to brown, setation comprised of white setae and brown macrosetae; pro coxa sparsely grey pubescent, long white setose; mes coxa sparsely grey pubescent, long white setose; met coxa laterally unsclerotized (membrane between coxa and metakatepisternum clearly visible), sparsely grey pubescent, long white setose; met trochanter setose medially; pro + mes femur light brown to brown, met femur light brown to brown, evenly clubbed in distal ¾, macrosetose, 1 antero-ventral and 1 postero-ventral row of macrosetae, postero-ventrally long white, erect setose with setae arranged in distinct row; pro tibia laterally arched; mes tibia laterally arched; met tibia laterally arched, met tibia cylindrical with distinct ventral keel terminating into distinct spur, postero-laterally sparse long white, erect setose with setae arranged in distinct row; pro + mes tarsomere 1 slightly longer than tarsomere 2, met tarsomere 1 slightly longer than tarsomere 2; pulvillus well-developed, as long as well-developed claw, and as wide as the base of the claw; setiform empodium absent.

***Wing*:** length = 7.4 mm; hyaline throughout, veins light brown, microtrichia absent; cells r_1, r_4, m_3, + cua closed, r_5 open; C terminating at junction with M_1 (or M_1+M_2); Sc long, terminating in C proximal to r-m; R_4 terminates in R_1; R_5 terminates in R_1; auxiliary vein (R_3) at base of R_4 absent; R_4 and R_5 widest apart medially; r-m indistinct, R_{4+5} and M_1 fused, forming an X; M_1 curves slightly anteriorly at r-m, M_1 (or M_1+M_2) terminates in C; base of M_3+M_4 present, M3+M_4 not terminating together in C (not reaching wing margin), M_4 and CuA split proximally to m-cu (cell m_3

Figures 47–49. *Lachnocorynus chobeensis* (♂ holotype of *Lachnocorynus kochi*, NMSA-Dip-43304, Zenodo https://doi.org/10.5281/zenodo.6083947): **47** dorsal (https://doi.org/10.5281/zenodo.6084035) **48** lateral (https://doi.org/10.5281/zenodo.6084037) **49** head anterior (https://doi.org/10.5281/zenodo.6084039). Scale bars: 5 mm.

narrow proximally); CuP straight, cell cup wide, CuP and wing margin further apart proximally than distally; alula well-developed; halter light brown, pubescent, dorsally asetose, ventrally yellow setose.

***Abdomen*:** brown, setation comprised of scattered short white setae, T2–4 parallel-sided and not constricted waist-like, T surface entirely smooth; T1–3 brown with white posterior margin, T4–7 brown; T apubescent; T1 long white setose, T2–7 short white setose; S1–7 light brown; S apubescent; S1–7 sparsely short yellow setose; bullae on T2 transversely elongate, brown, surface entirely smooth, T2 surface anterior to bullae smooth.

♀ ***abdomen and genitalia*:** densely arranged anteriorly directed setae present on T7–8 and S7–8; T8 anterior apodeme indiscernible (not dissected), auxiliary spiracle indiscernible (not dissected); T9 formed by wide, rectangular sclerite with median protuberance; T9+10 entirely fused (sclerites indistinguishable), T10 divided into 2 heavily sclerotized acanthophorite plates; 5 acanthophorite spines per plate.

Male. *Head*: black, in general grey pubescent, light brown, regular, cylindrical setae; width distinctly greater than thorax (at postpronotal lobe), interocular distance on vertex larger than at ventral eye margin; vertex between compound eyes ± horizontally straight, medially only slightly below dorsal eye margin, vertex grey pubescent, white setose; ocellar triangle apubescent; facial gibbosity distinct, well-developed and discernible

in lateral view, mystax covering entire facial gibbosity, light brown, white ventrally; parafacial area approximately as wide as ¾ width of central gibbosity (at same level); frons not elevated, medially apubescent, laterally grey pubescent, dark brown; occiput grey pubescent, white setose, median occipital sclerite brown macrosetose; pocl macrosetae absent; postgena sparsely grey pubescent, long, sparsely light brown setose; clypeus comprised of single sclerite, entirely sclerotized medially, recessed (concave), ventrally simple, posterior to proboscis, laterally connected to face by membranous cuticle; proboscis short, nob-like, occupying approximately ⅓ length of oral cavity, brown; labellum small, as wide as prementum, as long as prementum, unsclerotized laterally; maxillary palpus laterally compressed (triangular), brown, approximately ½ length of proboscis.

***Antenna*:** brown; scape white setose dorsally, asetose ventrally; pedicel light brown setose dorsally and ventrally; postpedicel cylindrical in proximal ½, symmetrically bulbous in distal ½, ≥ 3.0 times as long as combined length of scape and pedicel, asetose; apical seta-like sensory element situated apically in cavity on postpedicel.

***Thorax*:** black or brown, predominantly grey pubescent; scutum uniformly black, surface macrorugose (distinctly and deeply rugose), predominantly apubescent, paramedian stripes (merging on posterior margin) and lateral margins grey pubescent, scutal setation comprised of long white to yellow setae in pubescent areas; dc setae pre- and postsuturally white, acr setae absent, lateral scutal setae white, npl setae 0, spal setae 0, pal setae 0; proepisternum apubescent medially, grey pubescent laterally, long white setose; proepimeron grey pubescent, asetose; antepronotum antero-medially smooth (without any indentation); lateral postpronotum long white setose; postpronotal lobe light brown, grey pubescent, long white setose; scutellum grey pubescent, discal scutellar setae absent, apical scutellar setae absent; mesopostnotum grey pubescent, asetose; anatergite grey pubescent, asetose; katatergite apubescent, long white setose, elevated and smoothly convex; anepisternum sparsely grey pubescent, anteriorly asetose, posteriorly asetose, otherwise asetose; katepisternum dorsally sparsely grey pubescent, asetose; anepimeron apubescent, asetose; katepimeron sparsely grey pubescent, asetose; meron apubescent, asetose; metakatepisternum large; metanepisternum grey pubescent, asetose; metepimeron brown (same color as T1), grey pubescent, long white setose, ± flat, infra-halter sclerite absent.

***Legs*:** brown, setation comprised of white setae and brown macrosetae; pro coxa sparsely grey pubescent, long white setose; mes coxa sparsely grey pubescent, long white setose; met coxa laterally unsclerotized (membrane between coxa and metakatepisternum clearly visible), sparsely grey pubescent, long white setose; met trochanter setose medially; pro + mes femur brown, met femur brown, evenly clubbed in distal ¾, macrosetose, 1 antero-ventral and 1 postero-ventral row of macrosetae, postero-ventrally long white, erect setose with setae arranged in distinct row; pro tibia laterally arched; mes tibia laterally arched; met tibia laterally arched, met tibia cylindrical with distinct ventral keel terminating into distinct spur, postero-laterally sparse long white, erect setose with setae arranged in distinct row; pro + mes tarsomere 1 slightly longer than tarsomere 2, met tarsomere 1 slightly longer than tarsomere 2; pulvillus well-developed, as long as well-developed claw, and as wide as the base of the claw; setiform empodium absent.

***Wing*:** length = 6.0 mm; hyaline throughout, veins light brown, microtrichia absent; cells r_1, r_4, m_3, + cua closed, r_5 open; C terminating at junction with M_1 (or

M_1+M_2); Sc long, terminating in C proximal to r-m; R_4 terminates in R_1; R_5 terminates in R_1; auxiliary vein (R_3) at base of R_4 absent; R_4 and R_5 widest apart medially; r-m indistinct, R_{4+5} and M_1 fused, forming an X; M_1 curves slightly anteriorly at r-m, M_1 (or M_1+M_2) terminates in C; base of M_3+M_4 present, M_3+M_4 not terminating together in C (not reaching wing margin), M_4 and CuA split proximally to m-cu (cell m_3 narrow proximally); CuP straight, cell cup wide, CuP and wing margin further apart proximally than distally; alula well-developed; halter light brown, pubescent, dorsally asetose, ventrally yellow setose.

***Abdomen*:** brown, setation comprised of scattered short white setae, T2–4 parallel-sided and not constricted waist-like, T surface entirely smooth; T1 brown, T2–6 brown with white posterior margin, T7 brown; T sparsely grey pubescent; T1–2 long white setose, T3–7 short white setose; S1–6 light brown, S7 brown; S1–3 apubescent, S4–7 sparsely grey pubescent; S1–7 short white setose; bullae on T2 transversely elongate, light brown, surface entirely smooth, T2 surface anterior to bullae smooth.

♂ ***abdomen and terminalia*:** not dissected.

Type locality. Botswana: Chobe: Kabulabula, Chobe river (17°48'41"S, 024°56'48"E, -17.81139, 24.94667).

Material examined. Botswana: Chobe: 1♂ Kabulabula, Chobe river, 17°48'41"S, 024°56'48"E, 1930-07-11–1930-07-24, Vernay-Lang Kalahari Expedition (NMSA-DIP-43314, Holotype, NMSA); 1♀ Kabulabula, Chobe river, 17°48'41"S, 024°56'48"E, 1930-07-11–1930-07-24, Vernay-Lang Kalahari Expedition (NMSA-DIP-57787, Paratype, NMSA); Namibia: Ohangwena: 1♂ Oshikango, 17°24'00"S, 015°53'00"E, 1948-07-00, Koch, C. (NMSA-DIP-43304, Holotype *Lachnocorynus kochi*, NMSA).

Observations at iNaturalist. Botswana: Ngamiland: 18°57'56"S, 22°56'32"E, 2019-06-10, Taylor, R. (record URL www.inaturalist.org/observations/26760859).

Distribution, biodiversity hotspots, phenology, and biology. Known only from three localities in northern Botswana and north-central Namibia (Fig. 56). A rarely collected species known only from three specimens and two collecting events in 1930 and 1948 and one observation in 2019 (Table 1). The species is not known to occur in any currently recognized biodiversity hotspot. Adult flies are active in June–July in mid winter (Table 2), which corresponds to the dry season and lower temperatures (data for Kasane, Botswana, see https://worldweather.wmo.int/en/city.html?cityId=1545 and Oshikango, Namibia, see https://www.worldweatheronline.com/oshikango-weather-averages/ohangwena/na.aspx). Nothing is known of the biology.

Remarks. The male holotype of *L. kochi* is not well-preserved (Figs 47–49) and it cannot in any meaningful way be distinguished from *L. chobeensis*. The only differences of the male holotypes pertain to the abdominal colouration (T1 and T7 entirely brown in *L. chobeensis* and all tergites with yellow posterior margins in *L. kochi*). The male terminalia were not dissected but are morphologically very similar based on the externally visible structures. These minute differences in colouration cannot be utilized to delineate species and we, therefore, synonymize the two species. Both species were described by Hesse (1969) and he designated *L. chobeensis* as the type species of the genus. We, therefore, assign *L. chobeensis* as the senior synonym and this species has also been collected in both the female and male sex during the same collecting event.

***Lachnocorynus stenocephalus* sp. nov.**
http://zoobank.org/42B6D785-DD4A-4B33-951F-D18E986D00C4
GBIF https://www.gbif.org/species/1591101 (genus record)
Figs 50–52, 56

Diagnosis. The species is distinguished from congeners by the very narrow face (vertex much wider than face), the medially apubescent anepimeron (grey pubescent dorsally and ventrally), the apubescent katepimeron, and the apubescent abdominal tergites.

Etymology. Greek *steno* = narrow, *cephalos* = head. The specific epithet refers to the very narrow ventral face of this species.

Description. Female. unknown.

Male. ***Head*:** black, facial gibbosity brown, in general grey pubescent, white and light brown, regular, cylindrical setae; width distinctly greater than thorax (at postpronotal lobe), interocular distance on vertex distinctly larger than at ventral eye margin; vertex between compound eyes slightly depressed (less than 60° angle on median eye margin), vertex predominantly apubescent, only lateral margin grey pubescent, white setose; ocellar triangle apubescent; facial gibbosity distinct, well-developed and discernible in lateral view, mystax covering entire facial gibbosity, light brown, white ventrally; parafacial area approximately as wide as ½ width of central facial gibbosity (at same level); frons not elevated, medially apubescent, laterally grey pubescent, medially asetose, latero-ventrally brown; occiput grey pubescent, white setose, median occipital sclerite light brown macrosetose; pocl macrosetae absent; postgena sparsely grey pubescent, long, sparsely white setose; clypeus comprised of single sclerite, entirely sclerotized medially, recessed (concave), ventrally simple, posterior to proboscis, laterally connected to face by membranous cuticle; proboscis short, nob-like, occupying approximately ⅓ length of oral cavity, light brown; labellum small, as wide as prementum, as long as prementum, unsclerotized laterally; maxillary palpus cylindrical, light brown, longer than ½ length of proboscis.

***Antenna*:** brown; scape asetose; pedicel white setose dorsally and ventrally; postpedicel indiscernible (broken).

***Thorax*:** black, predominantly grey pubescent; scutum uniformly black, surface macrorugose (distinctly and deeply rugose), predominantly apubescent, paramedian stripes (merging on posterior margin) grey to light brown pubescent and lateral margins grey pubescent, scutal setation comprised of long white to yellow setae in pubescent areas; dc setae pre- and postsuturally white or yellow, acr setae absent, lateral scutal setae white, npl setae 0, spal setae 0, pal setae 0; proepisternum apubescent medially, grey pubescent laterally, long white setose; proepimeron grey pubescent, asetose; antepronotum antero-medially smooth (without any indentation); lateral postpronotum long white setose; postpronotal lobe yellow, grey pubescent, long white setose; scutellum sparsely grey pubescent, discal scutellar setae absent, apical scutellar setae absent; mesopostnotum partly grey pubescent, asetose; anatergite grey pubescent, asetose; katatergite apubescent, long white setose, slightly elevated, smoothly convex; anepisternum grey pubescent, anteriorly asetose, posteriorly asetose, otherwise asetose; katepisternum dorsally grey pubescent, ventrally apubescent, asetose; anepimeron dorsally

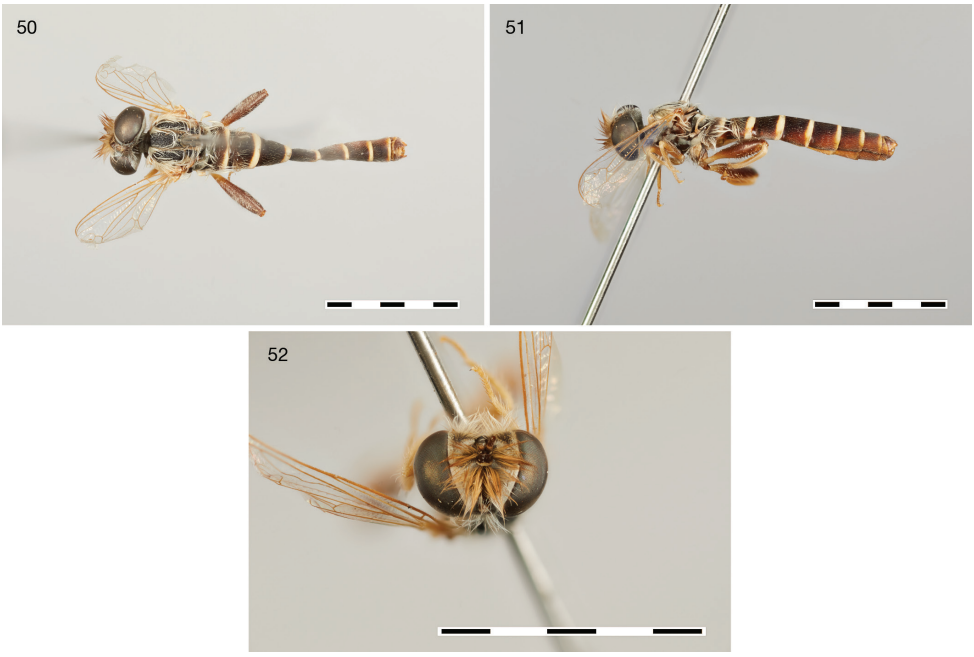

Figures 50–52. *Lachnocorynus stenocephalus* sp. nov. ♂ holotype (AAM-003060, Zenodo https://doi.org/10.5281/zenodo.6083951): **50** dorsal (https://doi.org/10.5281/zenodo.6084047) **51** lateral (https://doi.org/10.5281/zenodo.6084049) **52** head anterior (https://doi.org/10.5281/zenodo.6084051). Scale bars: 5 mm.

and ventrally grey pubescent, median stripe apubescent, asetose; katepimeron apubescent, asetose; meron grey pubescent, median stripe apubescent or white pubescent, median stripe apubescent, asetose; metakatepisternum large; metanepisternum grey pubescent, asetose; metepimeron brown (same color as T1), sparsely grey pubescent, long white setose, ± flat, infra-halter sclerite absent.

***Legs*:** yellow to brown, setation comprised of white setae and brown macrosetae; pro coxa sparsely grey pubescent, long white setose; mes coxa sparsely grey pubescent, long white setose; met coxa laterally unsclerotized (membrane between coxa and metakatepisternum clearly visible), sparsely grey pubescent, long white setose; met trochanter setose medially; pro + mes femur yellow, met femur brown, evenly clubbed in distal ¾, macrosetose, 1 antero-ventral and 1 postero-ventral row of macrosetae, 2 macrosetae anteriorly distally, postero-ventrally sparse, long white erect setose; pro tibia straight; mes tibia straight; met tibia laterally arched, met tibia cylindrical with distinct ventral keel terminating into distinct spur, postero-laterally short white, appressed setose; pro + mes tarsomere 1 approximately as long as individual tarsomeres 2, 3, or 4, met tarsomere 1 as long as individual tarsomeres 2, 3, or 4; pulvillus well-developed on pro and mes legs, smaller on met legs; setiform empodium absent.

***Wing*:** length = 5.7 mm; hyaline throughout, veins yellow, microtrichia absent; cells r_1, r_4, m_3, + cua closed, r_5 open; C terminating at junction with M_1 (or M_1+M_2); Sc long, terminating in C proximal to r-m; R_4 terminates in R_1; R_5 terminates in R_1;

Figures 53–55. Metathoracic coxa in lateral view: **53** *Eremohaplomydas gobabebensis* sp. nov. (USNMENT01518012, crop of Fig. 11) **54** *Haplomydas crassipes* (NMSA-DIP-77049, crop Fig. 36) **55** *Lachnocorynus chobeensis* (NMSA-Dip-43314, crop of Fig. 42).

auxiliary vein (R_3) at base of R_4 absent; R_4 and R_5 widest apart medially; r-m distinct, R_{4+5} and M_1 apart, connected by crossvein; M_1 curves slightly anteriorly at r-m, M_1 (or M_1+M_2) terminates in C; base of M_3+M_4 present, M_3+M_4 not terminating together in C (not reaching wing margin), M_4 and CuA split proximally to m-cu (cell m_3 narrow proximally); CuP straight, cell cup wide, CuP and wing margin further apart proximally than distally; alula well-developed; halter light yellow, pubescent, asetose.

***Abdomen*:** brown, setation comprised of scattered short white setae, T2–4 parallel-sided and not constricted waist-like, T surface entirely smooth; T1–7 dark brown dorsally, brown laterally, posterior margins yellowish; T apubescent; T1–2 long white setose, T3–7 short white setose; S1–5 yellow with white posterior margins, S6–8 light brown; S apubescent; S1 asetose, S2–7 sparsely white setose; bullae on T2 transversely elongate, light brown, surface entirely smooth, T2 surface anterior to bullae smooth.

♂ ***abdomen and terminalia*:** T1–7 well-developed, entirely sclerotized, T8 postero-medially weakly sclerotized, with anterior transverse sclerotized bridge connecting lateral sclerites. ♂ terminalia not dissected.

Type locality. Zimbabwe: Mashonaland East: Kotwa, Chimana Causeway (17°06'00"S, 032°38'00"E, -17.1, 32.63333).

Material examined. Zimbabwe: Mashonaland East: 1♂ Kotwa, Chimana Causeway, 17°06'00"S, 032°38'00"E, 1986-08-05, Lillig, M., Potel, S. (AAM-003060, Holotype, SNSB-ZSM).

Distribution, biodiversity hotspots, phenology, and biology. Known only from the type locality in north-eastern Zimbabwe (Fig. 56). A rarely collected species known only from a single specimen and collecting event in 1986 (Table 1). The species is not known to occur in any currently recognized biodiversity hotspot. Adult flies are active in late winter (Table 2), which corresponds to the dry season and lower temperatures (data for Mount Darwin, Zimbabwe, see https://worldweather.wmo.int/en/city.html?cityId=956). Nothing is known of the biology.

Key to species of *Eremohaplomydas*, *Haplomydas*, and *Lachnocorynus*

An online, illustrated version of the below dichotomous key is available at https://keys.lucidcentral.org/keys/v4/eremohaplomydas-dichotomous. An online, illustrated matrix-based, multi-access key is available at http://keys.lucidcentral.org/keys/v4/eremohaplomydas-matrix.

1 Proboscis distinct and long, almost reaching fronto-clypeal suture; widespread in southern Africa (Fig. 2) ..... ***Haplomydas crassipes***

– Proboscis short or minute, clearly not reaching fronto-clypeal suture; restricted geographically (see Fig. 2) **2**

2 Proboscis very small or minute (Figs 31–34); C terminating at R_1 (Fig. 10); pro and mes coxae anteriorly with either macrosetae or dorso-ventrally flattened setae; clypeus connected to face laterally by sclerotized cuticle; scutum surface smooth or only microrugose (slightly rugose 'imitating' pubescence)..... **4**

– Proboscis short and knob-like but easily discernible, occupying approximately 1/3 of oral cavity (Fig. 43); C terminating at M_1 (Figs 42, 46); pro and mes coxae anteriorly with only regular setae; clypeus connected to face laterally by membranous cuticle; scutum distinctly macrorugose (distinctly and deeply rugose)..... **3**

3 Interocular distance on vertex distinctly larger than at ventral eye margin, face ventrally very narrow (only males known, Fig. 52); mystax predominantly light brown (white dorsally); in males parafacial area approximately as wide as 1/2 width of central facial gibbosity; north-eastern Zimbabwe..... ..... ***Lachnocorynus stenocephalus* sp. nov.**

– Interocular distance on vertex only slightly larger than at ventral eye margin (Fig. 49); mystax predominantly white (brown dorsally); in males parafacial area approximately as wide as 3/4 width of central gibbosity; northern Botswana and north-central Namibia ..... ***Lachnocorynus chobeensis***

4 Alula well-developed; cell r_4 closed with R_4 and R_5 terminating together in R_1; anepisternum setose anteriorly and posteriorly; anepimeron setose **6**

– Alula entirely reduced; cell r_4 closed with R_4 and R_5 terminating independently in R_1; anepisternum asetose; anepimeron asetose..... **5**

5 Females with T3–8 apubescent, T1 entirely pubescent, T2 medially pubescent (Fig. 4); males with single macroseta on katepimeron (females asetose); larger flies with wing length 7.7–9.9 mm (1 male 5.6 mm); distributed in northern Namib desert (Fig. 56) ..... ***Eremohaplomydas desertorum***

– Females with T5–8 apubescent, T1–3 entirely pubescent, T4 medially pubescent (Fig. 23); katepimeron asetose in females and males; generally smaller flies with wing length 5–8 mm; distributed in central Namib desert (Fig. 57)..... ***Eremohaplomydas whartoni* sp. nov.**

6 All occipital setae setose only; base of vein M_3+M_4 absent (irregular wing venation); scutum entirely densely golden pubescent; distributed in central Namib desert (Fig. 56); females unknown ..... ***Eremohaplomydas gobabebensis* sp. nov.**

– Dorso-median occipital setae macrosetose; base of vein M_3+M_4 present (regular wing venation); scutum grey pubescent with broad median and 2 sublateral stripes brown pubescent; distributed in northern Namib desert (Fig. 57); males unknown..... ***Eremohaplomydas stomachoris* sp. nov.**

Key to genera of Afrotropical Mydidae

The present review of the genera *Eremohaplomydas*, *Haplomydas*, and *Lachnocorynus* revealed character state combinations that would prevent them from being properly identified using the key by Dikow (2017). For example, the posterior margin of the anepisternum being setose (couplet 6 in Dikow 2017) separates *Haplomydas* from most other Afrotropical Syllegomydinae (including *Eremohaplomydas* and *Lachnocorynus* in that key), but both *E. gobabebensis* sp. nov. and *E. stomachoris* sp. nov. are setose as well. Therefore, an updated key to the genera of the Afrotropical Region is necessary and provided here.

The online, illustrated version of the 2017 key has been updated and is available at https://keys.lucidcentral.org/keys/v4/Afrotropical-Mydidae-genera-dichotomous (version 2, 2022).

1 Antennal postpedicel composed of a single clubbed segment; mystacal (facial) setae absent..... ***Tongamya***

– Antennal postpedicel composed of a cylindrical proximal part and bulbous distal part separated by membranous cuticle; mystacal (facial) setae present..... **2**

2 Katatergite setose (at least a few short setae present, often densely setose)..... **6**

– Katatergite asetose..... **3**

3 Cell r_4 open; M_3+M_4 absent (not terminating together into C) (Rhopaliinae)... **5**

– Cell r_4 closed; M_3+M_4 present (terminating together into C) (Ectyphinae).... **4**

4 Auxiliary vein (R_3) connecting R_4 and R_2; anatergite setose; posterior margin of anepisternum setose..... ***Parectyphus***

– Auxiliary vein (R_3) extending from R_4 as a short stump vein, but not reaching R_2; anatergite asetose; posterior margin of anepisternum asetose ..... ***Ectyphus***

5 Proboscis long (extending beyond fronto-clypeal suture); cylindrical proximal part of postpedicel long, longer than bulbous distal part, this is more or less cylindrical; vertex slightly below median compound eye margin.....***Rhopalia***

– Proboscis minute; cylindrical proximal part of postpedicel short, much shorter than bulbous distal part, this proximally expanded and narrower distally; vertex elevated above median compound eye margin .....***Perissocerus***

6 Metathoracic coxa barrel-shaped, connected to metakatepisternum by 1 lateral and 1 median articulation point, membranous area between metakatepisternum and met coxa narrow **9**

– Metathoracic coxa not barrel-shaped, connected to metakatepisternum by 2 lateral articulation points, membranous area between metakatepisternum and met coxa large, easily visible in lateral view.....**7**

7 Proboscis distinct and long, almost reaching fronto-clypeal suture; females without bullae on postero-lateral margin of T2 .....***Haplomydas***

– Proboscis short or minute, clearly not reaching fronto-clypeal suture; females with bullae (even if small) easily discernible on postero-lateral margin of T2....**8**

8 Proboscis very small or minute; C terminating at R_1; pro and mes coxae anteriorly with either macrosetae or dorso-ventrally flattened setae; clypeus connected to face laterally by sclerotized cuticle; scutum surface smooth or only microrugose (slightly rugose 'imitating' pubescence)..... ***Eremohaplomydas***

– Proboscis short and nob-like but easily discernible, occupying approximately 1/3 of oral cavity; C terminating at M_1; pro and mes coxae anteriorly with only regular setae; clypeus connected to face laterally by membranous cuticle; scutum distinctly macrorugose (distinctly and deeply rugose) ..... ***Lachnocorynus***

9 Posterior margin of anepisternum asetose.....**18**

– Posterior margin of anepisternum setose (at least a few setae present, e.g., in *Oreomydas*, often densely setose) **10**

10 Mediotergite (mesopostnotum) asetose **12**

– Mediotergite (mesopostnotum) setose, at least laterally, usually also medially.....**11**

11 Proboscis minute to short, but never projecting beyond fronto-clypeal suture; cell r_5 (usually) closed; widespread sub-Saharan Africa with few species in southern Africa .....***Syllegomydas***

– Proboscis long to very long, invariably projecting beyond fronto-clypeal suture; cell r_5 open (even if only narrowly so); restricted to southern Africa, including southern Angola and southern Zambia .....***Afroleptomydas***

12 Infra-halter sclerite present and setose (Dikow and Leon 2014, p. 35); male with 2 phallic prongs fused medially.....***Namadytes***

– Infra-halter sclerite absent; male with 2 phallic prongs invariably separated medially.....**13**

13 Anatergite asetose **15**

– Anatergite setose **14**

14 Metathoracic femur cylindrical, not expanded distally; posterior margin of anepisternum densely setose; larger flies (wing length 11.2–17.7 mm) ..... ***Namibimydas***

– Metathoracic femur distinctly expanded distally; posterior margin of anepisternum only sparsely setose (1–4 setae); smaller flies (wing length 7.8–8.9 mm) ... ***Oreomydas***

15 Proboscis very long, projecting beyond tip of antennal postpedicel ..... ***Nothomydas***

– Proboscis long, projecting beyond fronto-clypeal suture, but never beyond tip of antennal postpedicel **16**

16 Abdominal tergal setae with small alveoli only, surface not punctate; scutum smooth ..... ***Heteroleptomydas* / *Nomoneuroides***

– Abdominal tergal setae with large, distinct alveoli, giving surface punctate appearance; scutum rugose..... **17**

17 Frons setose medially (at least few setae present, directly anterior to anterior ocellus); posterior margin of anepisternum only sparsely setose dorsally; restricted to easternmost South Africa and southernmost Mozambique ..... ***Neolaparopsis***

– Frons asetose medially (directly anterior to anterior ocellus); posterior margin of anepisternum densely setose from dorsal to ventral margin; restricted to northern Somalia ..... ***Afromydas***

18 Base of M_4 and middle section of CuA separated by m-cu (m-cu connecting M_3+M_4 and CuA); cell m_3 narrow proximally **20**

– Base of M_4 and middle section of CuA fused for considerable distance (m-cu absent, base of M_4 connecting M_3+M_4 and CuA); cell m_3 broad proximally ... **19**

19 Proboscis long, invariably extending well beyond fronto-clypeal suture, often projecting beyond tip of antennal postpedicel; anatergite asetose; metathoracic tibia with ventral keel at least proximally; commonly collected, but restricted to southern Namibia and Eastern, Northern, and Western Cape Provinces of South Africa ..... ***Cephalocera***

– Proboscis short, usually minute, except in a single species extending just beyond fronto-clypeal suture; anatergite setose; metathoracic tibia entirely cylindrical; rarely collected, but widely distributed throughout southern Africa ..... ***Cephalocerodes***

20 Proboscis long, invariably projecting beyond fronto-clypeal suture **25**

– Proboscis minute to short, but never projecting beyond fronto-clypeal suture..... **21**

21 Scutellum with 2 lateral tufts of discal scutellar setae ..... ***Halterorchis* / *Mimadelphus***

– Scutellum without any discal scutellar setae **22**

22 Parafacial area (between tentorial pit and median eye margin) more than 1/2 width of central facial swelling (at same level) (more pronounced in females);

light brown, grey pubescent, mostly asetose flies; restricted to southern Arabian Peninsula ..... ***Eremomidas***

– Parafacial area less than 1/2 width of central facial swelling; restricted to sub-Saharan Africa or Madagascar **23**

23 Cell d closed with long stalk (M_1 and M_3 merging before reaching r-m); auxiliary vein (R_3) on R_4 absent; restricted to Madagascar ..... ***Mahafalymydas***

– Cell d closed bluntly (M_1 and M_3 merging beyond r-m); auxiliary vein (R_3) on R_4 present; restricted to sub-Saharan Africa..... **24**

24 Median surface of metathoracic tibia with long, erect setae; metathoracic femur without ventral macrosetae; proboscis very short, only extending halfway to fronto-clypeal suture; restricted to north-westernmost Namibia..... ***Notosyllegomydas***

– Median surface of metathoracic tibia without long, erect setae; metathoracic femur with ventral macrosetae on elevated alveoli; proboscis short, but extending to fronto-clypeal suture; restricted to Kenya and Tanzania ..... ***Mydaselpis ngurumani***

25 Anepimeron and katepimeron asetose..... **27**

– Anepimeron and katepimeron setose (Leptomydinae in part) **26**

26 Restricted to Madagascar ..... ***Hessemydas***

– Restricted to Sudan..... ***Leptomydas***

27 Surface of abdominal tergites smooth (setae on tergites without obvious alveoli); T10 in females with acanthophorite spines..... **29**

– Surface of abdominal tergites punctate (setae on tergites with distinct alveoli); T10 in females without acanthophorite spines..... **28**

28 Male with phallic epimere (*sensu* Hesse 1969: 36) absent; restricted to southern Africa..... ***Mydaselpis***

– Male with phallic epimere distally simple and evenly rounded; throughout sub-Saharan Africa (within southern Africa only in Zimbabwe and northern South Africa) ..... ***Vespiodes***

29 Scutum rugose (except postalar callus); abdomen broad proximally and tapering slightly distally..... ***Arenomydas***

– Scutum smooth throughout, sometimes slightly punctate medially and paramedially; abdomen parallel-sided throughout **30**

30 Katatergite, antero-lateral scutum, and T1 densely long setose (females unknown); alula large, medially overlapping with scutellum (when wings folded over abdomen); frons and vertex densely long setose; restricted to southern Namibia and north-western South Africa..... ***Agaperemius***

– Katatergite, antero-lateral scutum, and T1 sparsely short setose in females and males; alula well-developed, but medially not touching scutellum (when wings folded over abdomen); frons and vertex sparsely short setose (virtually bare); restricted to eastern and southern South Africa ..... ***Nomoneura***

Discussion

Placement in Syllegomydinae

Hesse (1969), Bowden (1980), and Dikow (2017) place *Eremohaplomydas*, *Haplomydas*, and *Lachnocorynus* in the Syllegomydinae. This taxon was proposed by Bequaert (1963) in a review of the Afrotropical Mydidae to group those species with a two-pronged phallus and the absence of a joint M_3+M_4 vein reaching C on the posterior wing margin. Interestingly, the males of *Eremohaplomydas*, *Haplomydas*, and *Lachnocorynus* exhibit on first sight a single-pronged phallus, which is found in all Mydidae species, with the exception of Syllegomydinae, and their sister-group Apioceridae (Dikow 2009). Only a detailed study through dissections reveals that the phallus of the three genera is actually two-pronged. In the majority of Syllegomydinae species, the phallus has two distinct prongs arranged parallel to each other with openings for sperm deposition and an unpaired dorsal epimere. This configuration is most evident in species of *Afroleptomydas* and *Syllegomydas*. In *Eremohaplomydas*, *Haplomydas*, and *Lachnocorynus*, however, the two phallic prongs appear to be fused medially entirely and do not show distinctly visible openings for sperm deposition. The illustration of the posterior view of the male terminalia of *Lachnocorynus chobeensis* in Hesse (1969, see his Fig. 5, www.biodiversitylibrary.org/page/40724748) appears to show a single-pronged phallus. Our hypothesis is that there are two phallic prongs, which are fused medially and difficult to characterize individually. Entirely fused phallic prongs are also found in *Namadytes* Hesse, 1969 (Hesse 1972, see his Fig. 3 www.biodiversitylibrary.org/page/40942083, Dikow and Leon 2014), but the openings are distinctly visible providing evidence that there are two independent phallic prongs.

The wing venation in *Eremohaplomydas*, *Haplomydas*, and *Lachnocorynus* exhibits general features of other, but not all, Syllegomydinae genera (cell r_4 closed, cell r_5 open, C terminating anterior to wing tip at R_1 or M_1+$_2$, and M_3+M_4 not joining and terminating together into C).

While Bequaert (1963) included *Haplomydas* in his Syllegomydinae (despite postulating a single-pronged phallus), he explicitly excluded *Eremohaplomydas*, which he had described a few years earlier including illustrations of the male terminalia (Bequaert 1959), *Halterorchis* Bezzi, 1924 (males have only been reported recently, Dikow 2017), and *Eremomidas* Semenov, 1896 (now considered a Leptomydinae, but see discussion by Dikow 2017).

To date, representatives of five subfamilies of Mydidae are known from the Afrotropical Region, *i.e.*, Ectyphinae (2 genera, Lyons and Dikow 2010), Leptomydinae (3, see Dikow 2017), Megascelinae (1, Stuckenberg 1966; Yeates and Irwin 1996), Rhopaliinae (2, see Dikow 2017) and Syllegomydinae (24). Based on wing venation alone, *Eremohaplomydas*, *Haplomydas*, and *Lachnocorynus* cannot be placed in Ectyphinae, Megascelinae, and Rhopaliinae. The Leptomydinae fauna of the Afrotropical Region as currently understood is restricted to the Arabian Peninsula, the north-eastern Afrotropics and Madagascar (see Dikow 2017). We follow the hypotheses put forward by Hesse (1969) that all three genera should be placed in the Syllegomydinae. Morphological

and molecular phylogenetic studies of the entire Mydidae are currently being prepared by the junior author and these hypotheses will shed light on the evolutionary relationships of *Eremohaplomydas*, *Haplomydas*, and *Lachnocorynus*.

Distribution of the three genera

Eremohaplomydas is one of only two Mydidae genera known to be endemic to the Namib Desert (the other one is *Notosyllegomydas* Hesse, 1969 with a single species known from the northern Namib desert). *Eremohaplomydas* is known from two areas (with two collecting localities each) in the northern and central Namib Desert (Fig. 3).

Haplomydas is a widespread genus recorded here from some 67 specimens from 25 collecting events (Table 1) throughout southern Africa (Fig. 3). It is interesting to note though that *Haplomydas* has not been recorded from South Africa even though this country is the best sampled region of southern Africa and shares similar habitats with its neighbors Namibia, Botswana, Zimbabwe, and Mozambique along its northern and eastern borders. In addition, South Africa has the highest diversity of genera and species of Mydidae recorded within southern Africa (19 genera and 135 species) followed by Namibia (11 and 32), Zimbabwe (8 and 15), Mozambique (7 and 11), and Botswana (4 and 5, numbers include new species described herein). Several localities of *Haplomydas crassipes* in Botswana (Mochudi), Mozambique (Mapai), and Zimbabwe (Beit Bridge) are situated very close to the South African border (Fig. 3) supporting the hypothesis that it might only be a matter of time until this species will also be recorded from South Africa in similar habitats.

Lachnocorynus is known from four distant localities along the 17 degree southern latitude from northern Namibia, northern Botswana, and north-eastern Zimbabwe (Fig. 3). While the genus is currently restricted to southern Africa, one can postulate that it will also occur in Angola, Zambia, and Mozambique and potentially even further north.

Species pairs of *Eremohaplomydas*

It is interesting to observe that the four known species of *Eremohaplomydas* group together both geographically and morphologically in pairs. *E. desertorum* and *E. stomachoris* sp. nov. occur in the vicinity of Orupembe in north-western Namibia (Figs 56–57) while *E. gobabebensis* sp. nov. and *E. whartoni* sp. nov. occur in the vicinity of Gobabeb in west-central Namibia (Figs 56–57). The distance between these two sites is more than 600 km as the crow flies. Species within each pair appear to be isolated by different seasonal imago flight activity periods though as imagines of *E. desertorum* and *E. stomachoris* sp. nov. fly in early June and early May, respectively, and imagines of *E. gobabebensis* sp. nov. and *E. whartoni* sp. nov. fly in November and May, respectively (Table 2).

More striking is the morphological similarity of species pairs, which is opposite to that of the geographical pairs. *E. gobabebensis* sp. nov. and *E. stomachoris* sp. nov. imagines (Figs 10–12, 16–18) are very small and slender, have less expanded metathoracic femora, R_5 terminates in R_1 and R_4 simultaneously, and the alula is well-developed. In contrast, *E. desertorum* and *E. whartoni* sp. nov. (Figs 4–9, 19–24) are larger flies, have

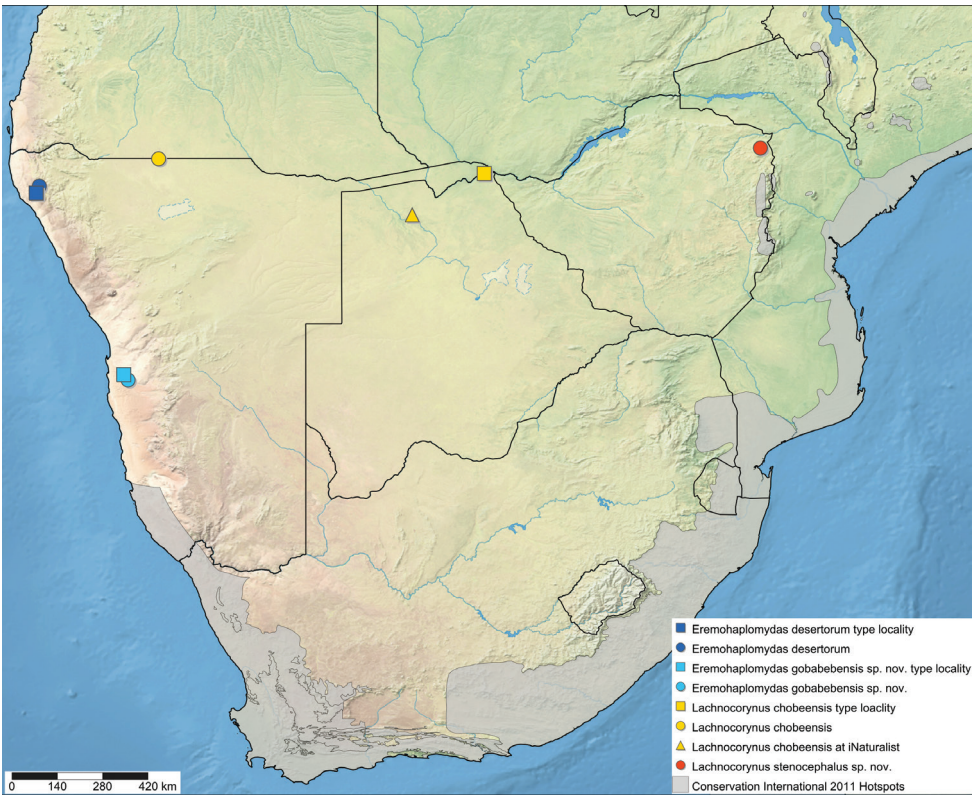

Figure 56. Map of southern Africa with elevational relief and biodiversity hotspots (*sensu* Conservation International in grey) and distribution of *Eremohaplomydas desertorum*, *Eremohaplomydas gobabebensis* sp. nov., *Lachnocorynus chobeensis*, and *Lachnocorynus stenocephalus* sp. nov. (SimpleMappr https://www.simplemappr.net/map/14089). Distribution and occurrence data available in Google Earth KML file https://www.simplemappr.net/map/14089.kml and also through GBIF (data-set https://www.gbif.org/dataset/993875DD-5915-4107-8707-835D5A8D1022, DOI https://doi.org/10.15468/awpjz9).

more pronounced expanded metathoracic femora, R_5 terminates into R_1 only, and the alula is greatly reduced to a small lobe. In this case, the two geographical areas exhibit each both morphological pairs: one large and robust species and one small and slender species.

Field-work in the Namib Desert might reveal the presence of *Eremohaplomydas* elsewhere and it will be interesting to learn whether such a pattern of sympatric distribution with different morphologies and seasonal imago flight activity will hold.

Morphological features

Metathoracic coxa and metakatepisternum

The development of the metathoracic coxa and the metakatepisternum in *Eremohaplomydas*, *Haplomydas*, and *Lachnocorynus* is unique within Mydidae. In general, metathoracic coxae in Mydidae are barrel-shaped and sclerotized on all sides. They move in

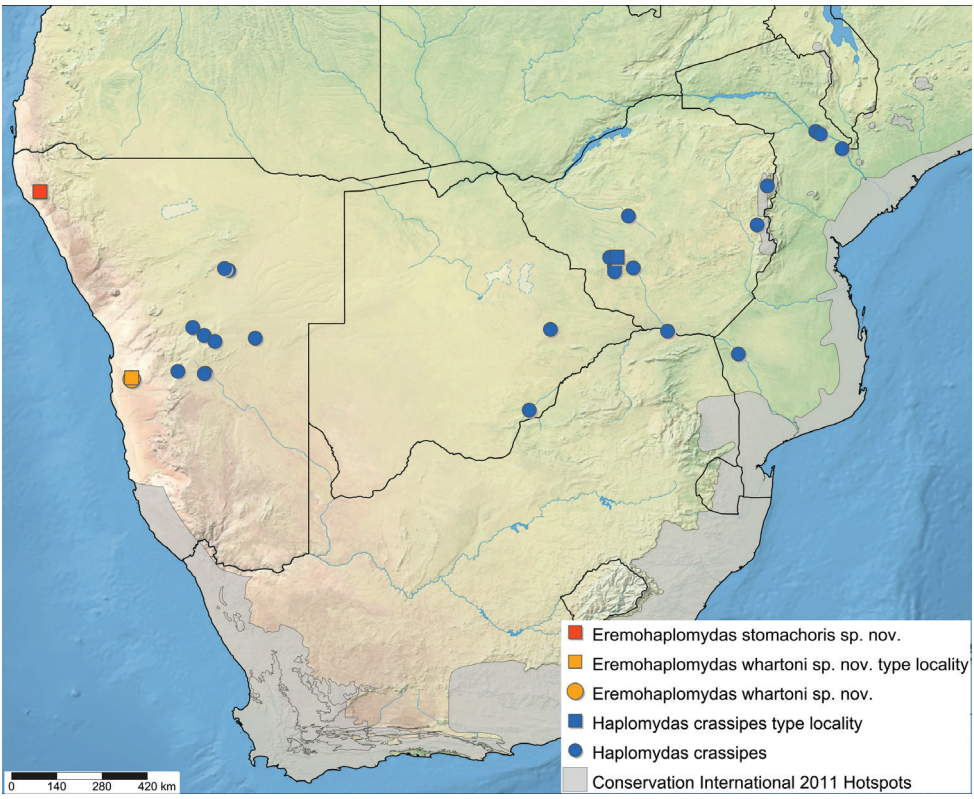

Figure 57. Map of southern Africa with elevational relief and biodiversity hotspots (*sensu* Conservation International in grey) and distribution of *Eremohaplomydas stomachoris* sp. nov., *Eremohaplomydas whartoni* sp. nov. (both localities only 5 km apart), and *Haplomydas crassipes* (SimpleMappr https://www.simplemappr.net/map/14090). Distribution and occurrence data available in Google Earth KML file https://www.simplemappr.net/map/14090.kml and also through GBIF (data-set https://www.gbif.org/dataset/993875DD-5915-4107-8707-835D5A8D1022, DOI https://doi.org/10.15468/awpjz9).

a plane from anterior to posterior (or if positioned more postero-ventrally in a plane from dorsal to ventral) through two articulations — one lateral and one median.

In lateral view, the metathoracic coxa of species of *Eremohaplomydas*, *Haplomydas*, and *Lachnocorynus* appears unsclerotized to a large extent (Figs 53–55) and is not cylindrical or barrel-shaped. The metakatepisternum is expanded laterally so that the median articulation point of the coxa is moved laterally. It is now positioned antero-ventrally and facing anteriorly (Fig. 54) so that it is visible in lateral view. It allows the coxa now to (potentially) move in a plane from median to lateral away from the thorax to position the legs out sideways. The only observation of a species of these genera in nature, *Lachnocorynus chobeensis* at iNaturalist (https://www.inaturalist.org/observations/26760859), illustrates this quite well. The unsclerotized and membranous area is formed by the membrane between the metakatepisternum and coxa and the coxa is itself less produced laterally.

More observations in nature are necessary to document the way the coxae and legs are being held in species of *Eremohaplomydas*, *Haplomydas*, and *Lachnocorynus*.

Wing venation of *Eremohaplomydas gobabebensis* sp. nov.

Eremohaplomydas gobabebensis sp. nov. is morphologically most similar to *E. stomachoris* sp. nov. (note that these species are only known from males and a single female, respectively). However, they differ distinctly in their wing venation. *E. gobabebensis* sp. nov. is unique among the species included here (and probably all Mydidae) in that the base of M_3+M_4 is absent (Fig. 10, view full-resolution file at Zenodo https://doi.org/10.5281/zenodo.6083969) and either the discal cell (d) is not developed or it is entirely fused to the basal medial cell (bm). The possibility exists that this unique arrangement of veins is a population-level anomaly. *Eremohaplomydas gobabebensis* sp. nov. has been collected at two different sites 21 km apart as the crow flies on consecutive days and most likely all collected specimens belong to the same population. The collection of additional specimens at different sites will provide evidence as to whether the peculiar wing venation is species-specific or only specific to the currently known population.

Clypeus development and minute proboscis in *Eremohaplomydas*

In Mydidae, the clypeus is developed as either an inverted U-shaped sclerite, an inverted U-shaped sclerite in which the dorsal half is sclerotized and forms a plate, or a single sclerite which is entirely sclerotized medially (Dikow 2009, p. 22). In *Haplomydas* and *Lachnocorynus* species the clypeus is formed by a single sclerotized plate, is recessed (concave), positioned posterior to the proboscis, and connected laterally to the face (or the facial swelling) by membranous cuticle. This specific arrangement is found in most Syllegomydinae but is considerably different in species of *Eremohaplomydas*. The most generalized and simple arrangement is found in *Eremohaplomydas gobabebensis* sp. nov. in which the clypeus is formed by an inverted U-shaped sclerite with the dorsal half sclerotized, is recessed (concave), is positioned posterior to the proboscis, but is connected laterally to the face (or the facial swelling) by sclerotized cuticle (Fig. 32). In *Eremohaplomydas stomachoris* sp. nov. the clypeus is formed by a single sclerotized plate, is flat to protruding (convex) ventrally, is positioned posterior to the proboscis, and is connected laterally to the face (or the facial swelling) by sclerotized cuticle (Fig. 33). The most bizarre arrangement is found in *Eremohaplomydas desertorum* and *Eremohaplomydas whartoni* sp. nov. in which the clypeus is formed by a single sclerotized plate, is protruding (convex) ventrally, is positioned anterior to the proboscis (almost covering the minute proboscis), and is connected laterally to the face (or the facial swelling) by sclerotized cuticle (Figs 31, 34). Not only is the proboscis minute in these two species, it is covered by the protruding clypeus, which might further reduce the potential for feeding on pollen or nectar. We believe this unique morphology of the clypeus (being anterior to the proboscis) is not caused by preservation as it is consistently found in the specimens studied and no other evidence would suggest that the clypeus was somehow transformed.

Wharton (1982) postulated that several Mydidae species do not feed as adults in the central Namib including *Eremohaplomydas whartoni* sp. nov., which he collected near Gobabeb (identified as *Eremohaplomydas* sp. in his Table 1). When *Eremohaplomydas gobabebensis* sp. nov. was collected in open sandy areas with sparse grass covering

(see Figs 1–2), no flowers were present in the immediate collecting area. While the absence of flowers in the area where a species was collected cannot be taken as evidence as to whether the species does or does not feed as imagines, it does provide additional data to evaluate the ability to feed. With the external mouthparts in form of the proboscis being minute and potentially non-functional, we can only support Wharton's hypothesis that species of *Eremohaplomydas* do not feed as adult flies. A comparative morphological study including CT scanning of several short-proboscis Mydidae species, which has been started by the junior author, will hopefully provide new data to further study this phenomenon.

Seasonal imago flight activity

Species of the three genera have been collected in the Southern Hemisphere late spring to winter (Table 2). *Eremohaplomydas* species are restricted in imago flight activity to either November in late spring (*Eremohaplomydas gobabebensis* sp. nov.) or late autumn (May) to early winter (June) (Table 2). Imagines of *Lachnocorynus* fly only in winter (June–August, Table 2) while the imago flight activity of *Haplomydas crassipes* is restricted to late summer (February) to late autumn (May, Table 2).

Biodiversity hotspots

Of the eight species included in this study, the only species that occurs within a currently recognized biodiversity hotspot *sensu* Conservation International is *Haplomydas crassipes*. Two collecting events of this species are within the Eastern Afromontane biodiversity hotspot in eastern-most Zimbabwe (Fig. 57).

Conclusion

With the description of four new species and the synonymy of one species, there are now 182 species of Mydidae in southern Africa and 483 species known in the world.

Acknowledgements

We would like to thank the many museum curators for making specimens available through loans and for their hospitality when visiting the collections. We would also like to graciously acknowledge the U.S. National Science Foundation (NSF) for funding the Research Experience for Undergraduates site grant at the NMNH entitled "Natural History Research Experience (NHRE)" (OCE 1560088; PI E. Cottrell, Co-PI E. Hunt). We thank Virginia Power, Liz Cottrell, and Gene Hunt for their constant support during the administration of the NHRE programme. We also acknowledge field-work support to the junior author from the NMNH for a project entitled, "Novel morphological data to decipher the character and life history evolution and

diversification of Asiloidea and Nemestrinoidea flies" (2017). John Hash (formerly NMNH) is thanked for taking the photographs of proboscides and Gillian Maggs-Kölling (Gobabeb Namib Research Institute) is thanked for help in identifying the grasses in Figs 1–2. We thank Marcus Guidoti and Donat Agosti (both Plazi) for developing the image repository at the Zenodo Biodiversity Literature Repository and help with uploading the image files. Furthermore, we thank the Namibian National Commission on Research, Science and Technology (NCRST) and the Ministry of Environment and Tourism (MET) for providing collecting and export permits in support of the field-work in Namibia. The junior author would like to thank Charlotte Alberts (UC Davis), Allan Cabrero (UC Berkeley), and Brandon Claridge (Utah State University) for accompanying him in the field in Namibia and Gillian Maggs-Kölling, Leena Kapulwa, and Eugene Marais (Gobabeb Namib Research Institute) for all the support prior and during our stay at the station. Lastly, we thank Jason Londt and an anonymous reviewer for their constructive comments during peer review.

References

Bequaert M (1959) Chapter 18. Diptera (Brachycera): Mydaidae. In: Hanström B, Brinck P, Rudebeck G (Eds) South African Animal Life (Results of the Lund University Expedition in 1950–1951), vol. 6, Almqvist and Wiksell, Lund, 356–372.

Bequaert M (1963) Contribution nouvelle a la connaissance des Mydaidae de la région Éthiopienne. Mémoires Institut Royal des Sciences Naturelles de Belgique 2(71): 3–68.

Bezzi M (1924) The South African Mydaidae (Diptera) as represented in the South African Museum. Annals of the South African Museum 19: 191–234. https://www.biodiversitylibrary.org/page/40677706

Bowden J (1980) 27. Family Mydidae. In: Crosskey RW (Ed.) Catalogue of the Diptera of the Afrotropical Region, London, 325–333.

Brunetti EA (1929) New African Diptera. Annals and Magazine of Natural History (ser. 10) 4(19): 1–35. https://doi.org/10.1080/00222932908673024

Catapano T (2010) TaxPub: An Extension of the NLM/NCBI Journal Publishing DTD for Taxonomic Descriptions. Proceedings of the Journal Article Tag Suite Conference. http://www.ncbi.nlm.nih.gov/books/NBK47081/

Cumming JM, Wood DM (2017) 3. Adult morphology and terminology. In: Kirk-Spriggs AH, Sinclair BJ (Eds) Manual of Afrotropical Diptera, vol. 1. Introductory chapters and keys to Diptera families. Suricata 4, SANBI, Pretoria, 89–133. http://hdl.handle.net/20.500.12143/6089

Dikow T (2009) Phylogeny of Asilidae inferred from morphological characters of imagines (Insecta: Diptera: Brachycera: Asiloidea). Bulletin of the American Museum of Natural History 319: 1–175. https://doi.org/10.1206/603.1

Dikow T (2017) 47. Mydidae (mydas flies). In: Kirk-Spriggs AH, Sinclair BJ (Eds) Manual of Afrotropical Diptera, vol. 2. Nematocerous Diptera and lower Brachycera. Suricata 5, SANBI, Pretoria, 1063–1095. http://hdl.handle.net/20.500.12143/6493

Dikow T, Leon S (2014) Review of the genus *Namadytes* Hesse, 1969 (Insecta: Diptera: Mydidae: Syllegomydinae). Biodiversity Data Journal 2: e1071. https://doi.org/10.3897/BDJ.2.e1071

Hesse AJ (1969) The Mydaidae (Diptera) of Southern Africa. Annals of the South African Museum 54: 1–388. https://www.biodiversitylibrary.org/page/40724360

Hesse AJ (1972) New Mydaidae (Diptera) from the Namib Desert and South-Western Africa. Annals of the South African Museum 60(3): 109–171. https://www.biodiversitylibrary.org/page/40942048

Lyons KM, Dikow T (2010) Taxonomic revision of *Ectyphus* Gerstaecker, 1868 and *Parectyphus* Hesse, 1972 with a key to world Ectyphinae (Insecta: Diptera: Mydidae). ZooKeys 73: 25–59. https://doi.org/10.3897/zookeys.73.840

Mittermeier RA, Myers N, Thomsen JB, da Fonseca GAB, Olivieri S (1998) Biodiversity hotspots and major tropical wilderness areas: Approaches to setting conservation priorities. Conservation Biology 12(3): 516–520. https://doi.org/10.1046/j.1523-1739.1998.012003516.x

Mittermeier RA, Gil PR, Hoffman M, Pilgrim J, Brooks TM, Mittermeier CG, Lamoreaux J, da Fonseca GAB (2005) Hotspots Revisited: Earth's Biologically Richest and Most Endangered Terrestrial Ecoregions. Conservation International, Washington, DC, 392 pp.

Myers N, Mittermeier RA, Mittermeier CG, da Fonseca GAB, Kent J (2000) Biodiversity hotspots for conservation priorities. Nature 403(6772): 853–858. https://doi.org/10.1038/35002501

Nichols SW (1989) The Torre-Bueno Glossary of Entomology. The New York Entomological Society, New York, 840 pp.

Pyle RL, Michel E (2008) Zoobank: Developing a nomenclatural tool for unifying 250 years of biological information. Zootaxa 1950(1): 39–50. https://doi.org/10.11646/zootaxa.1950.1.6

Séguy E (1929) Un Mydaidae nouveau de l'Afrique Orientale Portugaise. Annales de la Société Entomologique de France 98(1–2): 110–110.

Shorthouse DP (2010) SimpleMappr, an online tool to produce publication-quality point maps. http://www.simplemappr.net

Stuckenberg BR (1966) A remarkable new genus and species of Apioceridae in South Africa (Diptera). Revue de Zoologie et de Botanique Africaines 73(1–2): 106–120.

Stuckenberg BR (1999) Antennal evolution in the Brachycera (Diptera), with a reassessment of terminology relating to the flagellum. Studia Dipterologica 6(1): 33–48. https://doi.org/10.5281/zenodo.12390

van Oudtshoorn F (2012) Guide to grasses of southern Africa. Briza, Pretoria, 3rd revised edn., 287 pp.

Wharton RA (1982) Observations on the behaviour, phenology and habitat preferences of mydas flies in the central Namib Desert (Diptera: Mydidae). Annals of the Transvaal Museum 33(9): 145–151. https://hdl.handle.net/10520/AJA00411752_165

Wootton RJ, Ennos AR (1989) The implications of function on the origin and homologies of the dipterous wing. Systematic Entomology 14(4): 507–520. https://doi.org/10.1111/j.1365-3113.1989.tb00300.x

Yeates DK, Irwin ME (1996) Apioceridae (Insecta: Diptera): cladistic reappraisal and biogeography. Zoological Journal of the Linnean Society 116(3): 247–301. https://doi.org/10.1111/j.1096-3642.1996.tb00124.x

African Invertebrates 63(1): 77–88 (2022)
doi: 10.3897/AfrInvertebr.63.81092
https://africaninvertebrates.pensoft.net

RESEARCH ARTICLE

African Invertebrates
A journal of biodiversity research

Geometric morphometric analysis of gonopods in *Bicoxidens flavicollis* populations (Diplopoda, Spirostreptida, Spirostreptidae)

Tarombera Mwabvu[1,2], Adekunle Adebowale[3,4]

1 *School of Biology & Environmental Sciences, University of Mpumalanga, PB X11283, Riverside, Mbombela 1200, South Africa* **2** *School of Life Sciences, University of KwaZulu-Natal, Private Bag X54001, Westville campus, Durban, 4001, South Africa* **3** *Department of Botany, University of Otago, Dunedin 9016, New Zealand* **4** *Department of Botany, Rhodes University, Grahamstown 6140, South Africa*

Corresponding author: Tarombera Mwabvu (tarombera.mwabvu@ump.ac.za)

Academic editor: M. Hamer | Received 24 January 2022 | Accepted 11 May 2022 | Published 29 June 2022

http://zoobank.org/2ACDB517-A094-47ED-AA8D-8D08F7715113

Citation: Mwabvu T, Adebowale A (2022) Geometric morphometric analysis of gonopods in *Bicoxidens flavicollis* populations (Diplopoda, Spirostreptida, Spirostreptidae). African Invertebrates 63(1): 77–88. https://doi.org/10.3897/AfrInvertebr.63.81092

Abstract

Male gonopods are useful in taxonomic diagnoses and descriptions of millipedes, although they may vary intraspecifically in shape and size. To assess this intraspecific variation, we used geometric morphometric analysis to compare gonopod morphology among eight isolated populations of the colour-polymorphic southern African millipede *Bicoxidens flavicollis*. Our results showed that gonopod shapes vary significantly across the examined populations, and elucidated subtle variations. CVA cross-validation test indicates an average classification rate of 75% for the five populations for which we had more than one specimen. Although we had a small number of replicates for three populations, our results still illustrate the importance of applying quantitative approaches to what would otherwise be qualitative and subjective gonopod shape categories in millipedes. As such, the taxonomic assignment of the populations of *B. flavicollis* may require further investigation, and further revisions would be required with an integrative approach, including molecular data, in order to re-evaluate the taxonomic diversity and distribution data of this species. Finally, we highlight the conservation potential of divergent populations as evolutionary insurance against a dynamic and unpredictable climate, whether or not they undergo full speciation.

Keywords

cryptic species, millipedes, morphology, taxonomic diversity

Introduction

Morphological differences are important in taxonomy to delimit taxa (Jacob et al. 2004; Schlick-Steiner et al. 2007; Foley et al. 2017). In millipedes, gonopod morphology is central in species description because the male gonopods are divergent and species-specific. Recent studies have demonstrated that speciation may occur without changes in gonopod morphology in several invertebrates (see Bond and Sierwald 2002; Novo et al. 2010). Bond et al. (2003) reported that speciation occurred unaccompanied by gonopod divergence in a spirobolidan millipede, *Anadenobolus excisus* Karsch, 1881 species complex, and genetic change is uncorrelated to gonopod change. Although intraspecific variation in gonopods is common and differences in gonopod structure among taxa may be subtle (Pimvichai et al. 2011), male gonopods remain the key sources of traits that are used in millipede systematics (cf. Enghoff 2017; Frederiksen et al. 2012). Features of gonopods with consistent application in millipede taxonomy include the sternum, coxites and telopodite (Pimvichai et al 2011; Enghoff 2017), although Krabbe and Enghoff (1985) reported a case of considerable variability in gonopod coxite within a localised population of *Orthoporus antillanus*, suggesting that the variation in the character may not be exclusively geographic in origin.

The genus *Bicoxidens* Attems, 1928 comprises nine species which are endemic to southern Africa, occurring in diverse habitats such as Miombo woodland, riverine, and montane vegetation (Mwabvu et al. 2007). The species *Bicoxidens flavicollis* Attems, 1928 *sensu lato* is the most widely distributed species, with records from Zimbabwe and one from western Mozambique (Fig. 1) (Mwabvu et al. 2007). Although the male

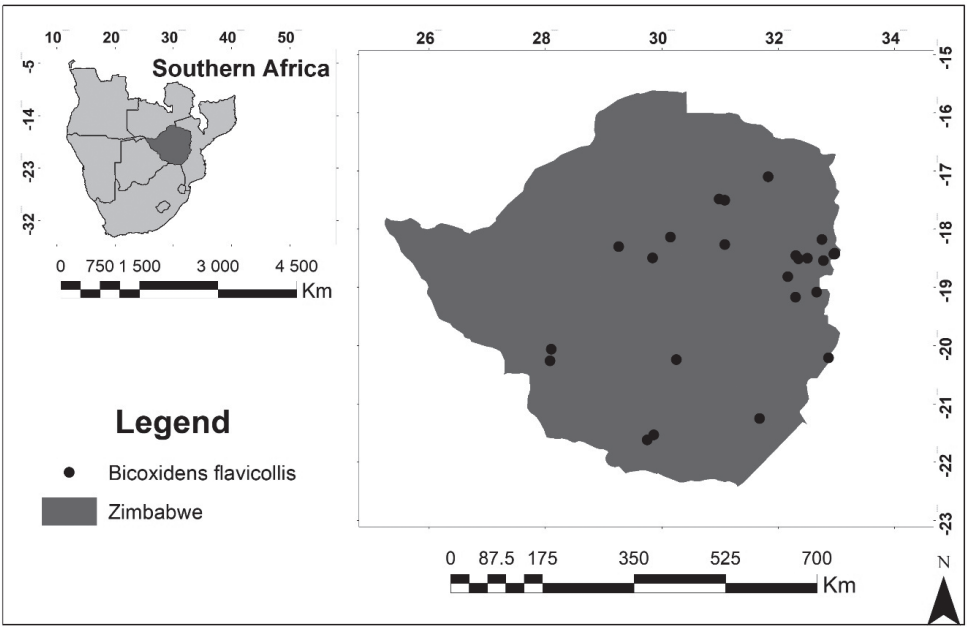

Figure 1. Distribution map of *B. flavicollis* in Zimbabwe, Southern Africa.

body size and gonopod shape in *B. flavicollis* populations appear identical, these observations have been based only on qualitative comparisons. According to Mwabvu et al. (2007), the pattern of body colour is related specifically to the locality of a determined population, with black, brown, or orange-yellow specimens having been recorded only in Zimbabwe, for instance. Nonetheless, quantitative comparisons of the gonopods are necessary in order to clarify the circumscription of this putative species complex. Furthermore, investigating intraspecific variations in gonopod morphology in populations of *B. flavicollis* could identify isolated populations and may lead to the recognition of undescribed diversity and a revision of distributional data.

Given the colour polymorphism and high genetic divergence (18% for CO1 and 6% for 16S rRNA) recorded in two populations of *B. flavicollis* (Mwabvu et al. 2013), we assessed the variation of gonopod morphology in differentiating colour polymorphic populations. We compared the shapes of gonopods from eight populations of *B. flavicollis*, predicting that gonopod shape would be highly conserved, and despite the variation in body colour, populations of *B. flavicollis* would not be differentiated using traditional comparative morphology of gonopods.

From this perspective, we employed in this study for the first time a geometric morphometric analysis to assess the taxonomic value of gonopod morphology in separating populations, and to test the hypothesis that gonopod morphology may underestimate the taxonomic diversity of a spirostreptidan species.

Materials and methods

Copulating and non-copulating males and females of *B. flavicollis* were collected by hand from eight geographically separate populations in Zimbabwe as summarised in Table 1.

All the specimens were preserved in 96% ethanol. The voucher specimens from each population were deposited in the Natural History Museum (NHMZ), Bulawayo, Zimbabwe, and the KwaZulu-Natal Museum (KZNM), Pietermaritzburg, South Africa. The total sample size on which our analysis was based was 40 (Table 1). The specimens were identified by T. Mwabvu after examining the male gonopods under a Carl Zeiss (Stemi DV4) dissecting microscope and using the species identification keys in Mwabvu et al. (2007). Male gonopods were photographed using Auto Montage software (Leica Microscope MZ12s with 3 CCD Toshiba Camera).

All the samples were photographed in the same oral view and magnifications. In total, eighteen landmarks for 40 specimens were obtained from the examined gonopods (Table 2; Fig. 2) using a suite of TPS programmes (TPS Util and TPSDig, Rohlf 2015). Considering the bilateral symmetry and to avoid any difference regarding gonopodal position only the right side was digitized. Procrustes standardisation was performed on the landmark coordinates to remove the effect of size, rotation, and position. To minimise the possibility of committing a type II error, we assessed measurement error on digitised landmarks using the intraclass correlation coefficient approach, also termed repeatability (Fisher 1958). To measure the repeatability of placing landmarks, an individual specimen from three randomly selected populations

Table 1. Details of the *B. flavicollis* populations and samples.

Population (sample size)	Coordinates	Province	Voucher	Vegetation/Habitat
Chegutu (1)	18°06'S, 30°09'E	Mashonaland West	NM 21954	Dry savanna
Chihota (1)	18°16'S, 31°05'E	Mashonaland East	NM-Myr 25833	Miombo woodland
Chitombo (12)	18°26'S, 32°58'E	Manicaland East	NM-Mil 25832	Miombo woodland
Marange (4)	19°10'S, 32°18'E	Manicaland West	NHMZ	Dry savanna
Mazowe (5)	17°29'S, 30°59'E	Mashonaland Central	NM 21958	Miombo woodland
Muterere (1)	18°26'S, 32°58'E	Manicaland East	NM-Mil 25831	Miombo woodland
Muzinga (5)	18°25'S, 32°58'E	Manicaland East	NM-Mil 25835	Miombo woodland
Sahumani (11)	18°32'S, 32°50'E	Manicaland East	NHMZ	Miombo woodland

(Chihota, Mazowe and Sahumani) was used to provide six replicates of gonopod images in a total of 18 images for each one. We then landmarked each replicate and performed a one-way ANOVA on the Procrustes standardised landmark coordinates using population as the categorical variable. Repeatability was computed according to the formula:

$$R = S_A^2 / (S_W^2 + S_A^2)$$

where R is the repeatability value, S_A^2 is the among-individuals component of variance, and S_W^2 is the within-individuals variance component (Sokal and Rohlf 1995; Arnqvist and Martensson 1998; Fruciano 2016).

For shape analysis, the variance-covariance matrix derived from the Procrustes coordinates were subjected to exploratory principal component analysis to reduce the dimensionality of the data to the most significant shape variables. As the first 15 principal components (PCs) accounted for about 95% of observed variance, the corresponding

Table 2. Description of *B. flavicollis* gonopod landmarks and semi-landmarks used for shape analysis.

Landmark number	Landmark definition (following Mwabvu et al. 2007)	Landmark type (after Bookstein 1997a; Bookstein 1997b)
1	Apex of median lobe of apical proplica	I
2	Apex of axe-shaped process (or apical axe-shaped process)	I
3	Tip of lobe of axe-shaped process	I
4	Base of lobe of axe-shaped process	I
5	Lateral mid-proplica	II (semi-landmark; midpoint between landmarks 4 and 6)
6	Apex of sternite (or apical sternite)	I
7	Base of sternite (or basal sternite)	I
8	Base of proplica (or basal proplica)	II (semi-landmark; the most distal part of the basal prolica)
9	Basal lateral edge of paracoxite	II (semi-landmark; furthest point on the lateral edge of paracoxite
10	Distal lateral paracoxite	I
11	Paracoxite apex	I
12	Telopodite (at midlength between knee and femoral lobe)	II (semi-landmark; midpoint between knee and femoral lobe)
13	Base of rounded lobe on proplica	I
14	Base/pit of telopodite knee	I
15	Apex of telopodite knee	I
16	Proximal edge of lateral process	I
17	Apex of lateral process	I
18	Apical groove between lateral process and median lobe	I

(14 of the landmarks were type I; 4 were type II *sensu* Bookstein 1997a, b).

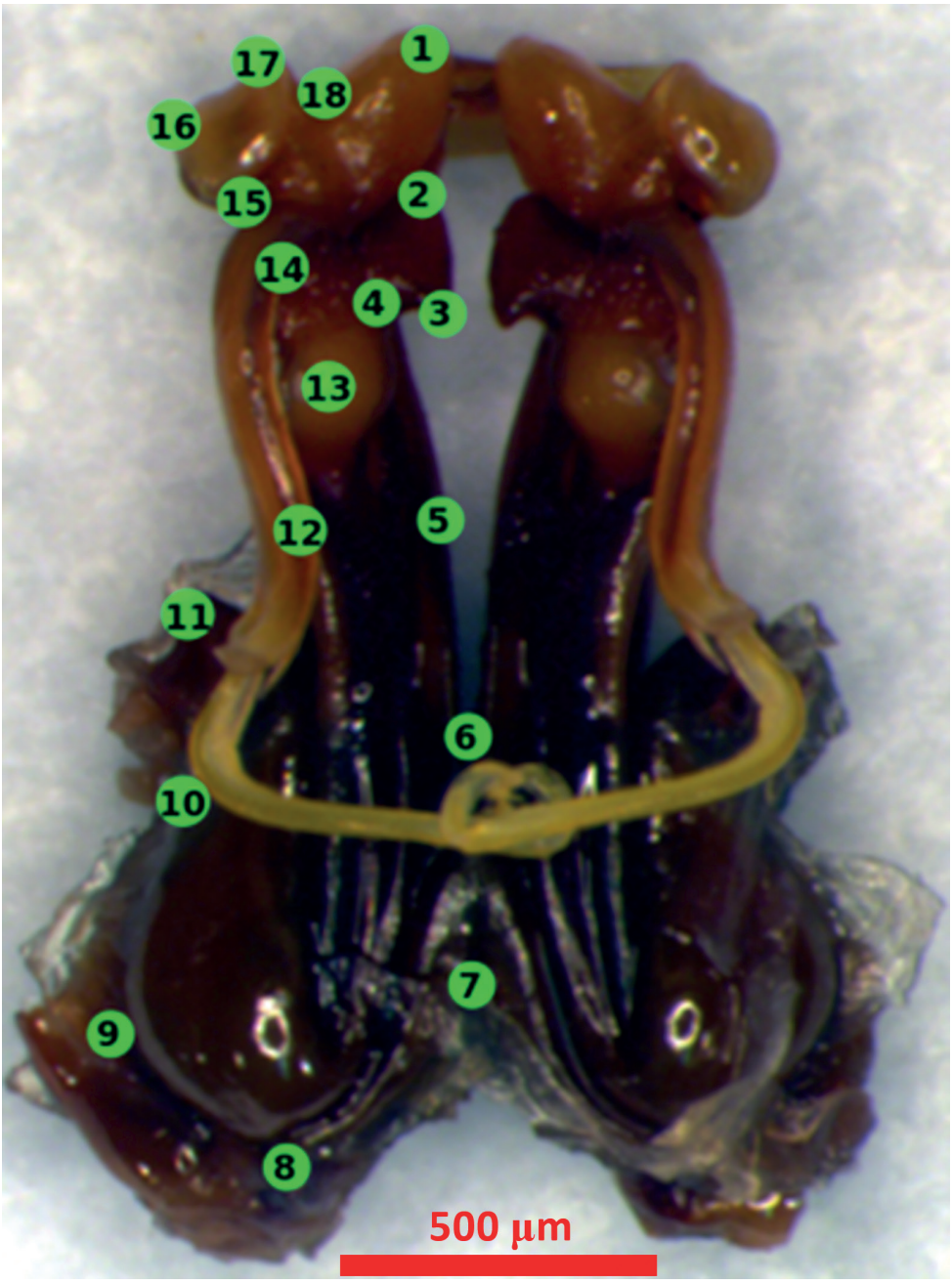

Figure 2. Landmarks used for analysis of gonopod shape variation in *B. flavicollis*.

PC scores were selected as variables for a canonical variates analysis (CVA) to assess shape discrimination across populations. This was followed with cross-validation tests to assess the rate of correct classification of specimens into their population groups. We tested the null hypothesis that gonopod shapes are not different among the eight

populations of *B. flavicollis* using the PC scores and population as dependent and predictor variables, respectively. All analyses were implemented in PAST (Hammer et al. 2001) and MorphoJ (Klingenberg 2011).

Results

The assessment of measurement errors arising from landmark digitisation demonstrates that variation between repeated digitisations of the same specimen is significantly lower than variation among different specimens, with an intraclass correlation coefficient of 0.99. The thin plate spline deformation grids (Fig. 3) depict some patterns of gonopod shape variations among the 18 landmarks, as well as among the various populations of *B. flavicollis*. Landmarks 6, 7 and 11 displayed the most visually perceptible variability. The overall shape changes along the first two principal component axes also identified the same sets of landmarks, in addition to semi-landmarks 8 and 9, as showing pronounced variability across all populations.

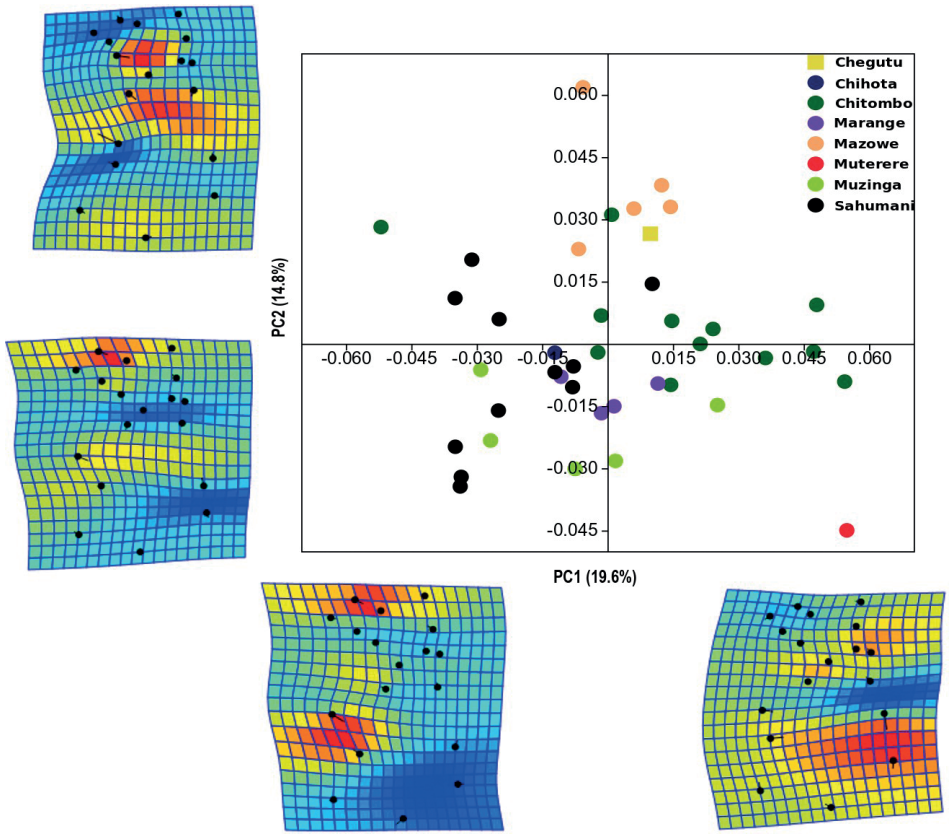

Figure 3. Principal component analysis of the first two PCs showing extremes of gonopod shape across eight populations of *B. flavicollis*. The thin plate spline deformation grids have been scaled up to illustrate shape differences along the respective PC axes.

Although a scatter plot of specimens along PC1 and PC2 (Fig. 3) does not show sufficient discrimination of the populations, the canonical variate analysis indicates a significant effect of population on gonopod shape (Wilk's $\lambda = 0.0029$, $F = 4.17$, $df = 60$ and 73, $P = 7.36 \times 10^{-9}$). PC1 and PC2 represent 34.4% of the total shape variation and correspond largely to the sternite/metaplica and the paracoxites, respectively. The gonopod shape space occupied by each specimen, as shown on the CV1 and CV2 axes, suggests clustering along population trajectories (Fig. 4).

Specimens from Chitombo, Marange, Mazowe, Muzinga, and Sahumani appear to occupy distinct morpho-space with minimal overlap. Despite the low sample size, cross-validation tests showed a relatively high percentage of correct specimen classification for populations with more than one specimen as follows: Chitombo (83%); Marange (75%); Mazowe (60%); Muzinga (75%); Sahumani (82%), and an overall classification rate of 75%.

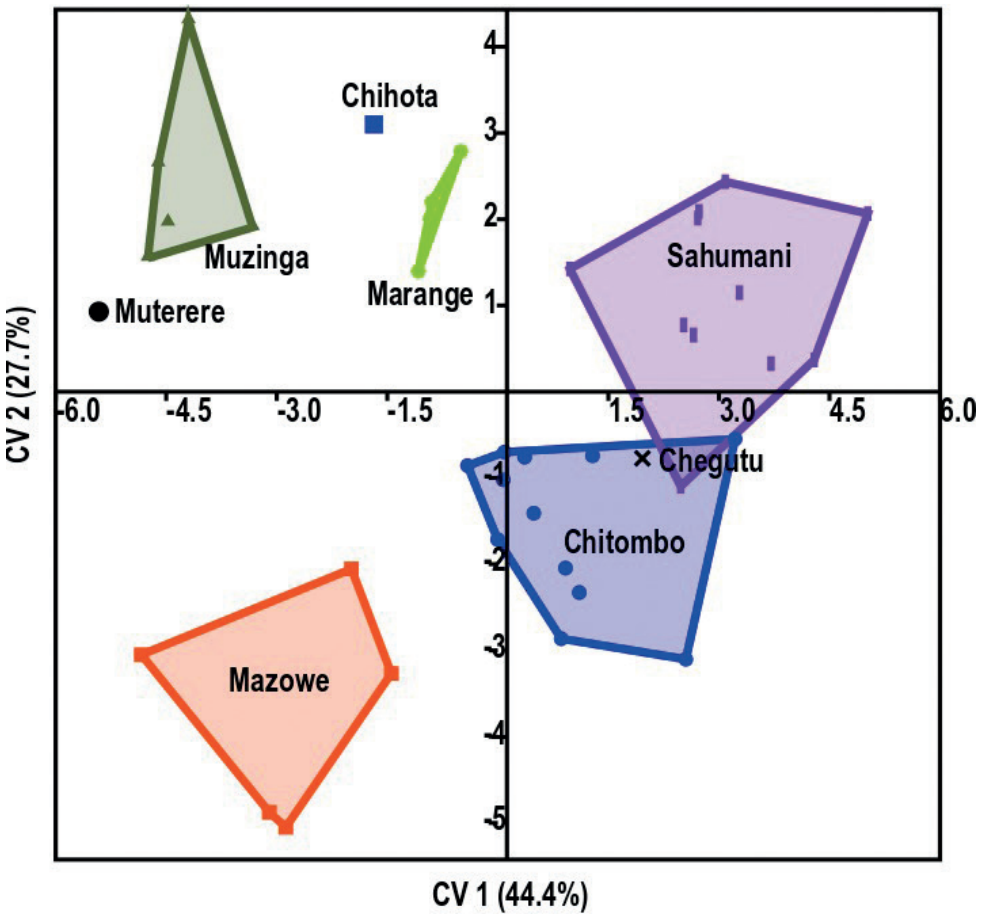

Figure 4. Canonical variate analysis based on the first 15 PC scores of gonopod shape across eight populations of *B. flavicollis*. Scatterplot indicates population grouping of sampled specimens along CV1 and CV2. Percentages indicate the proportion of variance explained by each CV axis.

Discussion

For any morphological structure in an organism, there are almost limitless possibilities of theoretical shapes that could evolve. However, only a few are evolutionarily viable due to functional, and thus adaptive constraints placed on such structures by natural selection (Mcghee 2007; Adebowale et al. 2012). These adaptive constraints may explain in part why comparatively only a limited set of shape configurations are encountered across the biological world, even among lineages with diverse genetic heritage.

Given this background and the significance of male gonopods in the reproductive success of arthropods, some levels of morphological stasis in gonopods would be expected in a species as widely distributed as *B. flavicollis*. Our results demonstrate that gonopod shape in *B. flavicollis* varies significantly among the eight populations, with landmarks 6, 7 and 11 showing pronounced shape changes along the first two PCs. However, it is conceivable that extensive sampling of Chihota and Muterere specimens would have blurred the distinction between them and their respective nearest neighbour population groups. The combination of landmarks 6 and 7, corresponding to the apex and base of the sternite, defines a spatial relation between two points that could be discriminatory at interspecific level of comparison. These three landmarks (6, 7, and 11) are regarded as type I (see Bookstein 1997a), and as such could be expected to hold some taxonomic or evolutionary significance for *B. flavicollis*. This is consistent with the finding of Enghoff (2017), who reported that the shapes of the sternite on gonopods of Spirostreptidae species are sufficiently variable to be of taxonomic value. While it is tempting to simplify the diagnostic attributes of the gonopod to the sternite, the proplica and the processes on the metaplica (however useful these are), it is equally noteworthy that the next eight PCs (PC3–PC10) capture 51.5% of shape variation. This indicates a more nuanced aspect to gonopod shape variation, and it is spread across most of the landmarks.

Based on the similarities of gonopods in a widely distributed African millipede genus *Doratogonus* Attems 1914, Hamer and Slotow (2000) reported that the diagnoses of the species could be too inclusive. Studies in other invertebrate groups, such as scorpions (Jacob et al. 2004), seem to support the assertion that morphology underestimates taxonomic diversity. However, these conclusions were based on qualitative assessments of gonopods, which is susceptible to subjective interpretations. A major strength of geometric morphometric methods is the quantification and analysis of shape information in a reproducible manner. This approach allows a more objective evaluation of important but cryptic shape variations that may be imperceptible to the human eye. Such cryptic variations, if heritable, could be the difference between operational taxonomic units (OTU). Furthermore, recent methodological advances in geometric morphometrics have seen the extraction of shape data and their incorporation into a phylogenetic matrix to infer evolutionary relationships (Smith and Hendricks 2013; Díaz -Cruz et al. 2021).

Although observations of conservatism in morphology have been reported in a number of animal taxa including spiders (Huber et al. 2005), copepods (Lajus et al. 2015) and rotifers (Fontaneto et al. 2007), our results support that gonopod shape

differs among populations in *B. flavicollis*. A high degree of genetic divergence documented between two populations of *B. flavicollis* (see Mwabvu et al. 2013) suggests that gonopod morphology and genetic divergence could be coupled. Our results further demonstrate that gonopod morphology, when rightly quantified, could serve as an additional tool for differentiating populations or taxa. Besides the clear discontinuity in colour patterns, the eight populations in the present study occupy distinct geographic areas, which suggests a limited gene flow between populations. Thus, the variation in environmental conditions at these localities could have influenced the subtle but significant divergence in genital morphology. In addition to molecular data and body colour patterns, gonopods have reliable diagnostic traits that identify unique populations in the *B. flavicollis*. The evidence suggests that *B. flavicollis* could be an inclusive complex requiring further studies to clarify the taxonomic assignment of the populations. On the other hand, the species could have a genetic machinery that allows for some degree of morphological latitude in gonopod divergence in differing environments.

Future work on *B. flavicollis* should include the use of nuclear markers to compare the levels of genetic divergence among the populations. Based on the similar pattern of body colour between populations, the high levels of genetic divergence reported by Mwabvu et al. (2013), and the differences in gonopod shapes observed in our study, *B. flavicollis* could be a species complex. Importantly, Pimvichai et al. (2011) reported identical gonopods in some species of *Thyropygus* Pocock, 1894 (Harpagophoridae) that had high DNA sequence divergence, and Frederiksen et al. (2012) observed identical gonopods in millipede populations of Julidae (Julida) that differ in body colouration and DNA sequences. These observations indicate that genetic diversity may not necessarily be matched by morphological changes, and strengthens the argument for thorough molecular analyses of *B. flavicollis* populations.

Conclusion

Even though three out of eight populations in our study had one specimen, our study highlights the importance of using quantitative methods in taxonomy. Our results support the position that population divergence and variation in male genitalia of *B. flavicollis* could be coupled. Bond et al. (2003) concluded based on gonopod morphology that the classification of millipedes may overlook taxonomic diversity due to OTU lumping. Although this might be true in some genera, it does not seem to be the case in *B. flavicollis*. In order to better assess the taxonomic importance of male gonopod shape variation in tropical millipedes, geometric morphometrics could be included routinely in these studies. Our results have conservation implications for *B. flavicollis* in particular, and millipedes in general. Populations of the same species in different environments represent opportunities for maintaining a large adaptive genetic base that may, or may not, proceed to full speciation. Conserving such populations and the processes that maintain them is akin to procuring an evolutionary insurance against the vagaries of unpredictable changes in the environment.

Acknowledgements

We wish to thank the KwaZulu-Natal Museum for granting access to the millipede collection, University of KwaZulu-Natal (Microscopy Unit, Pietermaritzburg) for making photographic equipment available and the National Research Foundation—through the Knowledge, Interchange and Collaboration (KIC) (Grant No. 92969)—for providing research funds to T. Mwabvu. We are grateful to Takudzwa Samuneta and Denounce Mukora for assisting in fieldwork.

References

Adebowale A, Nicholas A, Lamb J, Naidoo Y (2012) Elliptic Fourier analysis of leaf shape in southern African *Strychnos* section *Densiflorae* (Loganiaceae). Botanical Journal of the Linnean Society 170(4): 542–553. https://doi.org/10.1111/j.1095-8339.2012.01308.x

Arnqvist G, Martensson T (1998) Measurement error in geometric morphometrics: Empirical strategies to assess and reduce its impact on measures of shape. Acta Zoologica Academiae Scientiarum Hungaricae 44: 73–96.

Bond JE, Sierwald P (2002) Cryptic speciation in the *Anadenobolus excisus* millipede species complex on the island of Jamaica. Evolution; International Journal of Organic Evolution 56(6): 1123–1135. https://doi.org/10.1111/j.0014-3820.2002.tb01426.x

Bond JE, Beamer BA, Hedin MC, Sierwald P (2003) Gradual evolution of male genitalia in a sibling species complex of millipedes (Diplopoda: Spiroboloda: Rhinocricidae: Anadenobolus). Invertebrate Systematics 17(6): 711–717. https://doi.org/10.1071/IS03026

Bookstein FL (1997a) Morphometric tools for landmark data: Geometry and biology. Cambridge University Press. https://doi.org/10.2307/2534038

Bookstein FL (1997b) Landmark methods for forms without landmarks: Morphometrics of group differences in outline shape. Medical Image Analysis 1(3): 225–243. https://doi.org/10.1016/S1361-8415(97)85012-8

Díaz-Cruz JA, Alvarado-Ortega J, Ramírez-Sánchez MM, Bernard EL, Allington-Jones L, Graham M (2021) Phylogenetic morphometrics, geometric morphometrics and the Mexican fossils to understand evolutionary trends of enchodontid fishes. Journal of South American Earth Sciences 111: e103492. https://doi.org/10.1016/j.jsames.2021.103492

Enghoff H (2017) A new East African genus of spirostreptid millipedes (Diplopoda, Spirostreptida, Spirostreptidae), with notes on fungal ectoparasite *Rickia gigas*. Zootaxa 4273(4): 501–530. https://doi.org/10.11646/zootaxa.4273.4.3

Fisher RA (1958) Statistical methods for research workers. Hafner Publishers.

Foley NM, Goodman SM, Whelan CV, Puechille SJ, Teeling E (2017) Towards navigating the Minotaur's labyrinth: Cryptic diversity and taxonomic revision within the speciose genus *Hipposideros* (Hipposideridae). Acta Chiropterologica 19(1): 1–18. https://doi.org/10.3161/15081109ACC2017.19.1.001

Fontaneto D, Giordani I, Melone G, Serra M (2007) Disentangling the morphological stasis in two rotifer species of the *Brachionus plicatilis* species complex. Hydrobiologia 583(1): 297–307. https://doi.org/10.1007/s10750-007-0573-1

Frederiksen S, Peterson G, Enghoff H (2012) How many species are there of *Pachyiulus*? A contribution to the taxonomy of Europe's largest millipedes (Diplopoda: Julida: Julidae). Journal of Natural History 46(9–10): 599–611. https://doi.org/10.1080/00222933.2011.651636

Fruciano C (2016) Measurement error in geometric morphometrics. Development Genes and Evolution 226(3): 139–158. https://doi.org/10.1007/s00427-016-0537-4

Hamer ML, Slotow R (2000) Patterns of distribution and speciation in the genus *Doratogonus* (Diplopoda: Spirostreptidae). In: Wytwer J, Golovatch S (Eds) Progress in studies on Myriapoda and Onychophora. Fragmenta Faunistica (Supplement) 43: 295–311.

Hammer Ø, Happer D, Ryan P (2001) PAST: Paleontological Statistics Software: Package for Education and Data Analysis. Palaeontologia Electronica 4: 1–9.

Huber BA, Rheims CA, Brescovit AD (2005) Speciation without changes in genital shape: A case study on Brazilian pholcid spiders (Araneae: Pholcidae). Zoologischer Anzeiger 243(4): 273–279. https://doi.org/10.1016/j.jcz.2004.12.001

Jacob A, Gantebein B, Braunwalder ME, Nentwig W, Kropf C (2004) Complex male genitalia (hemispermatophores) are not diagnostic for cryptic species in the genus *Euscorpius* (Scorpiones: Euscorpiidae). Organisms, Diversity & Evolution 4(1–2): 59–72. https://doi.org/10.1016/j.ode.2003.11.002

Klingenberg CP (2011) MorphoJ: An integrated software package for geometric morphometrics. Molecular Ecology Resources 11(2): 353–357. https://doi.org/10.1111/j.1755-0998.2010.02924.x

Krabbe E, Enghoff H (1985) Morphological variability in a population of *Orthoporus antillanus* (Pocock, 1894) from Barbados, with notes on the taxonomic status of the species (Diplopoda: Spirostreptida, Spirostreptidae). Entomologica Scandinavica 15: 333–339.

Lajus D, Sukhikh N, Alekseev V (2015) Cryptic or pseudocryptic: Can morphological methods inform copepod taxonomy? An analysis of publications and a case study of the *Eurytemora affinis* species complex. Ecology and Evolution 5(12): 2374–2385. https://doi.org/10.1002/ece3.1521

Mcghee Jr GR (2007) The Geometry of Evolution: Adaptive Landscapes and Theoretical Morphospaces. Cambridge University Press. https://doi.org/10.1017/CBO9780511618369

Mwabvu T, Hamer M, Slotow R (2007) A taxonomic review and description of three new species; and phylogeny of the southern African millipede genus, *Bicoxidens* (Diplopoda: Spirostreptida: Spirostreptidae). Zootaxa 1452: 1–23. https://doi.org/10.11646/zootaxa.1452.1.1

Mwabvu T, Lamb J, Slotow R, Hamer M, Barraclough D (2013) Is taxonomy in millipedes based on gonopod morphology too inclusive? Observations on genetic variation and cryptic speciation in *Bicoxidens flavicollis* (Diplopoda: Spirostreptida: Spirostreptidae). African Invertebrates 54: 349–356. https://doi.org/10.5733/afin.054.0203

Novo M, Almodovar A, Fernandez R, Trigo D, Diaz Cosin DJ (2010) Cryptic speciation of hormogastrid earthworms revealed by mitochondrial and nuclear data. Molecular Phylogenetics and Evolution 56(1): 507–512. https://doi.org/10.1016/j.ympev.2010.04.010

Pimvichai P, Enghoff H, Panha S (2011) A revision of *Thyropygus allevatus* group. Part 3: the *T. induratus* subgroup (Diplopoda: Spirostreptida: Harpagophoridae). Zootaxa 2941(1): 47–68. https://doi.org/10.11646/zootaxa.2941.1.3

Rohlf FJ (2015) The tps series of software. Hystrix, the Italian Journal of Mammalogy 26: 9–12.
Schlick-Steiner BC, Seifert B, Stauffer C, Christian E, Crozier RH, Steiner FM (2007) Without morphology, cryptic species stay in taxonomic crypsis following discovery. Trends in Ecology & Evolution 22(8): 291–292. https://doi.org/10.1016/j.tree.2007.05.004
Smith UE, Hendricks JR (2013) Geometric Morphometric Character Suites as Phylogenetic Data: Extracting Phylogenetic Signal from Gastropod Shells. Systematic Biology 62(3): 366–385. https://doi.org/10.1093/sysbio/syt002
Sokal R, Rohlf F (1995) Biometry: the principles and practice of statistics in biological sciences. WH Free Company.

African Invertebrates 63(1): 89–103 (2022)
doi: 10.3897/AfrInvertebr.63.86661
https://africaninvertebrates.pensoft.net

RESEARCH ARTICLE

African Invertebrates
A journal of biodiversity research

Two new species of *Phronia* Winnertz, 1864 (Diptera, Mycetophilidae) from Taita Hills, Kenya

Olavi Kurina[1], Aleksander Pototski[2]

1 *Institute of Agricultural and Environmental Sciences, Estonian University of Life Sciences, Kreutzwaldi st 5-D, 51006 Tartu, Estonia* **2** *Estonian Society of Lepidopterologists; Lasnamäe Gymnasium, Pae 59, 13621 Tallinn, Estonia*

Corresponding author: Olavi Kurina (olavi.kurina@emu.ee)

Academic editor: Burgert Muller | Received 17 May 2022 | Accepted 15 June 2022 | Published 29 June 2022

https://zoobank.org/069C658B-35EE-497C-A41A-16C513542B52

Citation: Kurina O, Pototski A (2022) Two new species of *Phronia* Winnertz, 1864 (Diptera, Mycetophilidae) from Taita Hills, Kenya. African Invertebrates 63(1): 89–103. https://doi.org/10.3897/AfrInvertebr.63.86661

Abstract

Two new *Phronia* Winnertz, 1864 species—*P. hannarostiae* **sp. nov.** and *P. ristoi* **sp. nov.**—are described from Taita Hills in Kenya, representing the first named species of this genus in the African continent. The new species are morphologically similar to each other as well as to *P. flobertae* Matile – a species described from the Comoro Islands. These three species can be distinguished by details of the male terminalia, in particular by comparing the structures of the gonostyli. The new species are photographed and hand-drawn figures provided, and their taxonomy is discussed.

Keywords

Afrotropical region, fungus gnats, Kenya, new species, Sciaroidea, Taita Hills, taxonomy

Introduction

The genus *Phronia* Winnertz, 1864 was one of the first genera of fungus gnats (Diptera: Mycetophilidae) that was thoroughly studied in the 19th century. Namely, Henryk Dziedzicki (1889) published a monograph of European *Phronia* species including detailed descriptions of 51 species (some of them were later transferred to *Trichonta* Winnertz, 1864) supplemented by high quality figures, which are still invaluable in species delimitation today. Over the course of the next 130 years, a number of new species were described (e.g. Lundström 1906; Chandler 1992; Chandler and Ribeiro 1995;

Chandler 2001; Jakovlev and Polevoi 2008; Kurina 2008; Ševčík 2009; Salmela and Kolcsár 2017) along with several meticulous synopses devoted to Finnish (Hackman 1970), Nearctic (Gagné 1975) and European species (Plassmann 1977). Moreover, as a part of the latest Mycetophilidae monographs, Zaitzev (2003) and Chandler (2022) reviewed the species in Russia and Britain, respectively. All in all, about 150 species are currently known from all zoogeographical regions except Antarctica, including three of them from fossils (Evenhuis 1994; Fungus Gnats Online Authors 2022). However, the majority of the species have been discovered from the Palaearctic and Nearctic Regions, whereas only two are known from the Neotropical Region (Oliveira and Amorim 2014) and one from both Oriental and Australasian Regions (Bechev 2000). In the Afrotropical Region, four species of *Phronia* have so far been described, one from Seychelles and three from the Comoro Islands (Matile 1978). Matile (1978) additionally mentioned an undescribed species from Malawi and provided figures of male terminalia of all described Afrotropical species. Moreover, Søli (2017) noted that there are undescribed species known from Madagascar, South Africa, Tanzania and Uganda.

As a member of the tribe Mycetophilini, the genus *Phronia* has anepisternum with strong bristles, whereas within the tribe, the distinguishing characters include bare anepimeron, short cubital fork, subcostal vein ending free and the costal vein extending at most very slightly beyond apex of R_{4+5} (e.g. Søli et al. 2000). As usual for the majority of fungus gnats, the species-specific characters appear mostly in the structure of the male terminalia.

The current paper aims to describe two new species from Kenya, representing the first named *Phronia* species from the continental Africa.

Material and methods

The material was collected from Taita Hills in southern Kenya. The slopes of Taita Hills were formerly covered by moist montane forest of which only fragments are left, but these areas still accommodate a considerable diversity of species including endemic taxa (cf. Rosti et al. 2022).

The material was collected by handpicking specimens from a ground level rock cavity (Fig. 1) surrounded by tropical deciduous forest (Fig. 2) and preserved initially on a cotton-layer in an envelope. These specimens represent the only Mycetophilidae collected at this site. In the laboratory, all specimens were first kept in a high humidity relaxing chamber and when the specimens became pliable they were pinned and photographed. Thereafter, terminalia were detached from the abdomen and treated in a solution of hot KOH for maceration. The remaining chitinous parts were washed with distilled water, neutralized in acetic acid and transferred into glycerine. After examination, terminalia were stored in glycerine in a small plastic microvial together with the specimen.

The digital images of general habitus and terminalia were combined using the software LAS V.4.1.0. from multiple gradually focused images taken by a Leica DFC 450 camera attached to a stereomicroscope Leica 205C (see also Kurina et al. 2017). Topaz

Figure 1. The specimens were collected from a ground level rock cavity in Ngangao indigenous forest. Photo by H Rosti.

Figure 2. Ms. Hanna Rosti on fieldwork in tropical deciduous forest that surrounds the collecting locality in Taita Hills. The patronymic name *P. hannarostiae* honours her substantial contribution to make collecting of the fungus gnat material of this paper possible. Photo by A Pototski.

Sharpen Al v3.2.2 software was implemented to enhance the quality of the images. Black and white figures of the terminalia were prepared using a U-DA drawing tube attached to a compound microscope Olympus CX31. Adobe Photoshop CS5 was used for editing the figures and compiling the plates. The morphological terminology other than male terminalia follows that of Søli (2017). The terminology of male terminalia is used in accordance with Kjærandsen et al. (in press) and is explained also in Figs 4, 6, 7. The material is deposited in the Institute of Agricultural and Environmental Sciences, Estonian University of Life Sciences [former Institute of Zoology and Botany], Tartu, Estonia (**IZBE**).

Taxonomy

***Phronia hannarostiae* sp. nov.**
https://zoobank.org/BC67E7A9-C34A-48D0-AA50-6017CACFC40C
Figs 3A, 4A–F, 6B, 7B

Diagnosis. *Phronia hannarostiae* sp. nov. is closest morphologically to *P. flobertae* Matile, 1978 and *P. ristoi* sp. nov. but differs in characters of the male terminalia: gonocoxites anteroventrally with wide shallow incision; distal lobe of the ventral branch of the gonostylus elongated and stout; medial lobe of the ventral branch of the gonostylus sub-rounded with a strong long spine at dorsal margin medially; internal branch of the gonostylus bipartite, with ventral lobe apically widening, having combs of spines along posterior and dorsal margins, with dorsal lobe conical, having marginal lamellae; anterior branch of the gonostylus subrectangular, posteriorly somewhat widening, with four long setae subapically; aedeagal guides wide, narrower basally, rounded.

Etymology. The species is named after Ms. Hanna Rosti (Helsinki, Finland), a PhD student of the University of Helsinki. Her study project includes research and conservation of nocturnal mammals of Taita Hills. She generously assisted and guided Mr. Risto Haverinen (Vantaa, Finland) and the junior author, collectors of the material, around the named area.

Description. Male. Body length 3.1–3.2 mm (n = 4). **Coloration.** Head with vertex and frons brown, face and clypeus dark yellow, mouthparts yellow except palpus dark brown. Scape, pedicel and base of first flagellomere yellow, rest of flagellum brown. Thorax with scutum dull-yellow, having three longitudinal dull-brown strips, medial tapering posteriorly, ending before posterior margin; scutellum anteriorly brown, posteriorly yellowish to light brown; anepisternum, laterotergite and medial part of mediotergite brown, other thoracic lateral parts yellow. Thoracic setae brown. Wing hyaline, unmarked with slight yellowish tinge. Halter with stem yellow and knob brown. Legs yellow, hind coxa with lateral elongated brown macula, mid coxa with brown macula apically, hind femur entirely brown at apical fifth and brown dorsally at apical half, all tibiae with brown apical band, and tarsi yellow but seem darker because of dense brown setae. All setae on legs brown, tibial spurs brown. Abdomen brown, first 3–4 segments with large yellow anterolateral areas. Abdominal vestiture

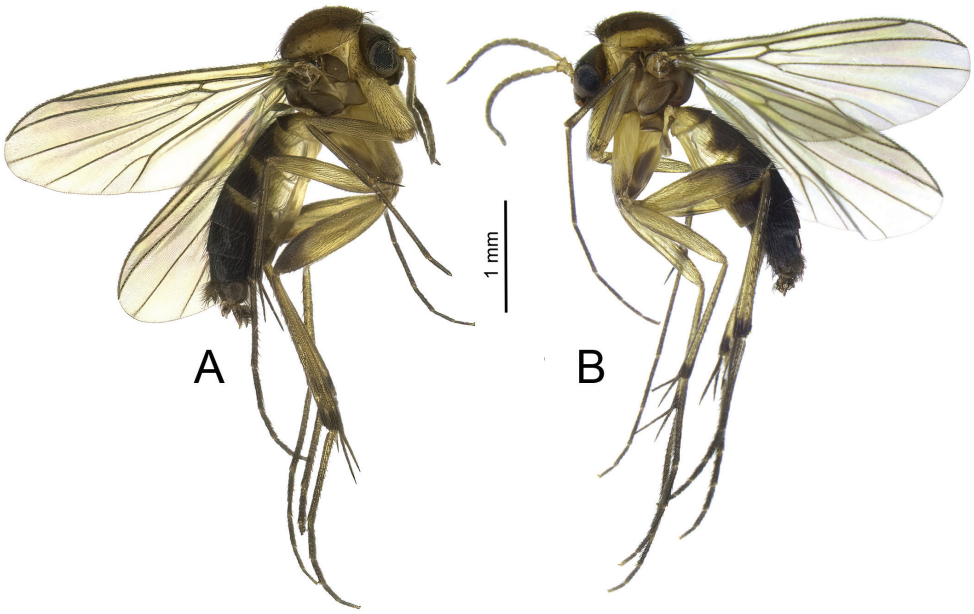

Figure 3. General habitus of Afrotropical *Phronia* species, lateral view **A** *P. hannarostiae* sp. nov. **B** *P. ristoi* sp. nov.

brown. Terminalia dark yellow. ***Head***. Ocelli two, touching eye margins. Frontal furrow complete. Clypeus rectangular. Fourth flagellar segment about as long as wide, apical flagellar segment 2.2 times as long as wide basally. Flagellar segments with dense whitish setae about one third of segments' width. ***Thorax.*** Scutum covered with setae, marginal setae stronger, two prominent prescutellar setae extending well over scutellum posteriorly. Scutellum with four strong marginal setae. Antepronotum with 4–5 strong and several weaker setae. Proepisternum with three strong and some weaker setae. Anepisternum with four strong setae at hind margin and several weak setae over surface. Katepisternum and anepimeron non-setose. Laterotergite setose with setae longer towards hind margin. Mediotergite non-setose. ***Wing.*** Length 2.88–3.00 mm, length to width 2.77–2.82. *Sc*, *bm-m*, *m-stem* and *CuP* non-setose, all other veins setose. *C* extending very slightly beyond apex of R_{4+5}. Length of *Sc* measured from *h* 0.47 of *r-stem*. *r-m* about as long as *m-stem*. Posterior fork begins well beyond furcation of anterior fork, at the level of basal third of anterior fork, ratio of M_2 to M_4 2.7. ***Legs.*** Ratio of femur to tibia for fore, mid and hind legs: 1.11–1.29; 0.95–1.03; 0.84–0.93. Ratio of tibia to basitarsus for fore, mid and hind legs: 1.00–1.13; 1.30–1.48; 1.67–1.77. Fore tibia with a spur 2.25–2.57 times of tibial maximum width. Mid tibia with anterior spur 3.11–3.25 times and posterior spur 3.89–4.25 times of tibial maximum width. Hind tibia with anterior spur 2.55–3.22 times and posterior spur 3.27–3.89 times of tibial maximum width. ***Terminalia*** (Figs 4A–F, 6B, 7B). Tergite 9 posteriorly rounded, with non-regular row of sub-marginal setae of different length, anteriorly with large U-shaped incision. Cerci long ovate, posteriorly blunt.

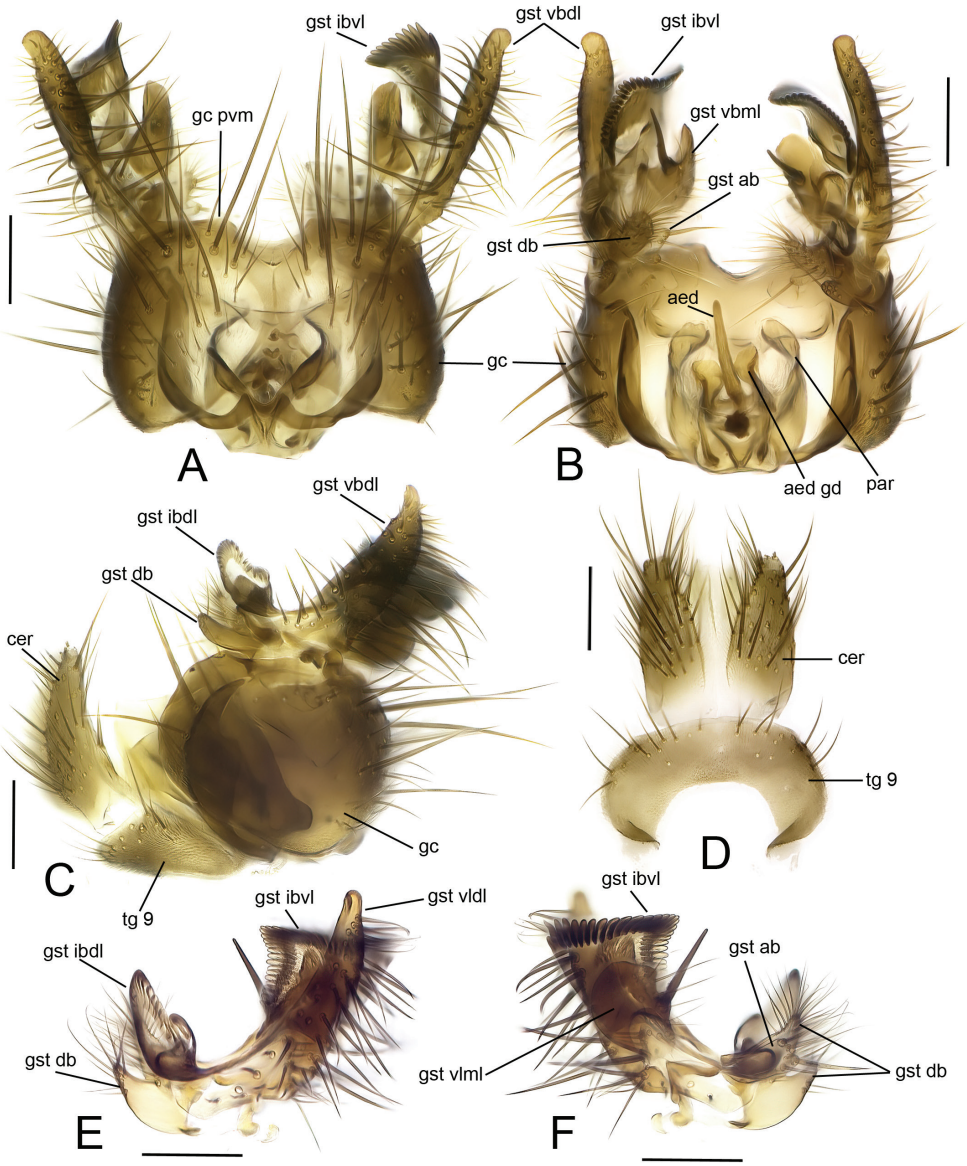

Figure 4. *Phronia hannarostiae* sp. nov., male terminalia **A** terminalia, ventral view **B** terminalia, dorsal view with cerci detached **C** terminalia, lateral view **D** cerci and tergite IX **E** gonostylus, lateral view **F** gonostylus, internal view. Abbreviations: aed = aedeagus, aed gd = aedeagal guide, cer = cercus, gc = gonocoxite, gc pvm = posteroventral margin of gonocoxite, gst ab = anterior branch of gonostylus, gst db = dorsal branch of gonostylus, gst ibdl = dorsal lobe of internal branch of gonostylus, gst ibvl = ventral lobe of internal branch of gonostylus, gst vbdl = distal lobe of ventral branch of gonostylus, gst vbml = medial lobe of ventral branch of gonostylus, par = paramere, tg 9 = tergite IX. Scale bars: 0.1 mm.

Gonocoxites fused, closed ventrally and open dorsally; anteroventrally with wide, shallow incision. Posteroventral margin of gonocoxites with medial incision, supplied by a dorsal fringe. Gonocoxites setose with setae erect, somewhat longer on posterior half,

deviating from other setosity of gonocoxites. Ventral branch of gonostylus with setose distal lobe, elongated and tapering in lateral view, posteriorly blunt and non-setose; setose medial lobe subrounded, with excavation at dorsal margin posteriorly and with a stout spine at dorsal margin medially. Internal branch of gonostylus formed of ventral and dorsal lobes; ventral lobe large, posteriorly widening, discernible partly between distal and medial lobe of ventral branch, with combs of spines along posterior and dorsal margin; dorsal lobe cone-shaped with lamellae along margins. Dorsal branch of gonostylus formed from two conical, posteriorly setose lobes. Anterior branch of gonostylus subrectangular, posteriorly slightly widening, with four subapical strong setae. Aedeagus digitate. Aedeagal guides apically widening, rounded. Parameres large, somewhat convoluted, not extending over aedeagus apically.

Female. Unknown.

Type material. ***Holotype.*** Kenya • ♂; Taita-Taveta County, Taita Hills, Ngangao indigenous forest; 3.3642°S, 38.3410°E alt. 1930 m; 4 February 2022; A. Pototski & R. Haverinen leg.; hand-picked (pinned, terminalia in glycerin, IZBE0228825). ***Paratypes.*** Kenya • 3 ♂♂, same data as for holotype (pinned, terminalia in glycerin, IZBE0228826, IZBE0228827, IZBE0228828).

Comments. Matile provided figures of male terminalia of all described Afrotropical *Phronia* species from ventral view (Matile 1978: figs 59–62) that regrettably do not describe all details of the gonostyli. However, the distal lobes of the ventral branch of the gonostylus and ventromedial margin of the gonocoxites have been provided in necessary details to allow an unambiguous delimitation of the species. *Phronia hannarostiae* sp. nov. shares the general outline of the gonostylus with *P. ristoi* sp. nov. but can be distinguished by (1) distal lobe of the ventral branch of the gonostylus stout, posteriorly blunt with subequal setae along the surface (slender, posteriorly tapering and bent, with aggregation of very long setae anteroventrally in *P. ristoi*), (2) medial lobe of the ventral branch of the gonostylus subrounded with a stout spine at dorsal margin medially (thumb-shaped, with a small hump at dorsal margin medially, with a sabre-like spine subapically in *P. ristoi*) and (3) internal branch of the gonostylus with ventral lobe large, posteriorly widening, with combs of spines along posterior and dorsal margin (large, conical, with comb of lamellae along dorsal margin in *P. ristoi*). Moreover, *P. hannarostiae* has (1) cerci long, ovate, posteriorly blunt (tapering posteriorly, with a mesial excavation in *P. ristoi*), (2) aedeagal guides apically widening, rounded (digitiform, apically pointed in *P. ristoi*) and (3) parameres large, somewhat convoluted, not extending over aedeagus apically (large, extending over aedeagus apically in *P. ristoi*).

Phronia ristoi sp. nov.

https://zoobank.org/409BD520-67BF-4B36-8AAA-070668D788B6
Figs 3B, 5A–F, 6A, 7A

Diagnosis. *Phronia ristoi* sp. nov. is closest to *P. flobertae* Matile, 1978 and *P. hannarostiae* sp. nov. but differs in characters of the male terminalia: gonocoxites anteroventrally with shallow U-shaped incision; distal lobe of the ventral branch of the gonostylus

elongated, tapering, apically bent; medial lobe of the ventral branch of the gonostylus thumb-like, with a strong long sabre-like spine subapically; internal branch of the gonostylus bipartite, with ventral lobe conical, having a comb of lamellae along dorsal margin, with dorsal lobe bipartite, having marginal lamellae; anterior branch of the gonostylus posteriorly rounded, with 3–4 long setae subapically; aedeagal guides digitiform, apically pointed.

Etymology. The species is named in honor of Mr. Risto Haverinen (Vantaa, Finland), a Finnish entomologist working mainly on macrolepidoptera. He was one of the collectors of the material of both species described in this paper and, additionally, contributed greatly towards successful fieldwork in Kenya.

Description. Male. Body length 2.9–3.0 mm (n = 2). **Coloration.** Head with vertex and frons dark brown, face and clypeus dark yellow to light brown, mouthparts yellow except palpus dark brown. Scape, pedicel and base of first flagellomere yellow, rest of flagellum brown.

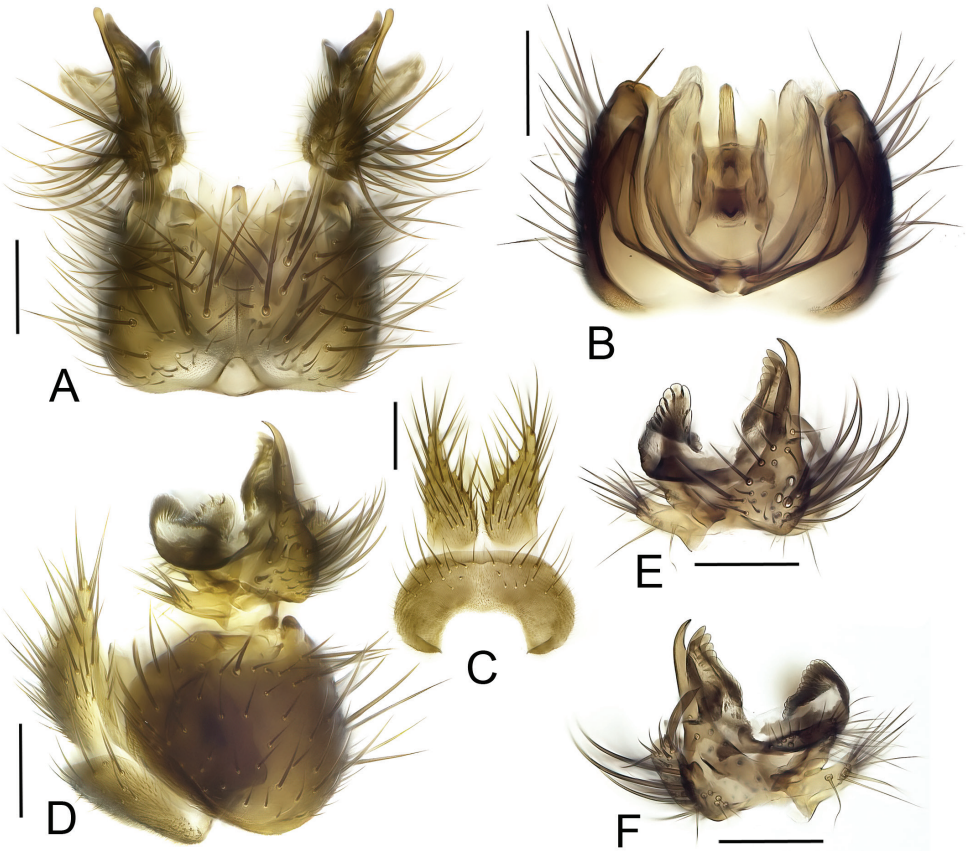

Figure 5. *Phronia ristoi* sp. nov., male terminalia **A** terminalia, ventral view **B** terminalia, dorsal view with gonostyli and cerci detached **C** terminalia, lateral view **D** cerci and tergite IX **E** gonostylus, lateral view **F** gonostylus, internal view. Scale bars: 0.1 mm.

Thorax with scutum dull-yellow, having three anteriorly fused longitudinal dull-brown strips, medial tapering posteriorly, ending before posterior margin; scutellum dull brown; antepronotum and proepisternum yellow, other thoracic lateral parts dull brown, posterior margin of laterotergite darker. Thoracic setae brown. Wing hyaline, unmarked with slight yellowish tinge. Halter with stem yellow and knob brown. Legs yellow, hind coxa with lateral elongated brown macula, hind femur entirely brown at apical fifth and brown dorsally at apical half, all tibiae with brown apical band, and tarsi yellow but seem darker because of dense brown setae. All setae on legs brown, tibial spurs brown. Abdomen brown, first 3–4 segments with yellow anterolateral areas. Abdominal vestiture brown. Terminalia dark yellow to brown. ***Head.*** Ocelli two, touching eye margins. Frontal furrow complete. Clypeus rectangular. Fourth flagellar segment about 1.2 times as long as wide, apical flagellar segment 2.1 times as long as wide basally. Flagellar segments with dense whitish setae about one third of segments' width. ***Thorax.*** Scutum covered with setae, marginal setae stronger, two prominent prescutellar setae extending well over scutellum posteriorly. Scutellum with four strong marginal setae. Antepronotum with four strong and several weaker setae. Proepisternum with three strong and some weaker setae. Anepisternum with 3–4 strong setae at hind margin and several weak setae over surface. Katepisternum and anepimeron non-setose. Laterotergite setose with setae longer towards hind margin. Mediotergite non-setose. ***Wing.*** Length 2.67–2.79 mm, length to width 2.53–2.65. *Sc*, *bm-m*, *m-stem* and *CuP* non-setose, all other veins setose. *C* extending very slightly beyond apex of R_{4+5}. Length of *Sc* measured from *h* 0.50 of *r-stem*. *r-m* about 0.75 times as long as *m-stem*. Posterior fork begins well beyond furcation of anterior fork, at the level of basal third of anterior fork, ratio of M_2 to M_4 2.4. ***Legs.*** Ratio of femur to tibia for fore, mid and hind legs: 0.96–1.00; 0.91–0.94; 0.87–0.91. Ratio of tibia to basitarsus for fore, mid and hind legs: 1.00–1.04; 1.43–1.50; 1.73–1.80. Fore tibia with a spur 2.67 times of tibial maximum width. Mid tibia with anterior spur 3.00–3.57 times and posterior spur 4.29 times of tibial maximum width. Hind tibia with anterior spur 2.50–2.70 times and posterior spur 3.10–3.50 times of tibial maximum width. ***Terminalia*** (Figs 5A–F, 6A, 7A). Tergite 9 posteriorly rounded, with non-regular row of sub-marginal setae of different length, anteriorly with large U-shaped incision. Cerci long ovate, tapering posteriorly, with well discernible excavation mesially. Gonocoxites fused, closed ventrally and open dorsally; anteroventrally with shallow U-shaped incision. Posteroventral margin of gonocoxites medially membranous with a shallow incision. Gonocoxites setose with erect setae of sub-equal length. Ventral branch of gonostylus with setose distal lobe, anteriorly shoe-shaped, anteroventral part with an aggregation of long curved setae, posterior part non-setose, slightly bent; setose medial lobe thumb-shaped, with a small hump at dorsal margin medially and with a sabre-like spine subapically. Internal branch of gonostylus formed of ventral and dorsal lobes; ventral lobe large, conical, discernible partly between distal and medial lobe of ventral branch, with comb of lamellae along dorsal margin; dorsal lobe bipartite with lamellae along margins. Dorsal branch of gonostylus formed from two conical setose lobes. Anterior branch of gonostylus thumb-shaped, with 3–4 subapical long setae. Aedeagus digitate. Aedeagal guides digitiform, apically pointed. Parameres large, extending over aedeagus apically.

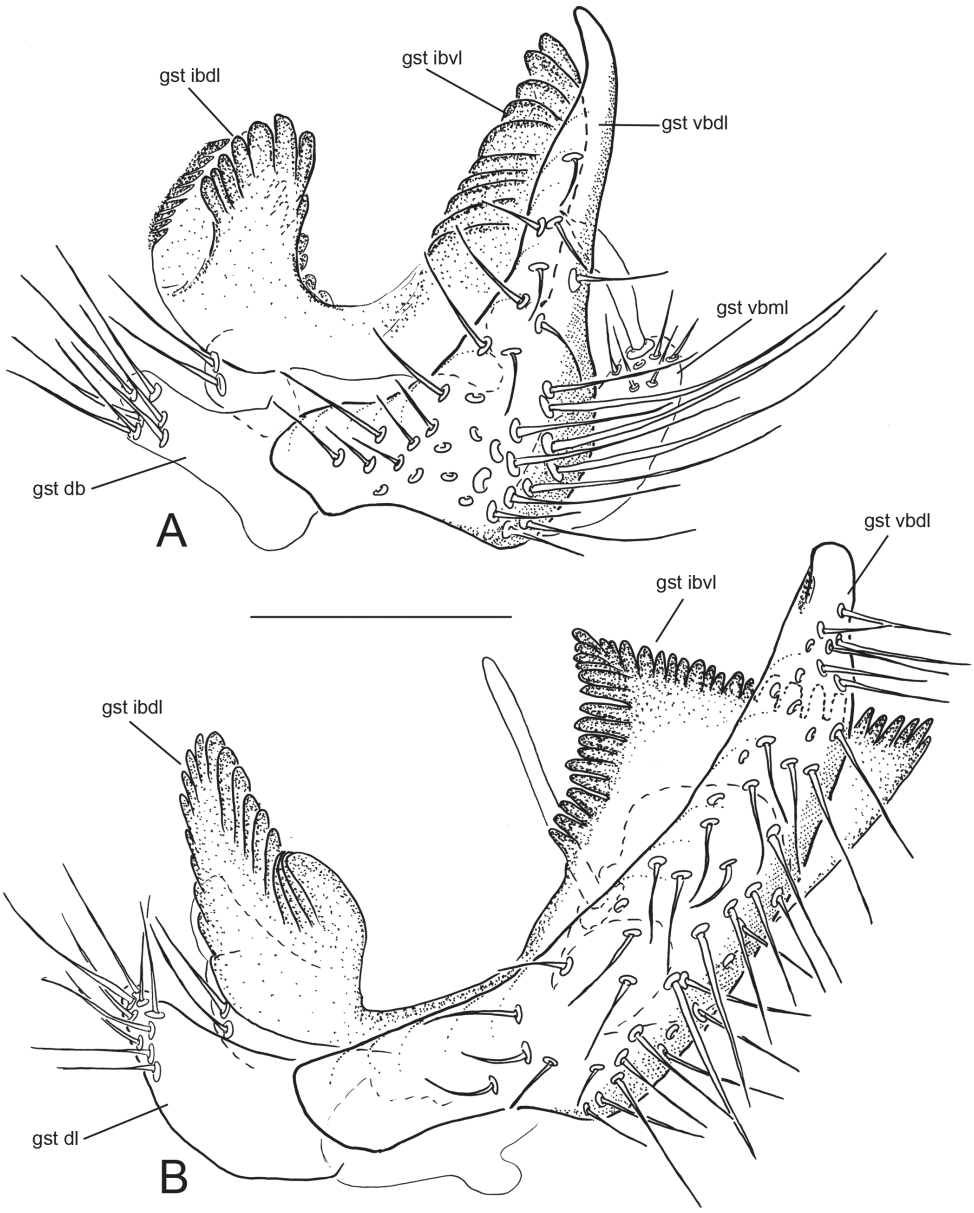

Figure 6. Gonostylus, lateral view **A** *Phronia ristoi* sp. nov. **B** *Phronia hannarostiae* sp. nov. For abbreviations see Fig. 4. Scale bar: 0.1 mm.

Female. Unknown.

Type material. ***Holotype.*** Kenya • ♂; Taita-Taveta County, Taita Hills, Ngangao indigenous forest; 3.3642°S, 38.3410°E; alt. 1930 m; 4 February 2022; A. Pototski & R. Haverinen leg.; hand-picked (pinned, terminalia in glycerin, IZBE0228829). ***Paratypes.*** Kenya • ♂, same data as for holotype (pinned, terminalia in glycerin, IZBE0228830).

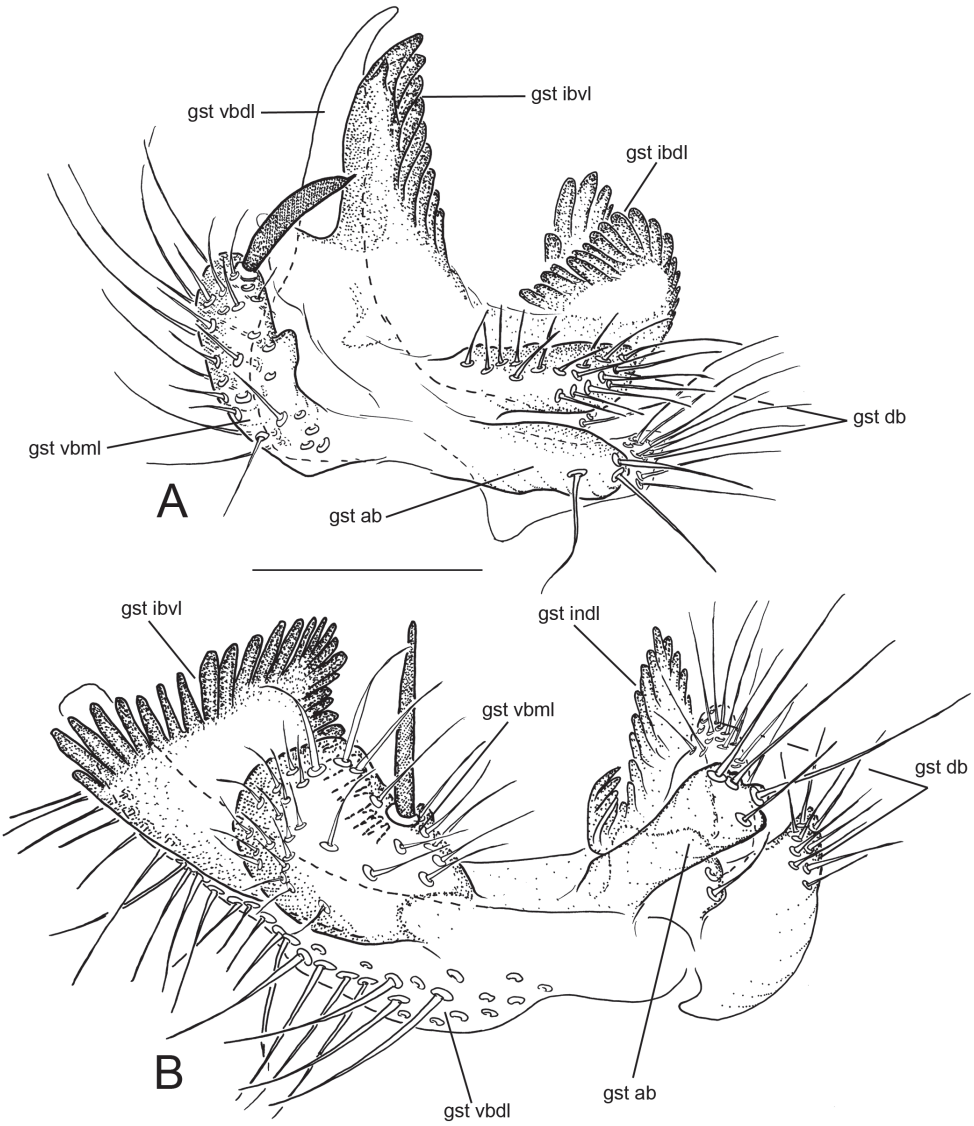

Figure 7. Gonostylus, internal view **A** *Phronia ristoi* sp. nov. **B** *Phronia hannarostiae* sp. nov. For abbreviations see Fig. 4. Scale bar: 0.1 mm.

Comments. For distinguishing *P. ristoi* sp. nov. from *P. hannarostiae* sp. nov. see comments under the latter. *Phronia ristoi* resembles also *P. flobertae* Matile, 1978 as both species have distal lobe of ventral branch of the gonostylus evenly tapering posteriorly. However, *P. ristoi* has (1) the medial lobe of ventral branch of the gonostylus with strong sabre-like subapical spine, well discernible also from ventral view (without any spine in *P. flobertae*) and (2) the ventral lobe of internal branch of the gonostylus conical, in subequal length with the distal lobe of the ventral branch (subrectangular, about half length of the distal lobe of the ventral branch in *P. flobertae*).

Discussion

Afrotropical fungus gnats (Diptera: Mycetophilidae) are rather superficially studied, with only about 10% of the real diversity known (Kirk-Spriggs and Stuckenberg 2009). Although a number of additional species have been described during the past decade (e.g. Hippa and Kurina 2012; Hippa et al. 2019; Magnussen et al. 2018; Kurina 2020; Lindemann et al. 2021), the family remains one of the least studied among Diptera in the Afrotropical region. From Kenya, only 12 species of Mycetophilidae are known to date (Matile 1980, 1992; Magnussen et al. 2018; Lindemann et al. 2021).

Taita Hills in Kenya constitute the most northeastern massive of the Eastern Arc Mountains (EAM) and the only section of this chain outside Tanzania. The EAM are known as the smallest and most fragmented biodiversity hotspots in the world (Myers et al. 2000). About ten million years ago, the savanna changed into a dominating biome in lowland, whereas the mountain ranges covered with moist tropical forest survived as isolated "islands" with a high degree of endemic species (Schabel 2006; World Wildlife Fund 2014). In terms of fungus gnats, several supposedly endemic species have been described from EAM earlier, particularly from Usambara Mountains in Tanzania (Søli 1993, 1997; Kjærandsen 1994; Magnussen et al. 2018). The described two *Phronia* species represent the first named species of this genus from continental Africa as well as the first fungus gnats from Taita Hills in Kenya.

Acknowledgements

We are much obliged to Ms. Hanna Rosti (Helsinki, Finland) and Mr. Risto Haverinen (Vantaa, Finland), who participated in fieldwork in Kenya, including collecting the specimens for this study. We are also thankful to Mr. Benson Mwakachola Lombo, a nature guide in the Taita Hills area, who assisted and led the team in the field. We are grateful to Peter Chandler (Melksham, UK) and Trude Magnussen (Oslo, Norway) for comments on an earlier draft of the manuscript.

References

Bechev D (2000) World distribution of the genera of fungus gnats (Diptera: Sciaroidea, excluding Sciaridae). Studia Dipterologica 7(2): 543–552.

Chandler P (1992) A review of the British *Phronia* Winnertz, and *Trichonta* Winnertz (Dipt., Mycetophilidae). Entomologist's Monthly Magazine 128: 237–254.

Chandler P (2001) Fungus gnats (Diptera: Sciaroidea) new to Britain. British Journal of Entomology and Natural History 13: 215–243.

Chandler P (2022) Fungus Gnats (Diptera: Mycetophilidae: Mycetophilinae). RES Handbooks for the Identification of British Insects 9(8), 398 pp.

Chandler P, Ribeiro E (1995) The Sciaroidea (Diptera) (excluding Sciaridae) of the Atlantic Islands (Canary Islands, Madeira and the Azores). Boletim do Museu Municipal do Funchal (Suplemento 3): 1–170. [Historia Natural]

Dziedzicki H (1889) Revue des espèces européennes du genre *Phronia* Winnertz avec la description des deux genres nouveaux: *Macrobrachius* et *Megophthalmidia*. Horae Societatis Entomologicae Rossicae 23: 404–532.

Evenhuis N (1994) Catalogue of the Fossil Flies of the World (Insecta: Diptera). Backhuys, Leiden, 600 pp.

Fungus Gnats Online Authors (2022) Fungus Gnats Online. https://sciaroidea.myspecies.info/ [accessed 10 May 2022]

Gagné RJ (1975) A revision of the Nearctic species of the genus *Phronia* (Diptera, Mycetophilidae). Transactions of the American Entomological Society 101: 227–318.

Hackman W (1970) New species of the genus *Phronia* Winnertz (Diptera, Mycetophilidae) from Eastern Fennoscandia and notes on the synonymies in this genus. Notulae Entomologicae 50: 41–60.

Hippa H, Kurina O (2012) New species and new records of Afrotropical *Manota* Williston (Diptera, Mycetophilidae), with a key to the species. Zootaxa 3455(1): 1–48. https://doi.org/10.11646/zootaxa.3455.1.1

Hippa H, Søli G, Kurina O (2019) New data on the genus *Manota* Williston (Diptera: Mycetophilidae) from Africa, with an updated key to the species. Zootaxa 4652(3): 401–441. https://doi.org/10.11646/zootaxa.4652.3.1

Jakovlev J, Polevoi A (2008) Two new species of the genus *Phronia* Winnertz (Diptera: Mycetophilidae) from Finland and Russian Karelia. Entomologica Fennica 19(4): 199–206. https://doi.org/10.33338/ef.84436

Kirk-Spriggs AH, Stuckenberg BR (2009) Afrotropical Diptera—rich savannas, poor rainforest. In: Pape T, Bickel D, Meier R (Eds) Diptera Diversity: Status, Challenges and Tools. Brill Academic Publishers, London, 155–196. https://doi.org/10.1163/ej.9789004148970.I-459.31

Kjærandsen J (1994) Three new species of *Pseudexechia* Tuomikoski from Tanzania and Thailand (Diptera: Mycetophilidae). Tijdschrift voor Entomologie 137: 325–330.

Kjærandsen J, Jakovlev J, Polevoi A, Salmela J, Kurina O (in press) A rarely seen taxonomic revision with immense value 41 years on: reflections on the 1981 monograph of *Trichonta* Winnertz, 1864 (Diptera, Mycetophilidae) by Raymond Gagné, with an integrative revision of the *Trichonta vulcani* (Dziedzicki, 1889) species complex. Proceedings of the Entomological Society of Washington 123.

Kurina O (2008) Sciaroidea excl. Sciaridae. In: Ziegler J (Ed.) Diptera Stelviana. A dipterological perspective on a changing alpine landscape (Vol. 1). Studia Dipterologica. Supplements 16: 245–293.

Kurina O (2020) New species and new records of *Sciophila* Meigen (Diptera: Mycetophilidae) from the Afrotropical region. Zootaxa 4722(4): 339–351. https://doi.org/10.11646/zootaxa.4722.4.3

Kurina O, Mantič M, Ševčík J (2017) A remarkable new genus of Keroplatidae (Insecta, Diptera) from the Afrotropical region, with DNA sequence data. African Invertebrates 58(1): 93–105. https://doi.org/10.3897/afrinvertebr.58.12655

Lindemann JP, Søli G, Kjærandsen J (2021) Revision of the *Exechia parva* group (Diptera: Mycetophilidae). Biodiversity Data Journal 9: e67134. https://doi.org/10.3897/BDJ.9.e67134

Lundström C (1906) Beiträge zur Kenntnis der Dipteren Finlands. 1.Mycetophilidae. Acta Societatis pro Fauna et Flora Fennica 29: 1–50.

Magnussen T, Kjærandsen J, Johnsen A, Søli GE (2018) Six new species of Afrotropical *Allodia* (Diptera: Mycetophilidae): DNA barcodes indicate recent diversification with a single origin. Zootaxa 4407(3): 301–320. https://doi.org/10.11646/zootaxa.4407.3.1

Matile L (1978) Diptères Mycetophilidae de l'archipel des Comores. Mémoires du Museum national d'histoire naturelle, Serie A. Zoologie 109: 247–306.

Matile L (1980) Superfamily Mycetophiloidea 15. Family Mycetophilidae. In: Crosskey RW (Ed.) Catalogue of the Diptera of the Afrotropical Region. British Museum (Natural History), London, 216–230.

Matile L (1992) Review of the Afrotropical Gnoristinae (Diptera: Mycetophilidae), with descriptions of nine new species and first record of *Synapha* Meigen. Annals of the Natal Museum 33(1): 189–202.

Myers N, Mittermeier RA, Mittermeier CG, da Fonceca GAB, Kent J (2000) Biodiversity hotspots for conservation priorities. Nature 403(6772): 853–858. https://doi.org/10.1038/35002501

Oliveira SS, Amorim DS (2014) Catalogue of the Neotropical Diptera. Mycetophilidae. Neotropical Diptera 25: 1–87. http://revistas.ffclrp.usp.br/Neotropical_Diptera

Plassmann E (1977) Revision der europäishen Arten der Pilzmückengattung *Phronia* (Diptera: Mycetophilidae). Deutsche Entomologische Zeitschrift N.F. 24(4–5): 305–344. https://doi.org/10.1002/mmnd.19770240406

Rosti H, Heiskanen J, Loehr J, Pihlström H, Bearder S, Mwangala L, Maghenda M, Pellikka P, Rikkinen J (2022) Habitat preferences, estimated abundance and behavior of tree hyrax (*Dendrohyrax* sp.) in fragmented montane forests of Taita Hills, Kenya. Scientific Reports 12(1): e6331. https://doi.org/10.1038/s41598-022-10235-7

Salmela J, Kolcsár L (2017) New and poorly known Palaearctic fungus gnats (Diptera, Sciaroidea). Biodiversity Data Journal 5: e11760. https://doi.org/10.3897/BDJ.5.e11760

Schabel HG (2006) Forest Entomology in East Africa. Forest Insects of Tanzania. Springler, Dordrecht, 328 pp.

Ševčík J (2009) Two new species and other new records of fungus gnats (Diptera: Mycetophilidae and Keroplatidae) from Slovakia and the Czech Republic. Časopis Slezského zemského muzea, Série A, Vedy prírodní (Opava) 58: 55–60.

Søli GEE (1993) New East African species of *Manota* (Diptera, Mycetophilidae). Journal of African Zoology 107: 451–465.

Søli GEE (1997) Afrotropical species of *Sciophila* Meigen (Diptera, Mycetophilidae). Journal of African Zoology 111(3): 149–190.

Søli GEE (2017) 20. Mycetophilidae (Fungus Gnats). In: Kirk-Spriggs AH, Sinclair BJ (Eds) Manual of Afrotropical Diptera (Vol. 2) (Nematocera & Lower Brachycera). SANBI Publishing, Pretoria, 533–555. https://www.nhm.ac.uk/our-science/our-work/biodiversity/manual-afrotropical-diptera.html

Søli GEE, Vockeroth JR, Matile L (2000) A. 4. Families of Sciaroidea. In: Papp L, Darvas B (Eds) Contributions to a Manual of Palaearctic Diptera. Appendix. Science Herald, Budapest, 49–92.

Winnertz J (1864) Beitrag zur einer Monographie der Pilzmücken. Verhandlungen der Zoologisch-Botanischen Gesellschaft in Wien 13: 637–964. https://doi.org/10.5962/bhl.title.9961

World Wildlife Fund (2014) Eastern Arc Forests. http://editors.eol.org/eoearth/wiki/Eastern_Arc_Forests [accessed 10 May 2022]

Zaitzev AI (2003) Fungus gnats (Diptera, Sciaroidea) of the fauna of Russia and adjacent regions. Part 2. International Journal of Dipterological Research 14: 77–386.

Volume 63 Issue 2

African Invertebrates 63(2): 105–119 (2022)
doi: 10.3897/AfrInvertebr.63.90530
https://africaninvertebrates.pensoft.net

RESEARCH ARTICLE

African Invertebrates
A journal of biodiversity research

Redescription of the poorly known genus *Ikuma* Lawrence, with synonymy and description of a new species from Namibia (Araneae, Palpimanidae)

Sergei Zonstein[1], Yuri M. Marusik[2,3]

1 *Steinhardt Museum of Natural History, Klausner 12, 69978 Tel-Aviv, Israel* **2** *Zoological Museum, Biodiversity Unit, University of Turku, FI-20014, Finland* **3** *Department of Zoology & Entomology, University of the Free State, Bloemfontein 9300, South Africa*

Corresponding author: Sergei Zonstein (znn@tauex.tau.ac.il)

Academic editor: Galina N. Azarkina | Received 19 July 2022 | Accepted 20 September 2022 | Published 4 October 2022

https://zoobank.org/9043366D-4428-449A-BC61-D7310BA183D4

Citation: Zonstein S, Marusik YuM (2022) Redescription of the poorly known genus *Ikuma* Lawrence, with synonymy and description of a new species from Namibia (Araneae, Palpimanidae). African Invertebrates 63(2): 105–119. https://doi.org/10.3897/AfrInvertebr.63.90530

Abstract

The spider genus *Ikuma* Lawrence, 1938, endemic to Namibia, is rediagnosed and redescribed based on the characters both species originally included in the genus and of the newly described *I. larseni* **sp. nov.** A new synonymy is proposed: *I. squamata* Lawrence, 1938, described from a sole female is recognized a junior synonym of the type species *I. spiculosa* (Lawrence, 1927), based on a single juvenile. The currently described *I. larseni* **sp. nov.** differs from the generotype in the eye arrangement, structure of the abdominal scuta, and details of the colouration. The copulatory organs of both males and females belonging to *Ikuma* are studied, described and depicted for the first time. The previously known genus range confined to the far north of Namibia extends to the mid-western part of this country.

Keywords

Afrotropic, Aranei, Namibia, Palpimaninae, spider, taxonomy

Introduction

The small spider genus *Ikuma* was established by Lawrence (1938) to encompass two species: *I. spiculosa* (Lawrence, 1927) (transferred from *Palpimanus* Dufour, 1820) and *I. squamata* Lawrence, 1938. The genus was not diagnosed in detail, only briefly compared in the character of the body pubescence and of the eye arrangement with *Palpimanus* and *Diaphorocellus* Simon, 1893 (sub *Iheringia* Keyserling, 1891). The type species, *I. spiculosa*, has originally been recognised as based on a juvenile. The only known specimen of *I. squamata*, when described, was claimed to be an adult female; however, no evidence of this statement has been provided.

Many decades have passed since its description, and both the genus concept and the key generic characters of *Ikuma* have continued to be unclear. Platnick (1981) briefly reviewed the Palpimaninae and considered that this subfamily could be divided into two groups, each probably of the genus rank. Both these groups could be delimited by possessing an entire or divided abdominal scutum in the females. The species with an entire abdominal sclerite in the females he has undoubtedly assigned to *Palpimanus*. The question as to whether all of the remaining species also form a monophyletic group (for which, in his opinion, the name *Ikuma* would be available), Platnick intended to consider in a subsequent study which, however, has never been conducted and published.

The reason for Platnick (1981) considering the difference between *Palpimanus* and *Ikuma* as based chiefly on the aforenoted criterion remains uncertain. Lawrence (1938), when establishing *Ikuma*, did not textually describe the abdominal sclerites in *Ikuma*, and Platnick himself had not noted any of the two known species of *Ikuma* within the studied material. Nevertheless, this assumption was then mentioned by Dippenaar-Schoeman and Jocqué (1997), who cited the mentioned review, refraining from their own comments. Until now, *Ikuma* has been thus treated as a once described and then completely forgotten taxon with dubious characters.

The present attempt to find criteria for reliably distinguishing between the genera of Palpimaninae was triggered by two interdependent events. First, among the studied palpimanids from Namibia, we have revealed a few palpimanine spiders that looked completely different to *Palpimanus* spp. On the other hand, by our request we have received a fortunate opportunity to look, albeit remotely, at the holotype of *Ikuma spiculosa*. As a result, we identified the noted specimens as certainly belonging to *Ikuma* and representing a yet-undescribed species. The type series of this new congener is diagnosed, described and illustrated herein.

Materials and methods

Used museum acronyms

DNMNH Ditsong National Museum of Natural History, Pretoria, South Africa;
KZNM KwaZulu-Natal Museum, Pietermaritzburg, South Africa;
MNB Museum für Naturkunde, Berlin, Germany;

NCA National Collection of Arachnida, ARC-Plant Protection Research Institute, Pretoria, South Africa;
NHML Natural History Museum, London, UK;
NMSA Natal Museum, the former abbreviation for KZNM, used in the labels;
RMCA Royal Museum for Central Africa, Tervuren, Belgium;
SAM Iziko South African Museum, Cape Town, South Africa;
SMNH Steinhardt Museum of Natural History, Tel Aviv, Israel.

Comparative material used in this study

Palpimanus Dufour, 1820: males and females of *P. gibbulus* Dufour, 1820 from La Palma, Mallorca (NHML), *P. schmitzi* Kulczyński, 1909 and *P. simoni* Kulczyński, 1909 from different localities in Israel (SMNH); the types of *P. namaquensis* Simon, 1910 from South Africa (MNB 13859) and *P. nubilus* Simon, 1910 from Namibia (MNB 13860).

Diaphorocellus Simon, 1893: the types of *D. isalo* Zonstein & Marusik, 2020 (RMCA ARA 200305) and *D. jocquei* Zonstein & Marusik, 2020 (RMCA ARA 201275), all from Madagascar; males and females of *D. biplagiatus* Simon, 1893 from Beaufort-West, South Africa (NCA 2008/4675) and *D. rufus* (Tullgren, 1910) from Mkomazi, Tanzania (RMCA ARA 215487).

Photographs were taken using an Olympus SZX16 stereomicroscope with a Canon EOS 7D (Turku) or Canon EOS 80D (Tel Aviv) camera and prepared using the Helicon Focus 7.6.2 Pro software (http://www.heliconsoft.com). Measurements were taken through the above-mentioned stereomicroscope to an accuracy of 0.01 mm. All measurements are given in millimetres. The maximum length of the clypeus along the midline was measured from the anterior edge to the perpendicular line connecting the anterior edge of both AME; the smaller lateral clypeus length, measured from the anterior edge of ALE and the closest point of the anterior clypeus edge, follows the maximum clypeus length, being enclosed in brackets. The length of the sternum was measured along a straight line between the posterior tip of the sternum and the hindmost part of the labium. Lengths of leg and palp segments were measured on the dorsal side, with lengths of every measured segment from the midpoint of the anterior margin to the midpoint of the posterior margin.

Illustrations of the dissected vulva, placed into a small Petri dish filled with a 85% lactic acid, were made after cleaning the object in 10% potassium hydroxide aqueous solution for several hours and exposing it for a few minutes in an alcohol solution of Chlorazol Black.

Abbreviations

AER anterior eye row;
ALE anterior lateral eye;
AME anterior median eye;
CL carapace length;
CW carapace width;

CyL clypeus length;
MOQ median ocular quadrangle;
PER posterior eye row;
PLE posterior lateral eye;
PME median lateral eye;
TL total body length in dorsal view.

Other abbreviations used are encoded in the text and in the captions.

Taxonomy

Family Palpimanidae Thorell, 1870

Note. Since Platnick (1975), the family is considered consisting of three subfamilies: the mostly Paleotropical Chediminae Simon, 1893, the purely Neotropical Otiothopinae Platnick, 1975, and the nominative subfamily Palpimaninae. The distributional peculiarities of the latter subfamily are considered below.

Subfamily Palpimaninae

Notes. This subfamily differs from the Otiothopinae by possessing accessory terminal sclerites in the male bulb (which are absent in the males belonging to the latter subfamily; see Platnick 1975). The Palpimaninae can be distinguished from the Chediminae in having eight eyes with widely spaced ALE and PLE vs. two, six or eight eyes with contiguous or lacking ALE and PLE in the chedimine spiders (Zonstein and Marusik 2017). The subfamily is distributed in the Old World, where its range is limited to the Mediterranean, Sahara-Sind region (including Middle East, Gujarat and Central Asia), and the mainland Sub-Saharan Africa. The record of *Palpimanus argentinus* Mello-Leitão, 1927 in South America, based only on the types, has not been confirmed by later field studies, and may refer either to a sole introduced species (Platnick 1975) or, even more likely, to the incorrectly interpreted collection data (Zonstein and Marusik 2017). The Palpimaninae are divided between two sharply uneven groups of the genus rank: a species-rich *Palpimanus* Dufour, 1820, with 38 named species distributed throughout the entire subfamily range (WSC 2022), and a small Namibian genus *Ikuma* Lawrence, 1938, embracing only two species.

Genus *Ikuma* Lawrence, 1938

Ikuma Lawrence, 1938: 217.

Type species. *Palpimanus spiculosus* Lawrence, 1927, by original designation.

Emended diagnosis. *Ikuma* (I.) well differs from *Palpimanus* (P.) in the shape of the carapace (anteriorly narrowed, ovoidal and gently elevated from the edges to the domed central part in I. vs. round-oval and steeply edged in P.), in the clypeus (inclined in I., vertical in P.), and in the shape of the sternum (longer and visually narrower, ending posteriorly behind coxae IV in I. *vs*. shorter, looking subrounded, and ending posteriorly at the axes of coxae IV in P.). The whitish adpressed pubescence on the dorsal and lateral surface of the carapace is much longer and denser in I. (where it is present also on the dorsal abdomen) than in P. (where a similar pubescence is much shorter and sparser, and confined only to the carapace). The embolus is small, fragile and membranous in I. vs. relatively large, branched and with partially sclerotized structures in P. The adult females of these genera can be distinguished by the structure of the endogyne, either possessing (P.) or lacking (I.) heavily sclerotized parts.

Redescription. Medium-sized to large palpimanids with carapace length ranging 4.4–5.8 in adult specimens. Dorsal body (both carapace and abdomen) densely covered with pale adpressed pubescence (Figs 1, 2); most sclerotized parts (carapace, chelicerae, sternum and abdominal scuta) finely granulated, as in Figs 1–4, 5A, B. Carapace (Figs 1C, 3A, B) narrowed anteriorly, ovoidal, with raised central part gently sloping toward edges and elevated hump between eye group and thoracic fovea. Short T-shaped thoracic fovea deeply excavated, foveal sulci poorly discernible. Clypeus moderately long. Eight eyes (Figs 1C, 3); AME largest, other eyes relatively smaller and subequal in size. AER recurved; PER nearly straight and noticeably wider than AER; both rows form wide trapezoidal figure. MOQ slightly wider than long. Chilum inconspicuous. Chelicerae about twice longer than clypeus; stridulatory ridges absent; cheliceral fang serrated; cheliceral furrow armed with several (5–6 in *Ikuma larseni* sp. nov.) peg teeth. Maxillae triangular. Labium long and narrow, notched anteriorly (Fig. 4B). Sternum densely granulated, covered with fine short hairs and extending backward between coxae IV (Figs 1D, 4A, D).

Palps short, legs I–IV moderately long. Leg formula: 4132. Leg I robust, with considerably swollen and laterally flattened femur, with patella longer that tibia, and tarsus longer than metatarsus (Figs 1B, 2B, D). Tibia and metatarsus I with wide and dense prolateral scopula. Leg tarsi II–IV relatively short; two tarsal claws narrow and provided with several short teeth. Claw tufts well-developed (as in Fig. 7A).

Abdomen fusiform, in unsclerotised part with contrasting dorsal pattern or uniformly pale coloured. Abdominal scuta conforming a rather short pedicel tube; dorsal portion of scutum narrow, small and narrowly separated from both pedicel tube and large scoop-like ventral portion. Small spinneret group set on low mound (see Fig. 7B). AMS small, cylindrical, two-segmented; PMS and PLS reduced to a few sessile spigots in females and absent in males.

Composition. *Ikuma* includes two species: *I. spiculosa* (Lawrence, 1927) and *I. larseni* sp. nov.

Distribution. The genus is currently known only from Namibia.

***Ikuma spiculosa* (Lawrence, 1927)**
Fig. 1

Palpimanus spiculosus Lawrence, 1927: 23 (j).
Ikuma spiculosa: Lawrence 1938: 217.
Ikuma squamata Lawrence, 1938: 217, fig. 3 (j), syn. nov.

Types. *Palpimanus spiculosus*: ***Holotype*:** juvenile, Namibia, Oshikoto Region, Namutoni, 18°48.5'S, 16°56.5'E, 1100 m, unspecified collector, most seemingly G.C. Shortridge (see Thomas 1926), 29.viii.1923 (SAM-ENW-B006293), seen from the full-colour and high-resolution macro-photographs kindly provided by N. Larsen.

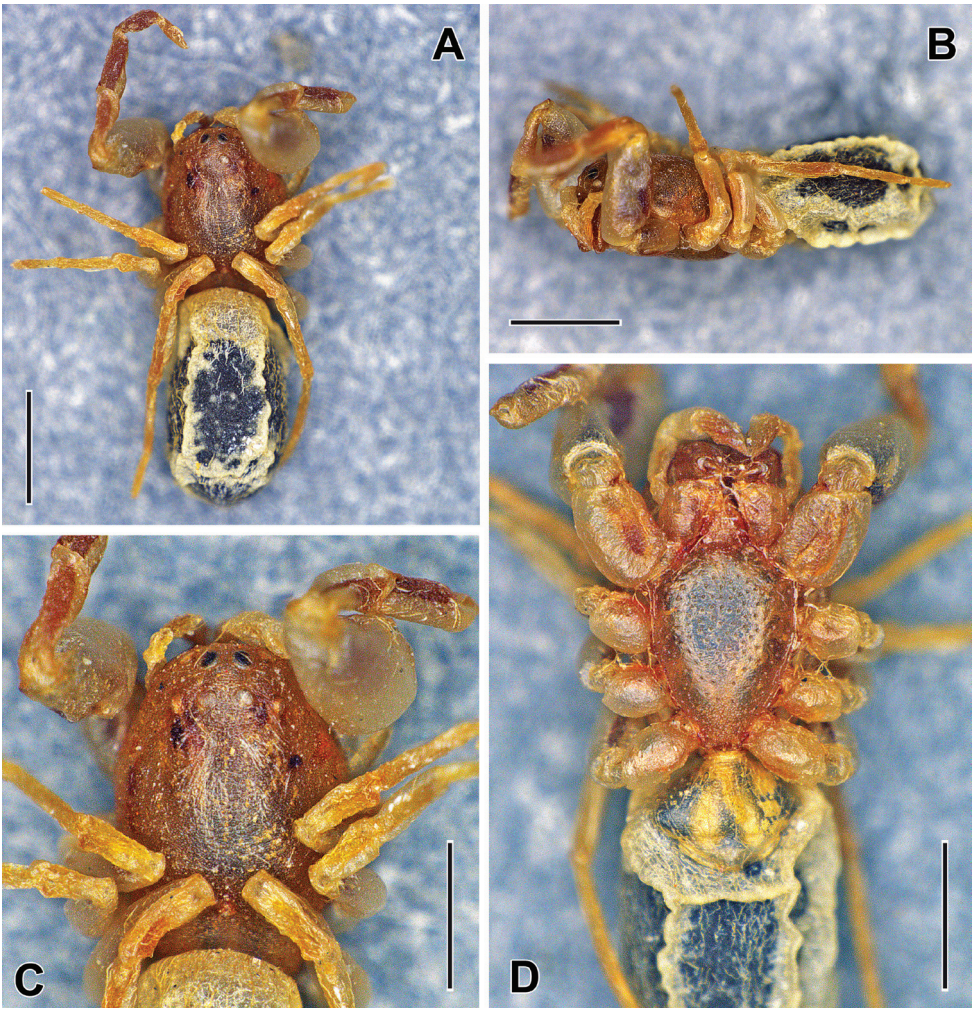

Figure 1. *Ikuma spiculosa*, immature holotype specimen SAM-ENW-B006293 **A, B** spider in dorsal and lateral view, respectively **C** carapace, dorsal **D** body, ventral. Scale bars: 1 mm.

Ikuma squamata: ***Holotype*:** juvenile (or subadult specimen), the same collection data as the preceding but Ikuma (Ekuma) River Valley, approximately 18°34'S, 16°00'E, 1100 m, further details uncertain, presumably deposited in the Transvaal Museum (currently DNMNH); however, it was not found there.

Diagnosis. There are a number of significant differences between *Ikuma spiculosa* and *I. larseni* sp. nov. It concerns the coloration of the abdomen (contrastingly bicolorous vs. uniformly pale), position of the appressed pubescence on the carapace (mostly subcentral vs. sublateral), and the relative length of interdistance AME-AME (longer than AME-ALE vs. shorter than AME-ALE).

Description (based on seemingly non-adult specimens). The species was in fairly sufficient details described by Lawrence (1927, 1938). See also Fig 1.

Distribution. Oshikoto Region in northern Namibia.

Notes. The aerial distance between the type localities of *Ikuma spiculosa* and *I. squamata*, Namutoni and Ikuma River, is less than 100 km. Both are situated at the same elevation, and they adjoin the same saline depression Etosha Pan. The holotype specimens of the two species do not differ in the peculiarities and details of their pubescence and overall colouration. Judging from the original descriptions, these types can be distinguished only by their size (TL 3.6 in *I. spiculosa* vs. 5.5 in *I. squamata*). Applied to the difference in the body size between these specimens and the type series of *I. larseni* sp. nov. (TL 10.7–12.1), it may simply indicate that these non-adult specimens can be, respectively, a younger and an elder instars belonging to the same species. Hence, *Palpimanus spiculosus* Lawrence, 1927 is considered here a senior synonym of *Ikuma squamata* Lawrence, 1938, syn. nov.

***Ikuma larseni* sp. nov.**

https://zoobank.org/1F29B626-F711-4AE9-84A1-AC15B19E42CE

Figs 2–8

Etymology. The specific name is a patronym after Norman Larsen (Cape Town, South Africa) who kindly provided us with the macro-photographs of the preceding *Ikuma* species.

Types. ***Holotype*** ♀, Namibia, Erongo Region, Namib-Naukluft National Park, Gobabeb, 23°34'S, 15°03'E, 8–9.ii.1969, B. Lamoral (NMSA-SPI-26895). ***Paratypes*:** 1♀, same collection data but 14.iv.1969, E. Holm (NMSA-SPI-26881); 1♀, same collection data but 14.iii.1970, no collector's name indicated (NMSA-SPI-11682); 1♀, same collection data but 1–29.ii.1972, B. Lamoral (NMSA-SPI-11210); 1♂, same collection data but Narras Valley 10 km W Gobabeb, 570 m (1700 feet), 2.x.1984, C. Griswold (NMSA-SPI-26894).

Diagnosis. *Ikuma larseni* sp. nov. can be distinguished from *I. spiculosa* by the colouration and pubescence (carapace with densest pubescence along margins vs. in subcentral part of the carapace); the new species has a uniformly pale abdomen vs. bicolorous in *I. spiculosa* (Fig. 2A, C cf. Fig. 1). The interdistance AME-AME is longer than AME-ALE in *I. larseni* sp. nov. and shorter in *I. spiculosa*. Since characters of

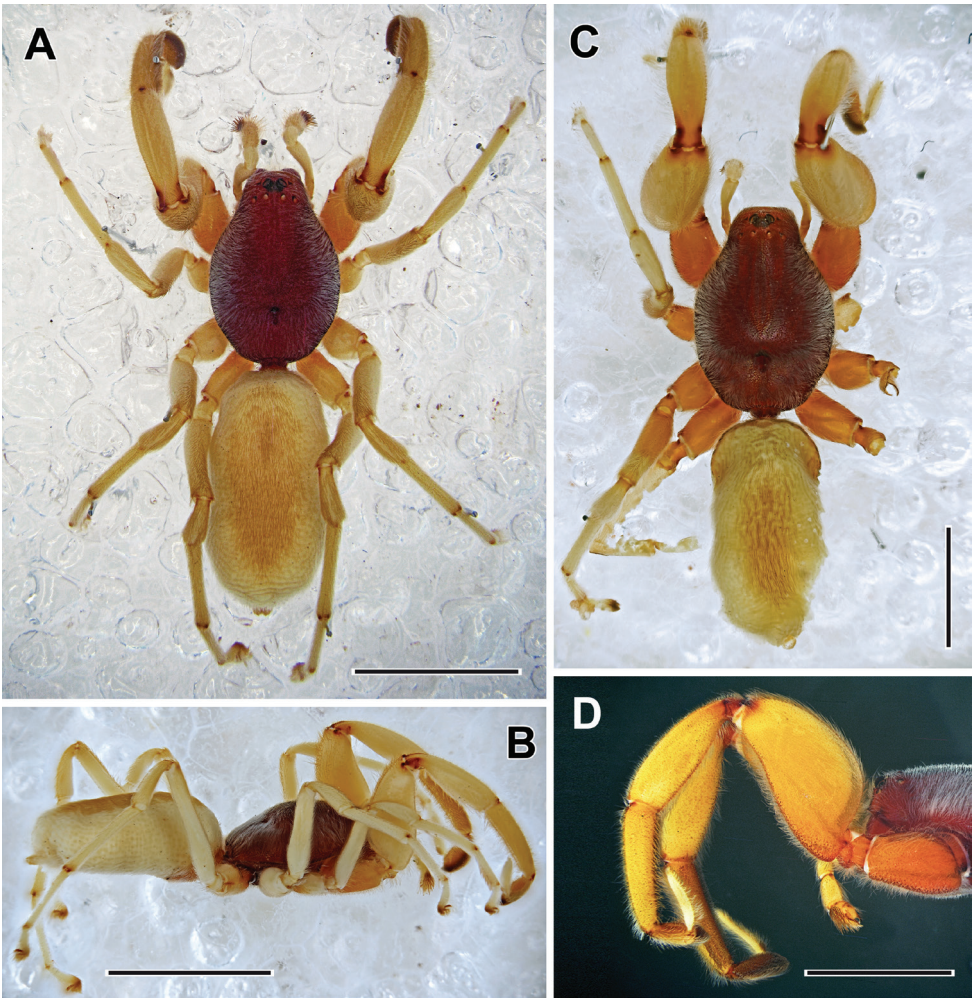

Figure 2. *Ikuma larseni* sp.n., holotype female NMSA-SPI-26895 (**A, C**) and paratype male NMSA-SPI-26894 (**B, D**) **A, B** spider in dorsal view **C, D** same, lateral. Scale bars: 5 mm.

I. spiculosa seem to be based on the juvenile or subadult specimens, the comparison of the copulatory organs remains impossible.

Description. Female. NMSA-SPI-26895 (holotype).

Habitus: as in Fig. 2A, B. *Colour in alcohol*: carapace and chelicerae dark carmine red; maxillae, coxae I–IV and abdominal scuta light to intensely orange; palp and legs I–IV from femora to tarsi pale yellowish orange (leg I slightly darker than legs II–IV, with more noticeable difference between corresponding tibiae and metatarsi); sternum, labium and pedicel tube medium carmine red; abdomen very pale yellowish orange, dorsally with large slightly darker oval median marking; spinnerets yellowish white. Carapace and abdomen laterally covered with dense flattened and adpressed whitish pubescence. ***Measurements***: TL 11.15. CL 4.81, CW 3.22, CyL 0.56 (0.43), Femur I L/W 2.29 (3.41/1.49). ***Carapace***: with moderately coarse granulations (Fig. 3A). ***Eyes***

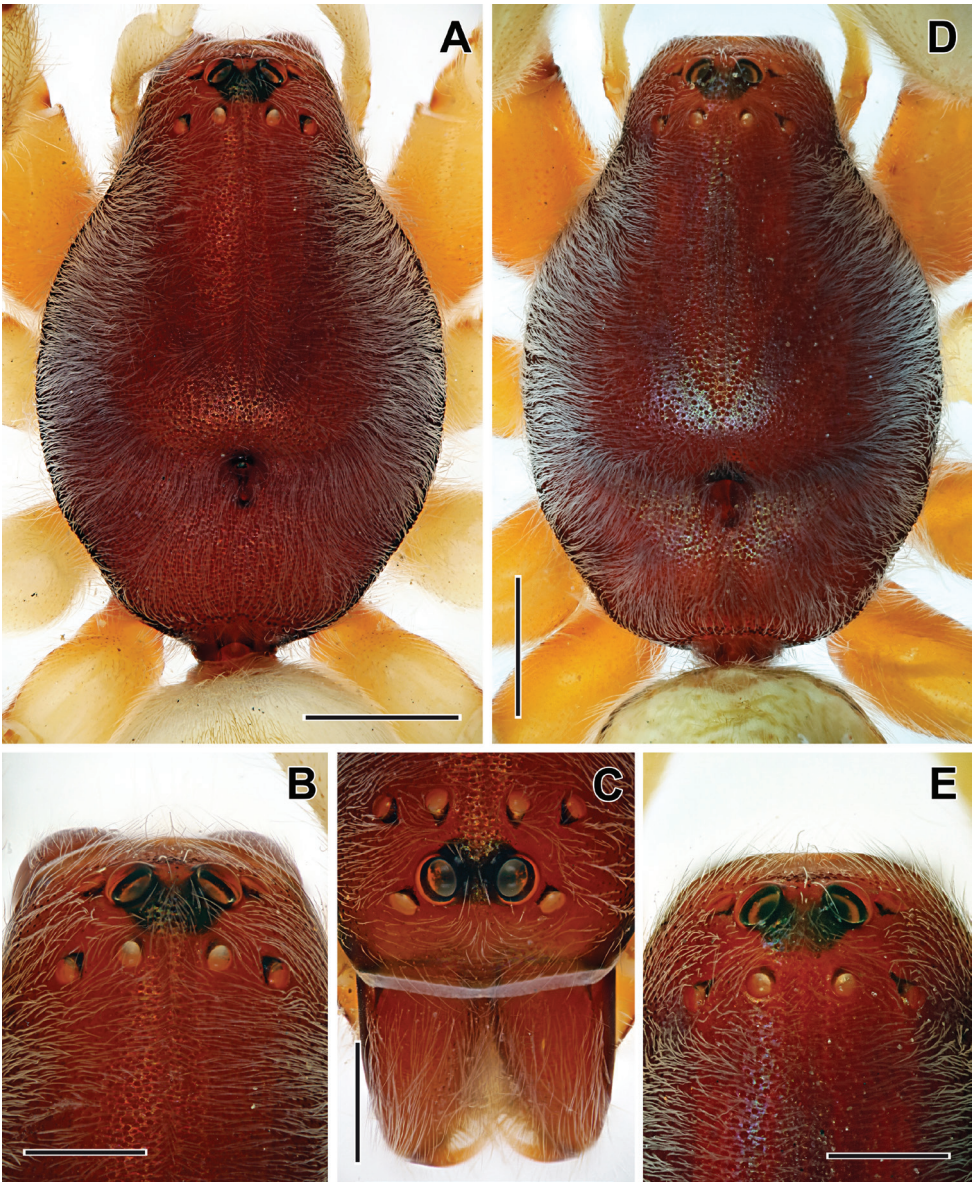

Figure 3. *Ikuma larseni* sp.n., holotype female NMSA-SPI-26895 (**A, C, D**) and paratype male NMSA-SPI-26894 (**B, E**) **A, B** carapace in dorsal view **C, E** eye group, clypeus and chelicerae, dorsal **D** same, lateral. Scale bars: 1 mm (**A, D**); 0.5 mm (**B, C, E**).

(Fig. 3B, C): AME 0.27, ALE 0.16, PME 0.13, PLE 0.13; AME-AME 0.16, AME-ALE 0.11, AME– PME 0.20, ALE-PLE 0.41, PLE-PME 0.18, PME-PME 0.31. ***Mouthparts***: labium with slightly notched anterior edge (Ln; Fig. 4B). ***Legs*** I–IV: tarsi with paired claw tufts of dense long setae and multipectinate paired claws each armed with 8–10 teeth (Fig. 7A). ***Abdominal sclerites***: short pedicel tube (Pt) widely funnel-shaped (Figs 4C, 5A, B); small hexagonal dorsal shield (Ds) clearly separated from

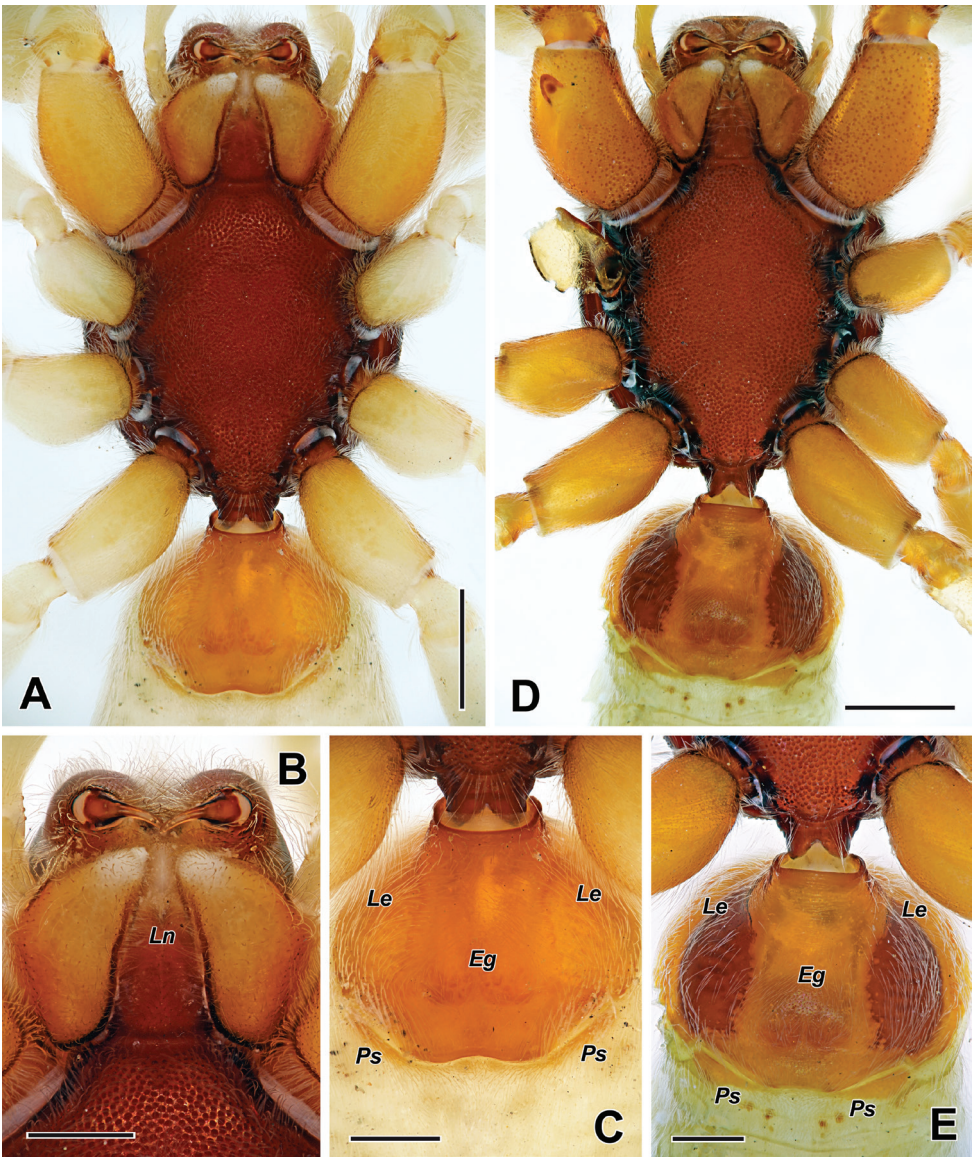

Figure 4. *Ikuma larseni* sp.n., holotype female NMSA-SPI-26895 (**A, C, D**) and paratype male NMSA-SPI-26894 (**B, E**) **A, B** cephalothorax and basal abdomen in ventral view **C** chelicerae, labium and maxillae, ventral **D, E** pedicel and abdominal scuta, ventral. Abbreviations: *Eg* epigastral plate; *Le* lateral extensions of scutum; *Ln* labial notch; *Ps* postgastral scuta. Scale bars: 1 mm (**A, D**); 0.5 mm (**B, C, E**).

and not fused with lateral sclerotized extensions (Le; Fig. 5A); epigastral plate (Eg) in intact specimen (before dissection) uniformly coloured, posterior part slightly concave; postgaster with one thin bow-shaped scutum (Fig. 4C); posterior edge nearly straight. *Spinnerets* as shown in Fig. 7B.

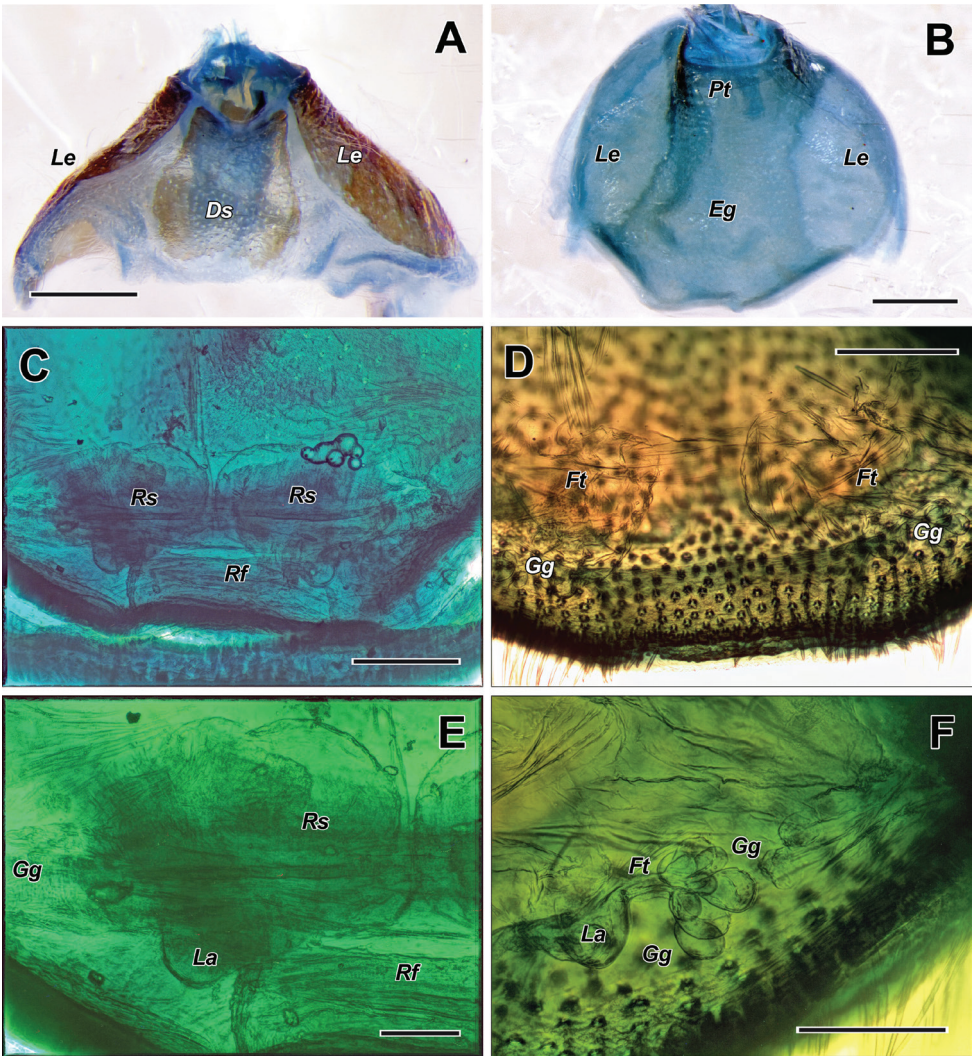

Figure 5. *Ikuma larseni* sp.n., paratype female NMSA-SPI-26881 **A, B** dissected, macerated and Chlorazol-tinted abdominal scuta in dorsal and ventral view, respectively **C–F** structures of endogyne, dorsal (inside). Abbreviations: *Ds* dorsal scutum; *Eg* epigastral plate; *Ft* fine threads; *Gg* grape shaped glands; *La* lateral apophyse of endogynal fold; *Le* lateral extensions of scutum; *Pt* petiolar tube; *Rf* basolateral fold of endogyne; *Rs* membranous sac like part of receptacle. Scale bars: 0.5 mm (**A, B**); 0.25 mm (**C, D**); 0.1 mm (**E, F**).

***Copulatory organs*:** as in Figs 5C–F, 6. Endogyne weakly sclerotized (unlike partially heavy-sclerotized one in *Palpimanus* spp.); main supporting structure, wide trapezoidal endogynal fold (Rf), carries two lateral apophyses (La); membranous sacs of receptacles (Rs) bell-shaped, about as long as wide, each receptacle accompanied by brushes of fine threads (Ft) and approximately 7–8 grape-shaped glands (Gg), glands with stalks about as long as head, pore glands indiscernible (seems absent).

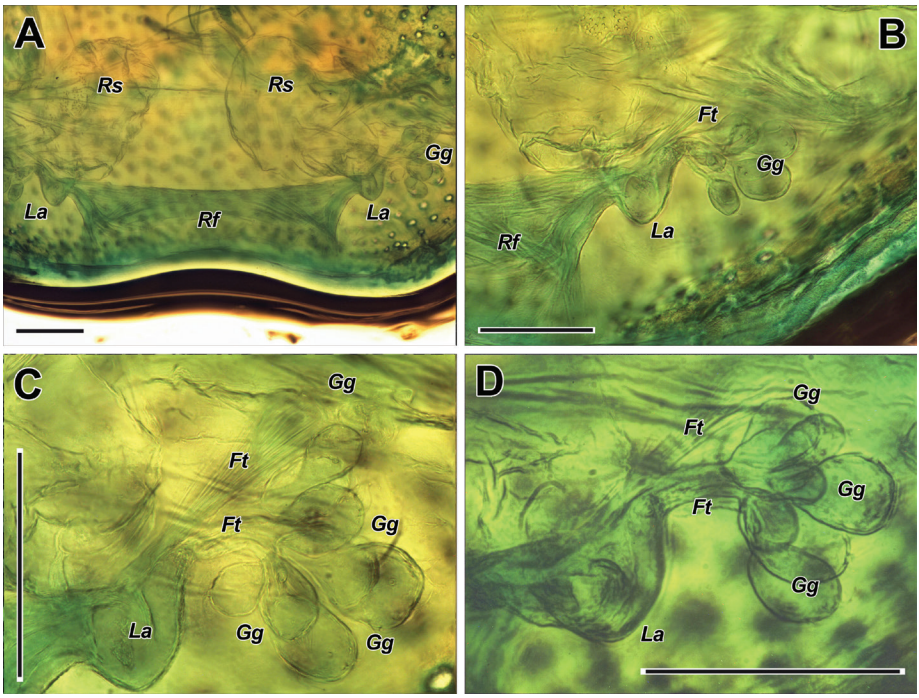

Figure 6. *Ikuma larseni* sp.n., paratype female NMSA-SPI-26881 **A–D** structures of endogyne, close up dorsal (inside) view. Abbreviations: *Eg* epigastral plate; *Ft* fine threads; *Gg* grape shaped glands; *La* lateral apophyse of endogynal fold; *Rf* basolateral fold of endogyne; *Rs* membranous sac like part of receptacle. Scale bars: 0.1 mm.

Figure 7. *Ikuma larseni* sp.n., holotype female NMSA-SPI-26895 (**A, B**) and paratype male NMSA-SPI-26894 (**C, D**) **A** tarsus IV in retrolateral view **B** spinnerets, ventral **C** entire leg II, retrolateral **D** palpal segments from patella to cymbium, retrolateral. Scale bars: 0.5 mm (**A, D**); 0.25 mm (**B**); 1 mm (**C**).

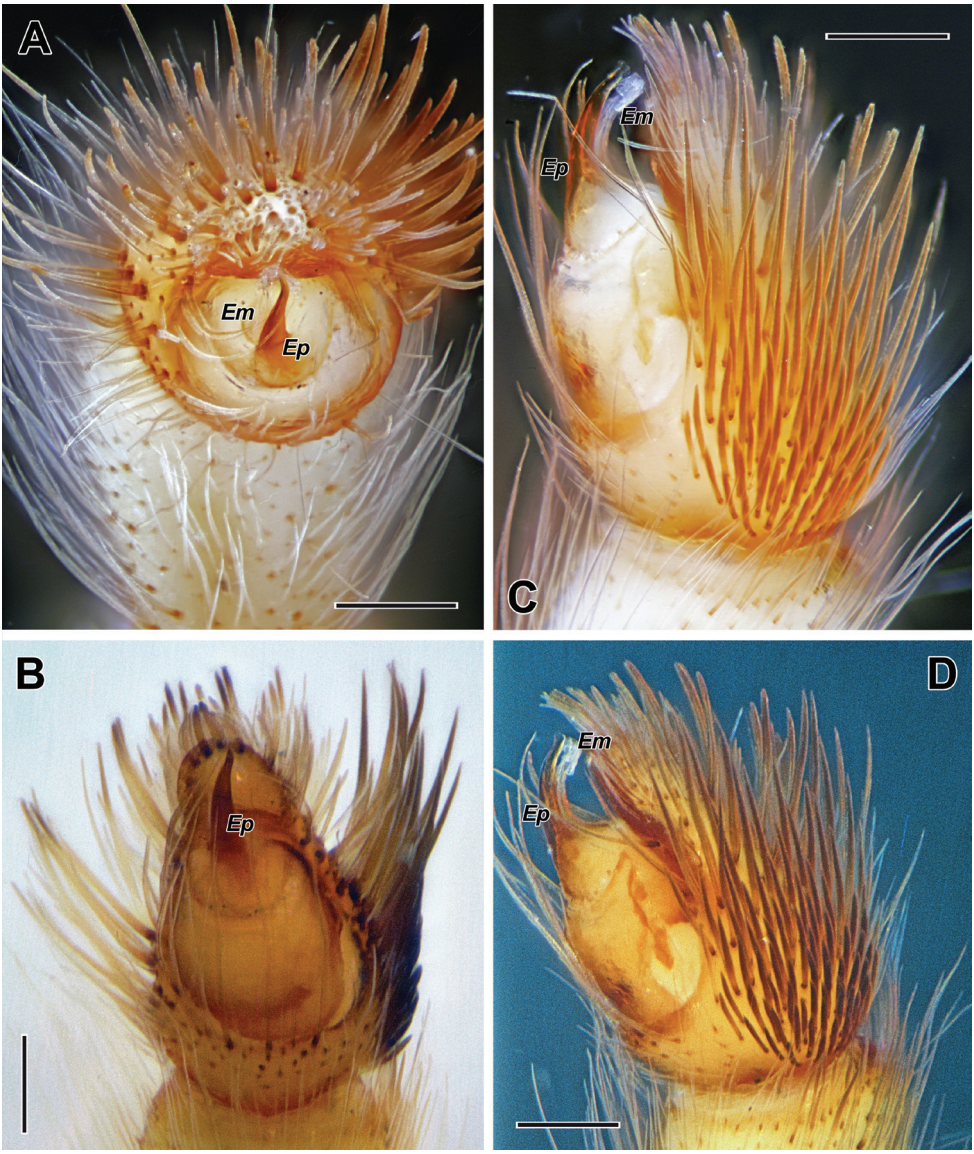

Figure 8. *Ikuma larseni* sp.n., paratype male NMSA-SPI-26894, cymbium and palpal bulb **A** in frontal view **B** same, ventrofrontal **C**, **D** same, retrolateral. Abbreviations: *Em* embolus; *Ep* embolic process. Scale bars: 0.25 mm.

***Leg measurements*:** female NMSA-SPI-26895 (male NMSA-SPI-26894 in brackets):

	Femur	Patella	Tibia	Metatarsus	Tarsus	Total
Palp	1.09 (1.18)	0.45 (0.51)	0.85 (0.77)	–	0.65 (0.78)	3.04 (3.24)
Leg I	3.41 (4.23)	3.03 (3.62)	2.72 (3.16)	1.41 (1.57)	1.55 (1.74)	12.12 (14.32)
Leg II	2.68 (3.37)	1.61 (2.01)	1.93 (2.35)	1.29 (1.50)	0.88 (0.97)	8.39 (10.20)
Leg III	2.98 (3.42)	1.59 (1.93)	2.06 (2.42)	1.75 (1.81)	0.95 (1.46)	9.33 (11.04)
Leg IV	4.28 (4.48)	1.99 (2.28)	3.11 (3.32)	2.39 (2.87)	1.10 (1.52)	12.87 (14.47)

Male. NMSA-SPI-26894 (paratype).

Habitus*:** as in Fig. 2C, D. ***Colour in alcohol*:** as in female, but coxae I–IV evenly orange and tarsus I pale yellow, much lighter than metatarsus I. ***Measurements*:** TL 12.37. CL 5.78, CW 3.95, CyL 0.29, Femur I L/W 1.91 (4.23/2.21). ***Carapace*:** longer, with slightly coarser granulations than in female (Fig. 3D). ***Eyes (Fig. 3E): AME 0.28, ALE 0.18, PME 0.15, PLE 0.14; AME-AME 0.22, AME-ALE 0.12, AME-PME 0.34, ALE-PLE 0.46, PLE-PME 0.22, PME-PME 0.35. ***Mouthparts*:** as in female (see Fig. 4B). ***Legs*** I–IV: metatarsi and tarsi armed with long ventral bristles as in female (Fig. 7C); claw tufts and dentition as in female. ***Abdominal sclerites*:** epigastral scutum with clearly darkened book-lungs; postgaster with two large long subtriangular scuta (distinguishable in form from the corresponding scuta in other palpimanids), and two pairs of dot-like scuta (see Fig. 4E).

***Copulatory organs*:** Palp as shown in Figs 7D, 8. Femur nearly 3 times longer than wide, 1.5 times longer than cymbium and tibia, 2.3 times longer than patella; patella elongate, 1.5 times longer than wide; tibia elongate, not swollen, length/maximal width ratio ca. 1.6, subequal in length to cymbium, covered with dense and long whitish setae; cymbium about twice longer than wide; bulb droplet-shaped; tegulum as wide as long, lacking any processes (apophyses), retrolateral part of tegulum membranous; embolic division with 2 outgrowths: slightly bent spine-like chitinized embolic process (Ep), sigmoid in anterior view (see Fig. 8A), and membranous embolus (Em).

Variation. In paratype females, the length of the carapace varies from 4.4 to 5.6 mm.

Habitat. According to the collecting data, the specimens were obtained by sand sifting.

Distribution. Known only from the type locality.

Note. Since the only available male of *Ikuma larseni* sp. nov. was found partially damaged (probably when collected), we preferred to designate one of the better preserved females as the holotype.

Acknowledgements

We thank Norman Larsen (SAM), Kirstin Williams and Matabaro Ziganira (KZNM), Ansie Dippenaar-Schoeman and Petro Marais (NCA), Janet Beccaloni (NHML), Arnaud Henrard and Rudy Jocqué (RMCA), and Jason Dunlop (MNB), for providing us with macro-photographs of the holotype of *Ikuma spiculosa* and loaning us the material used for this study. We also thank Charles Haddad and an anonymous reviewer for their valuable comments and recommendations. Special thanks go to Ilari Sääksjärvi and Seppo Koponen (Zoological Museum, University of Turku) for providing us with museum facilities. This study was supported in part by the Ministry of Absorption, Israel.

References

Dippenaar-Schoeman AS, Jocqué R (1997) African Spiders: An Identification Manual. Plant Protection Research Institute Handbook 9, 392 pp.

Lawrence RF (1927) Contributions to a knowledge of the fauna of South-West Africa V. Arachnida. Annals of the South African Museum 25(1): 1–75.

Lawrence RF (1938) Transvaal Museum Expedition to South-West Africa and Little Namaqualand, May to August 1937. Spiders. Annals of the Transvaal Museum 19: 215–226.

Platnick NI (1975) A revision of the palpimanid spiders of the new subfamily Otiothopinae (Araneae, Palpimanidae). American Museum Novitates 2562: 1–32.

Platnick NI (1981) A review of the spider subfamily Palpimaninae (Araneae, Palpimanidae). Bulletin - British Arachnological Society 5(4): 169–173.

Thomas O (1926) On Mammals from Ovamboland and the Cunene River, obtained during Capt. Shortridge's third Percy Sladen and Kaffrarian Museum Expedition into South-West Africa. Proceedings of the Zoological Society of London 1926(1): 285–312. https://doi.org/10.1111/j.1096-3642.1926.tb01549.x

World Spider Catalog (2022) World Spider Catalog. Natural History Museum Bern, version 23.5. http://wsc.nmbe.ch [accessed on 4.vii.2022]

Zonstein SL, Marusik YM (2017) Descriptions of the two-eyed African spider genera *Chedimanops* gen. n. and *Hybosidella* gen. n. (Araneae, Palpimanidae, Chediminae). African Invertebrates 58(1): 23–47. https://doi.org/10.3897/AfrInvertebr.58.11448

African Invertebrates 63(2): 121–130 (2022)
doi: 10.3897/AfrInvertebr.63.94095
https://africaninvertebrates.pensoft.net

SHORT COMMUNICATION

African Invertebrates
A journal of biodiversity research

First occurrence of the rare siphonophore *Lilyopsis* Chun, 1885 (Hydrozoa, Siphonophora, Prayinae) in South Africa

Gillian M. Mapstone[1], Craig N. Foster[2], Mark J. Gibbons[3]

1 *Department of Life Sciences, The Natural History Museum, London, UK* **2** *Seachange Science Lab, 41 Freesia Rd., Murdock Valley South, Simonstown, South Africa* **3** *Department of Biodiversity and Conservation Biology, University of the Western Cape, Private Bag X17, Belleville 7535, South Africa*

Corresponding author: Mark J. Gibbons (mgibbons@uwc.ac.za)

Academic editor: S. Stainbank | Received 26 August 2022 | Accepted 21 September 2022 | Published 25 October 2022

https://zoobank.org/86C22FAA-9951-48F4-8B4A-5E919BA82197

Citation: Mapstone GM, Foster CN, Gibbons MJ (2022) First occurrence of the rare siphonophore *Lilyopsis* Chun, 1885 (Hydrozoa, Siphonophora, Prayinae) in South Africa. African Invertebrates 63(2): 121–130. https://doi.org/10.3897/AfrInvertebr.63.94095

Abstract

A colony of the rare hydrozoan siphonophore *Lilyopsis* Chun, 1885, was observed for the first time in shallow water in False Bay, South Africa, swimming amongst kelp. A study of a high-quality image of this individual found it to share some characters with the prayine prayid *L. fluoracantha* Haddock, Dunn & Pugh, 2005, so far known only from Monterey Bay, California, in the eastern Pacific. No *Lilyopsis* species has previously been reliably identified from either the South Atlantic or the Indian Ocean, so this record represents an expansion of the known worldwide distribution for this genus.

Keywords

Agulhas Current, Benguela ecosystem, Calycophorae, community science, diversity, photo identification, Prayid

Introduction

Siphonophores can be abundant members of coastal and oceanic zooplankton (e.g. Gili et al. 1991), where they play a role as predators (Purcell 1981; Choy et al. 2017; Hetherington et al. 2022) and prey (Bieri 1966; Bjorndal 1997; Nakamura et al. 2015; Eduardo et al. 2020; Hetherington et al. 2022). Although their populations

may fluctuate in size (Blackett et al. 2014, 2015, 2016), they are widely regarded as indicators of water mass movement (Russell 1935). However, their value in the latter context relies on up-to-date information regarding distribution, as this allows us to track potential range expansions in response to, for example, changing ocean circulation. Traditionally, the reporting of new species in areas outside known distributional ranges has been the purview of professional scientists, but this is rapidly changing as we harness the interest, enthusiasm and effort of community scientists (e.g. Gibbons et al. 2021). Here, we report on a genus of siphonophore not previously recorded from the South Atlantic from an image taken by one such community scientist.

Materials and methods

A specimen of a siphonophore was photographed by CF taken on 10 May 2018, at a depth of 1.5 m from within a kelp bed along the western shore of False Bay (34°12.484'S, 018°27.662'E, Fig. 1), and a high-resolution copy of the photograph (Fig. 2) used to identify the specimen. The photo was taken using natural light. The length of the colony was estimated at 7 cm based on the distance of the specimen from the camera.

Glossary of terminology used in this paper:

Basigaster – proximal thickened region of gastrozooid where nematocysts are produced.
Bract – protective asexual zooid of cormidium, typically rounded in prayids with lobed distal margin but in *Lilyopsis* extending into a spur on one side.
Calyconula larva – later larval stage of a calycophoran siphonophore.
Cormidium – serially repeated (iterative) group of zooids on the main stem, or siphosome, each including a gastrozooid, one or more gonophores and typically a bract.
Cormidial bell – a special nectophore in the cormidia of *Lilyopsis*, some other prayines and some other siphonophores.
Gastrozooid – asexual feeding zooid in a cormidium, with tentacle arising from proximal end.
Nectophore – asexual swimming bell present in most siphonophores, having a muscular nectosac for locomotion opening distally via an aperture termed the ostium.
Siphosome – posterior part of the stem, bearing cormidia in all siphonophores.
Tentilla – specialized side branches on a siphonophore tentacle comprising a complex nematocyst battery.

Results and discussion

The specimen illustrated in Fig. 2, can be identified as the fragile prayine siphonophore genus *Lilyopsis* Chun, 1855, for its distinctive closely spaced cormidia on the siphosome, each with a cormidial bell, and a pair of extremely transparent nectophores, swimming away from the camera on the right. *Lilyopsis* nectophores have very large nectosacs relative to those of other prayines. Each nectosac opens via an enlarged ostium oriented

at a 45° angle relative to the long axis of the nectophore and one such ostium is just visible in Fig. 2B. The bracts in the siphosomal cormidia of *Lilyopsis* are spurred, also clearly visible in Fig. 2B (see Fig. 3).

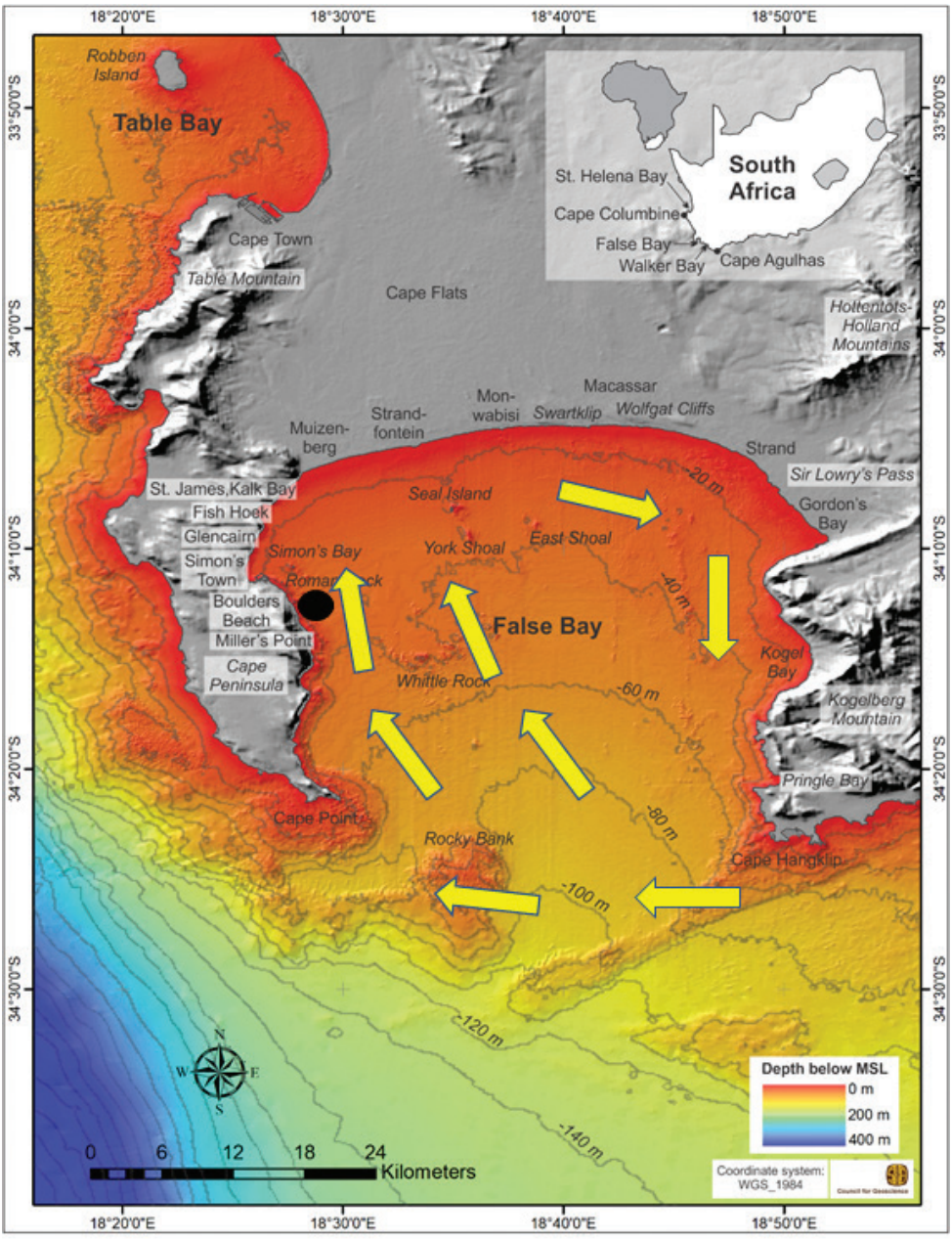

Figure 1. Bathymetric chart of False Bay (From Pfaff et al. 2019, https://doi.org/10.1525/elementa.367.f1). Location where the image was taken indicated by black circle; approximate direction of prevailing surface circulation during SE winds shown by yellow arrows.

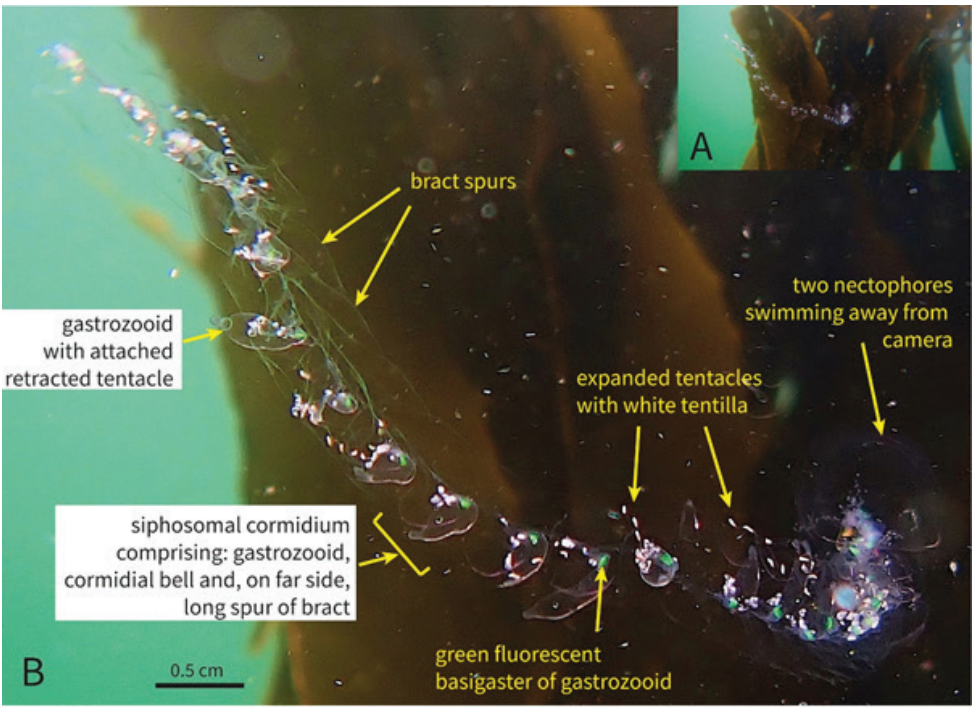

Figure 2. A photograph of a specimen of *Lilyopsis* taken against a background of the kelp *Ecklonia maxima* at a depth of 1.5 m in False Bay on 10 May 2018 **A** original image **B** enlarged *Lilyopsis* colony with explanatory labels. The length of the colony was estimated to be 7 cm.

There are two species currently identified as belonging to the genus *Lilyopsis: L. medusa* (Metschnikoff & Metschnikoff, 1871) and *L. fluoracantha*, Haddock, Dunn and Pugh 2005. *Lilyopsis medusa* was first introduced as *Praya diphyes* by Graeffe (1860), but because this name was already preoccupied by another prayine prayid, precedence for the species name *medusa* went to the specimen described by Metschnikoff and Metschnikoff (1871) from Villefranche as *Praya medusa*. Later, Chun (1885) introduced a new genus *Lilyopsis* for three prayine species with the generic characters noted above. These included Chun's own species *L. rosea* from Naples which he considered different from the *L. medusa* of Metschnikoff and Metschnikoff (1871) and from the *Praya diphyes* of both Kölliker (1853) and Vogt (1854). *Lilyopsis rosea* has been considered a junior synonym of *L. medusa* for some time, although usage of the specific name did not change until the error was pointed out by Pugh (2009). *Praya diphyes* of Kolliker and Vogt is now referred to as *Desmophyes annectens* (Totton 1965).

Lilyopsis medusa was last studied in detail by Carré as *L. rosea*, based on specimens collected at Villefranche in the Mediterranean, including drawings and photographic images of the siphosome and of male and female cormidia (Carré 1969, figs 1, 2, pl. 1 fig. 5, pl. II fig. 5). More recently, the same species was imaged in the Southern California Bight by Luo et al. (2014, fig. 3ad), with a second image from the same site

included in Mapstone (2015, fig. 14E). In all these figures, and earlier ones reproduced by Totton (1965, figs 72A–C) and Bedot (1896, fig. 1), the bracts of the cormidia can be seen to have a spur extending from one side in a posterior direction, but this spur is not particularly elongate. In contrast, the bracteal spurs of *L. fluoracantha* are conspicuously longer as clearly shown by Haddock et al. (2005, fig. 5A–C) and noted in their species diagnosis.

The siphosome of the present colony from False Bay (Fig. 2) became twisted during swimming, and the most mature cormidia on the stem are on the left in Fig. 2B. In these cormidia each bract has a long posteriorly directed spur and further long spurs are also visible from bracts in cormidia on the right, closer to the nectosome. These bracteal spurs are longer than those shown for *Lilyopsis medusa* and are most similar to those illustrated and described for *L. fluoracantha* (Haddock et al. 2005), as shown in Fig. 3. Other similarities include the whitish tentilla on the tentacles of the gastrozooids in both the False Bay specimen and *L. fluoracantha*, which, although said to be yellowish in life in *L. fluoracantha*, appear whitish in the published figures (Haddock et al. 2005, fig. 6A, C, E). The gastrozooids of *L. fluoracantha* also appear similar to those of the present colony, except that they are relatively smaller in the published figure of *L. fluoracantha* and also have white basigasters (Haddock et al. 2005, fig. 6E).

Some characters of the present colony from South Africa fit well with those of both *Lilyopsis medusa* and *L. fluoracantha* (large transparent nectophores and closely spaced siphosomal cormidia, each with a cormidial bell), although nectophore details could not be directly compared since in the False Bay image only one of the two nectophores was visible, and in posterior view (Fig. 2B). Our colony measured c. 7 cm in length, which falls within the range of 5–10 cm for *L. medusa* (Carré 1969) and 3.6–12 cm for *L. fluoracantha* (Haddock et al. 2005, fig. 6A and p. 702). At least 18 cormidia can be identified in our colony (Fig. 2B). In *L. medusa*, 10 to 20 cormidia have been identified by Carré (1969) and up to 25 by Luo et al. (2014), and in *L. fluoracantha* up to 35 cormidia have been observed (Haddock et al. 2005). The main difference between our colony and those of *L. medusa* and *L. fluoracantha* is the bright green basigasters on the gastrozooids (Fig. 2B). In *L. fluoracantha* the gastrozooids were clear or whitish and cylindrical (Haddock et al. 2005) with a whitish basigaster, as noted above, and it is assumed here that those of *L. medusa* are similar, since no previous authors have commented on any pigment in this zooid (for example Carré 1969; Chun 1885). Cormidial bells are clearly present in each cormidium of our specimen, but further detail is not discernible (Fig. 2B). In *L. medusa* a small red disc is present on the two most anterior of the four cormidial radial canals and fine red spots are distributed all around the ostium, but in *L. fluoracantha* no red pigment was identified in the cormidial bells (Haddock et al. 2005).

Lilyopsis fluoracantha was described from just five specimens collected, or captured on video, between 1998 and 2004 near Monterey Bay, California, at depths between 327 and 476 m (Haddock et al. 2005), although 13 more have been identified in the same region (pers. comm. Kyra Schlining). There are more records for *L. medusa* which is considered a warmer water species worldwide, but rare. Most

Lilyopsis medusa bract, from below	*Lilyopsis fluoracantha* bract, from below
Quite flattened cushion, concave below with rounded right border and left border with short spur	Fluorescent green in life. Lower surface concave & draped over the stem, partly enclosing cormidial elements. Conspicuous elongate spur on left side, directed posteriorly.

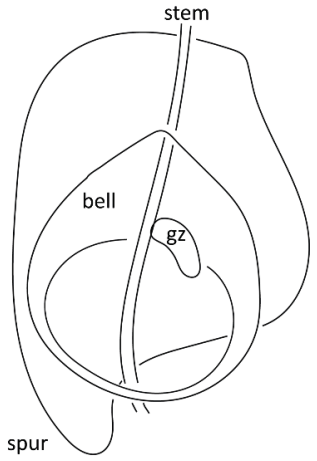

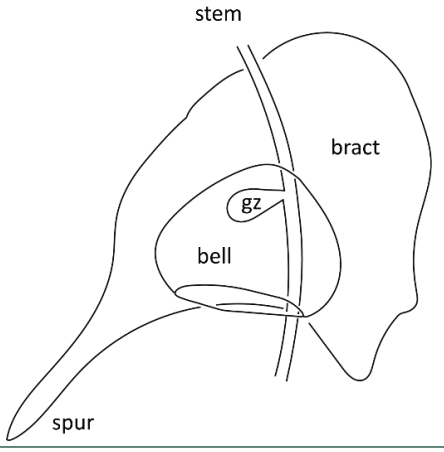

Figure 3. Bracts of the two known *Lilyopsis* species from below. *L. medusa* modified from Carré 1969 Fig. 1; *L.fluoracantha* modified from Haddock et al. (2005 Fig. 5A; bell – of cormidium; gz – gastrozooid).

specimens have been collected at Villefranche-sur-Mer in the Ligurian Sea of the Mediterranean where upwelling has been known since antiquity (Madin 1991). From this location, or nearby off Nice, *L. medusa* has been described by Graeffe (1860), Metschnikoff and Metschnikoff (1871), Fewkes (1883), Moser (1917), Carré (1969) and Carré and Carré (1969). However, it has also been reliably reported twice in the Tyrrhenian Sea off Naples (Chun 1885; Schneider 1898), in the North Atlantic once from the Canaries by Chun (1888), in the Caribbean (Minemizu et al. 2015) and elsewhere by Haddock et al. (2005). In the Pacific, *L. medusa* has been recorded from the Southern Californian Bight (Luo et al. 2014, at 84 m), from the central tropical Pacific in the Bay of Ambon (Moluccas Indonesia, Bedot 1896), in Sagami Bay (Lindsay and Miyake 2009) and in Suguru Bay (Minemizu et al. 2015) in the western Pacific, and also off Australia (Haddock et al. 2005). This species has been additionally collected as a calyconula larva by SCUBA divers in Monterey Bay, California (Pugh 2009). Other records for the genus exist but the specific identity is unknown (e.g. Hoving et al. 2020).

So far *Lilyopsis fluoracantha* has only been observed or collected in deep water from Monterey Bay where the water temperature varied between ~6.5 and 8.5 °C (pers. comm. from Kyra Schlining at MBARI, July 2020). In contrast, reliable records for *L. medusa* show that it typically inhabits shallower and warmer water worldwide, between, for example, 14 and 24 °C in Villefranche Bay (Villefranche Sea Temperature 2021), 13 and 28 °C in the Bay of Naples (Bay of Naples Sea Temperature 2021) and 27 and 29 °C in the Bay of Ambon, in the Moluccas (Bay of Ambon Sea Temperature 2021), although one record is from 84 m in the Southern California Bight, where the water temperature was only 8 to 11 °C (Luo et al. 2014). Our *Lilyopsis* specimen was imaged in False Bay during the austral autumn where the water temperature was c. 15 °C. False Bay is one of the largest true embayments in South Africa (Fig. 1), and although circulation is approximately clockwise, it is influenced by prevailing winds. Because the bay sits at the NW edge of the Agulhas Bank, it is also subject to the vagaries of the Agulhas Current (Gründlingh and Largier 1991, de Vos et al. 2021). SE winds predominate in summer, which lead to upwelling at Cape Hangklip in the SE corner of the bay, offshore water transport and the development of a strong northward temperature gradient (Pfaff et al. 2019). During winter, NW winds serve to mix waters in the bay, and they promote onshore water movement (Pfaff et al. 2019). While we can speculate as to its origin, it is clear that *Lilyopsis* is not resident in False Bay because it has only been observed once during the many years that one of us (CF) has been snorkeling daily at the site in False Bay. Neither has it been observed by another frequent community scientist, Peter Southward (see Gibbons et al. 2021).

Conclusions

In general, our specimen shares more characters with *L. fluoracantha* than it does with *L. medusa*, but the bright green basigasters of the gastrozooids do seem to be unique, although may not be a robust character for species separation. Perhaps, therefore, it represents a third *Lilyopsis* species, or maybe a variant of *L. fluoracantha*, since in both species the bracts have elongate spurs. It will be necessary to collect a specimen in the future for genetic analysis if this is ever possible, which could confirm its identity as *L. fluoracantha*. Meanwhile, we assign our specimen to the genus *Lilyopsis* Chun, 1885, in the subfamily Prayinae Chun, 1897, of the calycophoran family Prayidae Kolliker, 1853.

Acknowledgements

We thank Kyra Schlining of Monterey Bay Aquarium Research Institute for information about observations and samples of *Lilyopsis fluoracantha* from the Monterey Bay area. GMM thanks The Natural History Museum, London for access to literature and other facilities as an NHM Scientific Associate. We are grateful to Bert Hoeksema and Dhugal Lindsay for their comments on the manuscript, which have helped to clarify the text.

References

Bay of Ambon Sea Temperature (2021) Ambon Water Temperature. https://www.seatemperature.org/asia/indonesia/ambon.htm [Accessed 27/05/2021]

Bay of Naples Sea Temperature (2021) Naples Sea Temperature. https://www.seatemperature.org/europe/italy/naples.htm [Accessed 27/05/2021]

Bedot M (1896) Les siphonophores de la Baie d'Amboine. Etude suivie d'une revision de la famille des Agalmidae. Revue Suisse de Zoologie 13(3): 367–414. https://doi.org/10.5962/p.318236

Bieri R (1966) Feeding preferences and rates of the snail, *Ianthina prolongata*, the barnacle, *Lepas anserifera*, the nudibranchs, *Glaucus atlanticus* and *Fiona pinnata*, and the food web in the marine neuston. Publications of the Seto Marine Biological Laboratory 14(2): 161–170. https://doi.org/10.5134/175429

Bjorndal KA (1997) Foraging ecology and nutrition of sea turtles. In: Lutz PL, Musick JA (Eds) The biology of sea turtles. CRC Press, Boca Raton, USA, 199–231.

Blackett M, Licandro P, Coombs SH, Lucas CH (2014) Long-term variability of the siphonophores *Muggiaea atlantica* and *M. kochi* in the Western English Channel. Progress in Oceanography 128: 1–14. https://doi.org/10.1016/j.pocean.2014.07.004

Blackett M, Lucas CH, Harmer RA, Licandro P (2015) Population ecology of *Muggiaea atlantica* (Cnidaria, Siphonophora) in the Western English Channel. Marine Ecology Progress Series 535: 129–144. https://doi.org/10.3354/meps11423

Blackett M, Lucas CH, Cook K, Licandro P (2016) Occurrence of the siphonophore *Muggiaea atlantica* in Scottish coastal waters: Source or sink? Journal of Plankton Research 39(1): 122–137. https://doi.org/10.1093/plankt/fbw082

Carré C (1969) Sur le genre *Lilyopsis* Chun 1885, avec une redescription de l`èspece *Lilyopsis rosea* Chun 1885 (Siphonophore, Prayinae) et une description du sa phase calyconula. Cahiers de Biologie Marine 10: 71–81.

Carré C, Carré D (1969) Le développment larvaire de *Lilyopsis rosea* (Chun, 1885) siphonophore, calycophore, Prayidae. Cahiers de Biologie Marine 10: 359–364.

Choy CA, Haddock SHD, Robison BH (2017) Deep pelagic food web structure as revealed by *in situ* feeding observations. Proceedings of the Royal Society B 284(1868): 20172116. https://doi.org/10.1098/rspb.2017.2116

Chun C (1885) Über die cyklische Entwickelung der Siphonophoren. Sitzungsberichte der Königlich Preussischen Akademie der Wissenschaften zu Berlin for 1885, 511–529.

Chun C (1888) Berichte über eine nach den Canarischen Inseln im Winter 1887/88 ausgeführte Reise. Sitzungsberichte der Preussischen Akademie der Wissenschaften zu Berlin for 1888: 1141–1173. [English translation in The Annals and Magazine of Natural History, Series 6, 3: 214–246.]

Eduardo LN, Bertrand A, Mincarone MM, Santos LV, Frédou T, Assunção RV, Silva A, Ménard F, Schwamborn R, Le Loc'h F, Lucena-Frédou F (2020) Hatchetfishes (Stomiiformes: Sternoptychidae) biodiversity, trophic ecology, vertical niche partitioning and functional roles in the western Tropical Atlantic. Progress in Oceanography 187: 1–14. https://doi.org/10.1016/j.pocean.2020.102389

Fewkes JW (1883) The Siphonophores. V. The Diphyae. American Naturalist 17(8): 833–845. https://doi.org/10.1086/273435

Gibbons MJ, Haddock SHD, Matsumoto GI, Foster C (2021) Records of ctenophores from South Africa. PeerJ 9: e10697. https://doi.org/10.7717/peerj.10697

Gili JM, Pagès F, Fusté X (1991) Mesoscale coupling between spatial distribution of planktonic cnidarians and hydrographic features along the Galician coast (Northwestern Iberian Peninsula). Scientia Marina 55: 419–426.

Graeffe E (1860) Beobachtungen über Radiaten und Würmer in Nizza. Neue Denkschriften der allgemeinen Schweizerischen Gesellschaft fur die gesammten. Naturwissenschaften 17: 1–59.

Gründlingh ML, Largier JL (1991) Physical Oceanography in False Bay – a review. In: Jackson WPU (Ed.) False Bay 21 years on – an environmental assessment. Proceedings of the Symposium. Transactions of the Royal Society of South Africa 47: 387–400.

Haddock SHD, Dunn CD, Pugh PR (2005) A re-examination of siphonophore terminology and morphology, applied to the description of two new prayine species with remarkable bio-optical properties. Journal of the Marine Biological Association of the United Kingdom 85(3): 695–707. https://doi.org/10.1017/S0025315405011616

Hetherington ED, Damian-Serrano A, Haddock SHD, Dunn CW, Choy CA (2022) Integrating siphonophores into marine food-web ecology. Limnology and Oceanography Letters 7(2): 81–95. https://doi.org/10.1002/lol2.10235

Hoving HJT, Neitzel P, Hauss H, Christiansen S, Kiko R, Robison BH, Silva P, Körtzinger A (2020) In situ observations show vertical community structure of pelagic fauna in the eastern tropical North Atlantic off Cape Verde. Scientific Reports 10(1): e21798. https://doi.org/10.1038/s41598-020-78255-9

Kölliker A (1853) Die schwimmpolypen oder Siphonophoren von Messina. Leipzig: Wilhelm Engelmann, Leipzig, 96 pp. https://doi.org/10.5962/bhl.title.12447

Lindsay DJ, Miyake H (2009) A checklist of midwater cnidarians and ctenophores from Japanese waters: Species sampled during submersible surveys from 1993–2008 with notes on their taxonomy. Kaiyo Monthly 41: 417–438. [In Japanese with English abstract]

Luo JY, Grassian B, Tang D, Irisson J-O, Greer AT, Guigand CM, McClatchie S, Cowen RK (2014) Environmental drivers of the fine-scale distribution of a gelatinous zooplankton community across a mesoscale front. Marine Ecology Progress Series 510: 129–149. https://doi.org/10.3354/meps10908

Madin LP (1991) Distribution and Taxonomy of Zooplankton in the Alboran Sea and adjacent western Mediterranean. A literature survey and field guide. Technical Report Woods Hole Oceanographic Institution, 91–26. https://doi.org/10.1575/1912/954

Mapstone GM (2015) Systematics of Siphonophores. In: Gopalakrishnakone P, Malhotra A (Eds) Evolution of Venomous Animals and Their Toxins, 1–37. https://doi.org/10.1007/978-94-007-6727-0_14-1

Metschnikoff E, Metschnikoff L (1871) Contributions to the knowledge of siphonophores and medusae. Mémoires de la Société des Amis des Sciences Naturelles, de l'Anthropologie et de l'Ethnographie 8(1): 295–370. [In Russian]

Minemizu R, Kubota S, Hirano Y, Lindsay DJ (2015) A photographic guide to the jellyfishes of Japan. Heibonsha, Tokyo, 360 pp.

Moser F (1917) Die siphonophoren der Adria und ihre Beziehungen zu denen des Weltmeeres. Kaiserliche Akademie der Wissenschaften in Wien. Mathematisch-naturwissenschaftliche Klasse. 126(9): 703–763.

Nakamura I, Goto Y, Sato K (2015) Ocean sunfish rewarm at the surface after deep excursions to forage for siphonophores. Journal of Animal Ecology 84(3): 590–603. https://doi.org/10.1111/1365-2656.12346

Pfaff MC, Logston RC, Raemaekers SJPN, Hermes JC, Blamey LK, Cawthra HC, Colenbrander DR, Crawford RJM, Day E, du Plessis N, Elwen SH, Fawcett SE, Jury MR, Karenyi N, Kerwath SE, Kock AA, Krug M, Lamberth SJ, Omardien A, Pitcher GC, Rautenbach C, Robinson TB, Rouault M, Ryan PG, Shillington FA, Sowman M, Sparks CC, Turpie JK, van Niekerk L, Waldron HN, Yeld EM, Kirkman SP (2019) A synthesis of three decades of socio-ecological change in False Bay, South Africa: Setting the scene for multidisciplinary research and management. Elementa 7: 32. https://doi.org/10.1525/elementa.367

Pugh PR (2009) A review of the family Sphaeronectidae (Class Hydrozoa, Order Siphonophora), with the description of three new species. Zootaxa 2147(1): 1–48. https://doi.org/10.11646/zootaxa.2147.1.1

Purcell JE (1981) Dietary composition and diel feeding patterns of epipelagic siphonophores. Marine Biology 65(1): 83–90. https://doi.org/10.1007/BF00397071

Russell FS (1935) On the value of certain plankton animals as indicators of water movements in the English Channel and North Sea. Journal of the Marine Biological Association of the United Kingdom 20(2): 309–332. https://doi.org/10.1017/S0025315400045239

Schneider KC (1898) Mittheilungen über Siphonophoren. III. Systematische und andere Bemerkungen. Zoologischer Anzeiger 21: 51–57, 73–97,114, 133, 153–173, 185–200.

Totton AK (1965) A Synopsis of the Siphonophora. Trustees of the British Museum (Natural History), London, UK, 230 pp.

Villefranche Sea Temperature (2021) Villefranche-sur-Mer Sea Temperature. https://www.seatemperature.org/europe/france/villefranche-sur-mer.htm [Accessed 27/04/2021]

Vogt C (1854) Recherches sur les animaux inférieurs de la Méditerranée. 1. Sur les Siphonophores de la mer de Nice. Mémoires de l`Institut National Genèvois 1: 1–164.

Vos de M, Vichi M, Rautenbach C (2021) Simulating the Coastal Ocean Circulation Near the Cape Peninsula Using a Coupled Numerical Model. Journal of Marine Science and Engineering 9(4): e359. https://doi.org/10.3390/jmse9040359